STEADY STREAMING ASSOCIATED WITH SOME UNSTEADY VISCOUS FLOWS

by

WILLIAM HOWARD LYNE

Department of Mathematics

Imperial College of Science and Technology. July 1970.

ABSTRACT

The work in this thesis is concerned with the steady streaming generated by some unsteady viscous flows and two problems are considered in detail.

The first part of the thesis considers, in the main, the flow in a circular pipe of radius a, which is itself coiled in a circle. The pressure gradient along the pipe varies sinusoidally in time with frequency ω. Of especial interest is the so-called secondary flow generated by centrifugal effects in the plane of the cross-section of the pipe, for, if the parameter $\beta = (2\nu/\omega a^2)^{1/2}$ is sufficiently small, this is found to be steady in the interior of the pipe, and in the opposite sense to that predicted for a steady pressure gradient along the pipe (ν is the kinematic viscosity of the fluid). This is verified qualitatively by an experiment.

The second part is concerned with the steady streaming generated by an oscillating viscous flow over a wavy wall. A viscous shear-wave layer is formed on the wall, and if its thickness is much smaller than the amplitude of the wave, an existing theory may be used to calculate the steady streaming. This is only valid, however, when the amplitude of the oscillation of the fluid particles a long way from the wall is much smaller than the wavelength of the wall. A theory is developed for the case when the

thickness of the viscous layer is much greater than the amplitude of the wave, and it is found that, under certain conditions, the previous theory is still valid. In addition it proves possible to calculate the steady streaming when the amplitude of the oscillation of the fluid particles a long way from the wall is much greater than the wavelength of the wall.

ACKNOWLEDGEMENT

I would like to express my gratitude to Professor J. T. Stuart for his continual guidance and invaluable assistance throughtout the course of this work. I am also indebted to Dr. C. G. Caro for the provision of the experimental equipment.

CONTENTS

APPENDICES

GENERAL INTRODUCTION

The theoretical study of the steady streaming generated by unsteady viscous flows was initiated by Rayleigh (1884) in connection with certain acoustic phenomena of Kundt's dust tube. Considerable attention has since been focused on the fundamental problem of a body oscillating in an unbounded viscous fluid, and for a comprehensive review of the contributions to this topic the reader is referred to Riley (1967). The type of asymptotic analysis employed by Riley is used extensively in part one of this thesis.

This first part contains an investigation of the flow through a curved pipe under an oscillatory pressure gradient, the so-called secondary flow generated in the plane of cross-section being of especial interest. In the interior of the pipe, this secondary flow is found to be steady for sufficiently small values of the parameter $\beta = (2\nu/\omega a^2)^{1/2}$, and in the opposite sense to that predicted for a steady pressure gradient; this is confirmed by experiment (ω is the frequency of the oscillations, a is the radius of the pipe and ν is the kinematic viscosity of the fluid). This type of flow is of considerable physiological interest, and its implications for the cardiovascular system, and in particular the aorta, are considered. Because the secondary flow is induced by centrifugal effects, it is analogous to the steady streaming induced in a fluid bounded by two parallel

planes performing torsional oscillations about a common axis. This problem has recently been considered by Jones and Rosenblat (1969), following an earlier discussion by Rosenblat (1960).

In part two the steady streaming induced by an oscillatory viscous flow over a wavy wall is considered. A viscous layer is formed on the wall, and if its thickness is much smaller than the amplitude of the wave, the theory for a cylinder oscillating in an unbounded viscous fluid can be applied directly to predict the steady streaming. This theory, due originally to Schlichting (1932), is valid only when the amplitude of oscillation of the fluid particles is much smaller than the wavelength of the wall. The theory is extended for the case when the amplitude of the wave is much smaller than the thickness of the viscous layer, and it is found that, under certain conditions, the theory due to Schlichting may still be applied to predict the steady streaming. In addition it proves possible to calculate the steady streaming when the amplitude of the oscillations of the fluid particles is much greater than the wavelength of the wall.

PART I

FLOW IN A CURVED PIPE

CHAPTER I

INTRODUCTION

In this first part we consider the flow of an incompressible viscous fluid through a pipe of circular cross-section which is coiled in a circle. In particular attention is focused on the so-called secondary flow, which is induced in the plane of the cross-section of the pipe by centrifugal effects.

The steady problem of this kind was first analysed by Dean (1927 and 1928), who found that the motion depended on a parameter K, equal to $2Re^2 a/R$, Re being a Reynolds number for flow along the pipe, a the radius of the pipe and R the radius of curvature of its axis. The analysis employed by Dean was restricted to small values of K, but recently this has been extended numerically to moderately large values of K by McConalogue and Srivastava (1968). The work of the latter bridges the gap between the theory of Dean and that of Barua (1963), who developed an asymptotic boundary layer theory for very large values of K.

The knowledge of steady flow through a curved pipe is thus quite extensive. On the other hand, time dependent viscous flows in a curved pipe have not been studied, at least to the author's knowledge. Therefore we consider here the effects of unsteadiness on the motion.

This problem is of considerable interest in the study of the cardio-vascular system where the motion in the larger arteries is anything but steady, and where, unlike most engineering situations, the flow is laminar.

In order to simplify the problem, the radius of curvature of the pipe is assumed large in relation to its own radius, and the pressure gradient applied along the pipe sinusoidal in time with zero mean. In Chapter 2 the equations of motion are derived and the flow, being unsteady, is seen to depend on two parameters which are conveniently taken as

$$\epsilon = \frac{W}{a\omega} \cdot \left(\frac{a}{R}\right)^{1/2}, \quad R_s = \frac{W^2}{R\omega} \cdot \frac{a}{\nu} \qquad (1.1)$$

Here W is a typical velocity along the pipe, ω is the frequency and ν the kinematic viscosity of the fluid. The parameter ϵ may be recognised as the product of the ratio of the particle displacement amplitude $\frac{W}{\omega}$ for motion along the pipe to the radius of the pipe, and the square root of the ratio of the radius of the pipe to its radius of curvature. The problem has been formulated in such a way that ϵ is always small and this allows the equations to be simplified thus making the problem more amenable to analysis. It will be seen later that R_s plays the role of a conventional Reynolds number for the secondary flow. This choice of parameters was made to allow direct comparison with the analagous two-dimensional problem of flow

induced by a body oscillating in an unbounded viscous fluid, as described by Riley (1967) in a review article. Another parameter of major importance in our analysis is

$$\beta^2 = 2\nu/\omega a^2 = 2\epsilon^2/R_s \qquad (1.2)$$

and this also is assumed small. Clearly β represents the ratio of the Stokes layer thickness, which is proportional to $(2\nu/\omega)^{1/2}$, to the radius of the pipe. The smallness of β implies that, for the flow down the pipe, viscous effects are confined to a thin layer on the wall, while the main part of the flow is inviscid.

In Chapter 3 a solution is developed by the use of two matched asymptotic expansions, one expansion being valid near to the wall of the pipe, where the Stokes shear-wave layer exists (the inner region), and the other expansion being valid in the region away from the wall (the outer region). The expansion parameter in each case is β, and a common range of validity is assumed in which the matching takes place. In Chapter 4 these expansions are taken to $0(\beta^2)$ in both regions when R_s is small, but when R_s is large a solution to only $0(\beta^0)$ is attempted for the outer region, and is described in Chapter 5.

In the latter case we find that an outer boundary layer of thickness $0(aR_s^{-1/2})$ is formed at the edge of the Stokes layer, in which the velocity of the secondary motion is adjusted to the value dictated by the flow in the interior of the pipe. This interior, away

from all viscous boundary layers, will be referred to as the core, and differs from the outer region in that the latter comprises both the outer boundary layer and the core. Because the governing equations for the first order secondary flow in the outer region are steady, and the streamlines are closed, it will be seen that the secondary flow in the core of the pipe must, to first order, have uniform vorticity (see Batchelor (1956)). Because of symmetry about that diameter lying in the plane in which the pipe is coiled, the vorticity immediately above this diameter must be equal in magnitude, but of opposite sign, to that immediately below it. Harper (1963) has shown that this leads to the formation of a free boundary layer of thickness $0(a R_s^{-1/2})$ along this diameter. The equations of these boundary layers are linearised by assuming the velocities of the secondary motion in the layers are small perturbations to the velocities of the motion in the core. These linearised equations are solved to give an integral equation for the velocity profile at some station, the strength of the vortex in the core appearing as an eigenvalue. This equation is solved numerically, and the eigenvalue found.

In Chapter 6 the results are presented together with a discussion of their implications for the cardiovascular system. One of the striking features is that, for sufficiently small values of the parameter β, the secondary flow in the core of the pipe is in the

opposite sense to that predicted for steady flow along the pipe. Thus, whereas the intuitive idea of 'outwards centrifuging' is valid for steady flow, it is not valid in the unsteady flow that we discuss; rather the apparent centrifuging is negative and is therefore directed inwards! This has been verified experimentally using the apparatus described in Chapter 7.

In Chapter 8 the analysis is extended to embrace pipes of elliptic cross-section. The motivation for this is the hope that the linearisation used in the large R_s calculation may be more convincing. We shall find this to be the case in certain circumstances, and the results indicate that the linearisation may, in fact, be very good even for the circular pipe. This belief is reinforced by the numerical work of Kuwahara and Imai (1969) described in Chapter 6.

CHAPTER 2

THE EQUATIONS OF MOTION

Let us consider incompressible viscous flow in a pipe of circular cross-section of radius a, the pipe's own axis itself being coiled in a circle of radius R about the axis 0z (Fig. 2.1). Distance down the pipe is measured by $R\theta$, where θ is the angle which an axial plane (containing 0z) makes with some fixed axial plane. Within the pipe cross-section polar coordinates r, ψ are used (Fig. 2.1). The velocity vector $\underline{u}$ has components (u, v, w) corresponding to the spatial coordinates (r, ψ, θ), and we assume $\underline{u}$ is independent of θ. In addition we define p to denote the pressure, ρ the density, ν the kinematic viscosity and t the time.

The momentum equation written in vector form is

$$\frac{\partial \underline{u}}{\partial t} + \text{grad}\left(\frac{1}{2}\underline{u}^2\right) - \underline{u} \wedge \text{curl } \underline{u} = -\frac{1}{\rho}\,\text{grad } p - \nu \text{ curl curl } \underline{u} \qquad (2.1)$$

and the equation of continuity is

$$\text{div } \underline{u} = 0 \qquad (2.2)$$

For the derivation of these equations see, for example, Whitham (1963).

In this coordinate system the line element ds is given by

$$ds^2 = h_1^{\,2}\, dr^2 + h_2^{\,2}\, d\psi^2 + h_3^{\,2}\, d\theta^2 \qquad (2.3)$$

where

$$h_1 = 1, \quad h_2 = r, \quad h_3 = R + r\cos\psi \tag{2.4}$$

We use the following well known expressions for grad, div and curl

$$\left.\begin{aligned}
&\text{grad} \equiv \left(\frac{1}{h_1}\frac{\partial}{\partial r}, \frac{1}{h_2}\frac{\partial}{\partial \psi}, \frac{1}{h_3}\frac{\partial}{\partial \theta}\right) \\
&\text{div } \underline{u} = \frac{1}{h_1 h_2 h_3}\left\{\frac{\partial}{\partial r}(h_2 h_3 u) + \frac{\partial}{\partial \psi}(h_3 h_1 v) + \frac{\partial}{\partial \theta}(h_1 h_2 w)\right\} \\
&\text{and} \\
&\zeta_1 = \frac{1}{h_2 h_3}\left\{\frac{\partial}{\partial \psi}(h_3 w) - \frac{\partial}{\partial \theta}(h_2 v)\right\} \\
&\zeta_2 = \frac{1}{h_3 h_1}\left\{\frac{\partial}{\partial \theta}(h_1 u) - \frac{\partial}{\partial r}(h_3 w)\right\} \\
&\zeta_3 = \frac{1}{h_1 h_2}\left\{\frac{\partial}{\partial r}(h_2 v) - \frac{\partial}{\partial \psi}(h_1 u)\right\}
\end{aligned}\right\} \tag{2.5}$$

where $\underline{\zeta}\ (\zeta_1, \zeta_2, \zeta_3) = \text{curl } \underline{u}$

When the values of h_i are inserted the equations become, in component form,

$$\frac{\partial u}{\partial t} + u\frac{\partial u}{\partial r} + \frac{v}{r}\frac{\partial u}{\partial \psi} - \frac{v^2}{r} - \frac{w^2\cos\psi}{R+r\cos\psi} = -\frac{\partial}{\partial r}(p/\rho)$$

$$- \nu\left(\frac{1}{r}\frac{\partial}{\partial \psi} - \frac{\sin\psi}{R+r\cos\psi}\right)\left(\frac{\partial v}{\partial r} + \frac{v}{r} - \frac{1}{r}\frac{\partial u}{\partial \psi}\right) \tag{2.6}$$

$$\frac{\partial v}{\partial t} + u\frac{\partial v}{\partial r} + \frac{v}{r}\frac{\partial v}{\partial \psi} + \frac{uv}{r} + \frac{w^2\sin\psi}{R+r\cos\psi} = -\frac{1}{r}\frac{\partial}{\partial \psi}(p/\rho)$$

$$+ \nu\left(\frac{\partial}{\partial r} + \frac{\cos\psi}{R+r\cos\psi}\right)\left(\frac{\partial v}{\partial r} + \frac{v}{r} - \frac{1}{r}\frac{\partial u}{\partial \psi}\right) \tag{2.7}$$

$$\frac{\partial w}{\partial t} + u\frac{\partial w}{\partial r} + \frac{v}{r}\frac{\partial w}{\partial \psi} + \frac{uw\cos\psi}{R+r\cos\psi} - \frac{vw\sin\psi}{R+r\cos\psi} = \frac{-1}{R+r\cos\psi}\frac{\partial}{\partial\theta}(p/\rho)$$

$$+\nu\left[\left(\frac{\partial}{\partial r}+\frac{1}{r}\right)\left(\frac{\partial w}{\partial r}+\frac{w\cos\psi}{R+r\cos\psi}\right)+\frac{1}{r}\frac{\partial}{\partial\psi}\left(\frac{1}{r}\frac{\partial w}{\partial\psi}-\frac{w\sin\psi}{R+r\cos\psi}\right)\right] \tag{2.8}$$

The equation of continuity is

$$\frac{\partial u}{\partial r}+\frac{u}{r}+\frac{u\cos\psi}{R+r\cos\psi}+\frac{1}{r}\frac{\partial v}{\partial\psi}-\frac{v\sin\psi}{R+r\cos\psi}=0 \tag{2.9}$$

We now impose a simple sinusoidal pressure gradient along the pipe

$$-\frac{\partial}{\partial\theta}(p/\rho) = R\,W\,\omega\cos\omega t \tag{2.10}$$

where W has the dimensions of velocity and ω is the angular frequency. We may first note that the exact solution to (2.6) - (2.9) in the absence of viscosity is the potential flow solution

$$u = 0,\quad v = 0,\quad w = \frac{RW\sin\omega t}{R+r\cos\psi} \tag{2.11}$$

$$p/\rho = -R\theta W\,\omega\cos\omega t - \frac{W^2}{2}\left[\left(\frac{R}{R+r\cos\psi}\right)^2 - 1\right]\sin^2\omega t$$

The arbitrary function of integration has been chosen so that as $R \to \infty, p/\rho \to -R\theta W\,\omega\cos\omega t$, which can be identified as the pressure distribution when the pipe is straight. This solution satisfies the boundary condition of no flow through the pipe wall. There are no

components of secondary flow in the plane of the cross-section, there being a balance between the centrifugal force exerted by the flow along the pipe, and the pressure gradient in that plane. Now, when viscosity is present, a balance between the highest derivative and the driving pressure gradient in equation (2.8) must be set up, in order to satisfy the extra boundary condition of no slip on the pipe wall. Thus we must have

$$\nu \frac{\partial^2 w}{\partial r^2} \sim W \omega \qquad (2.12)$$

We now assume, in common with most boundary layer theories, that, for small viscosity, (2.11) is a valid representation for w away from the wall of the pipe. Hence we see $w = 0(W)$ and then (2.12) implies that viscous effects are confined to a layer of thickness $0(\nu/\omega)^{1/2}$ adjacent to the pipe wall. This layer is thin when $\beta = (2\nu/\omega a^2)^{1/2}$ is small, and is just the Stokes shear-wave layer referred to in numerous texts. Another consequence of this boundary layer assumption is that the pressure gradients, given by the expression for p in (2.11), are essentially unchanged within the viscous Stokes layer. However, the value of w will decay to zero as the wall of the pipe is approached, and thus there will no longer be a balance between the centrifugal force and the pressure gradients in equations (2.6) and (2.7). Therefore the latter now drive the so-called secondary

flow in the plane of the cross-section. Within the Stokes layer a balance must be set up between the pressure gradient and the highest derivative in order that all the boundary conditions may be satisfied. Therefore, from (2.7)

$$\frac{1}{r}\frac{\partial}{\partial \psi}(p/\rho) \sim \nu \frac{\partial^2 v}{\partial r^2} \qquad (2.13)$$

Within the layer this leads to the conclusion that $v = 0(\frac{W^2}{R\omega})$ and similarly $u = 0((\frac{W^2}{R\omega}) \cdot \beta)$. If this secondary flow persists away from the pipe wall, we may expect then that $v = 0(\frac{W^2}{R\omega})$ and $u = 0(\frac{W^2}{R\omega})$ from a consideration of the equation of continuity (2.9). Although u and v may no longer be zero, we shall see that the assumption that (2.11) is a valid representation of flow away from the pipe wall is still consistent within the framework of this boundary layer theory. The reason for this is that $u, v = 0(\frac{W^2}{R\omega}) = 0\left[\epsilon (\frac{a}{R})^{1/2} W\right]$. Thus, for small $\epsilon (\frac{a}{R})^{1/2}$, the secondary flow, though non-zero, is smaller than the flow along the pipe.

We now introduce the following non-dimensional notation

$$\delta = a/R, \quad r' = r/a, \quad w' = w/W, \quad u' = u/\frac{W^2}{R\omega}$$

$$v' = v/\frac{W^2}{R\omega}, \quad \tau = \omega t \ , \qquad (2.14)$$

$$p' = (p + \rho R\Omega W \cos \omega t) / \rho \delta W^2$$

remembering that, in due course, r' and u' will need to be suitably scaled within the Stokes layer. The momentum equations (2.6),

(2.7) and (2.8) now become

$$\frac{\partial u'}{\partial \tau} + \epsilon^2\left(u' \frac{\partial u'}{\partial r'} + \frac{v'}{r'} \frac{\partial u'}{\partial \psi} - \frac{v'^2}{r'}\right) - \frac{w'^2 \cos\psi}{1+\delta r'\cos\psi} = -\frac{\partial p'}{\partial r'}$$

$$- \frac{1}{2}\beta^2 \left(\frac{1}{r'} \frac{\partial}{\partial \psi} - \frac{\delta \sin\psi}{1+\delta r'\cos\psi}\right)\left(\frac{\partial v'}{\partial r'} + \frac{v'}{r'} - \frac{1}{r'} \frac{\partial u'}{\partial \psi}\right) \qquad (2.15)$$

$$\frac{\partial v'}{\partial \tau} + \epsilon^2\left(u' \frac{\partial v'}{\partial r'} + \frac{v'}{r'} \frac{\partial v'}{\partial \psi} + \frac{u'v'}{r'}\right) + \frac{w'^2 \sin\psi}{1+\delta r'\cos\psi} = -\frac{1}{r'} \frac{\partial p'}{\partial \psi}$$

$$+ \frac{1}{2}\beta^2 \left(\frac{\partial}{\partial r'} + \frac{\delta\cos\psi}{1+\delta r'\cos\psi}\right)\left(\frac{\partial v'}{\partial r'} + \frac{v'}{r'} - \frac{1}{r'} \frac{\partial u'}{\partial \psi}\right) \qquad (2.16)$$

and

$$\frac{\partial w'}{\partial \tau} + \epsilon^2\left(u' \frac{\partial w'}{\partial r'} + \frac{v'}{r'} \frac{\partial w'}{\partial \psi} + \frac{u'w'\delta\cos\psi}{1+\delta r'\cos\psi} - \frac{v'w'\delta\sin\psi}{1+\delta r'\cos\psi}\right)$$

$$= \frac{1}{1+\delta r'\cos\psi}\cos\tau + \frac{1}{2}\beta^2\left[\left(\frac{\partial}{\partial r'} + \frac{1}{r'}\right)\left(\frac{\partial w'}{\partial r'} + \frac{w'\delta\cos\psi}{1+\delta r'\cos\psi}\right)\right.$$

$$\left. + \frac{1}{r'} \frac{\partial}{\partial \psi}\left(\frac{1}{r'} \frac{\partial w'}{\partial \psi} - \frac{w'\delta\sin\psi}{1+\delta r'\cos\psi}\right)\right] \qquad (2.17)$$

The equation of continuity (2.9) becomes

$$\frac{\partial u'}{\partial r'} + \frac{u'}{r'} + \frac{u'\delta\cos\psi}{1+\delta r'\cos\psi} + \frac{1}{r'} \frac{\partial v'}{\partial \psi} - \frac{v'\delta\sin\psi}{1+\delta r'\cos\psi} = 0 \qquad (2.18)$$

In order to simplify the equations and allow some progress to be made, δ is taken to be very small and all terms of $0(\delta)$ are neglected.

Equation (2.18) now becomes

$$\frac{\partial u'}{\partial r'} + \frac{u'}{r'} + \frac{1}{r'} \frac{\partial v'}{\partial \psi} = 0 \qquad (2.19)$$

We satisfy equation (2.19) by introducing the non-dimensional stream

function χ for flow in the cross-section, defined as follows.

$$u' = \frac{1}{r'}\frac{\partial \chi}{\partial \psi} \quad , \quad v' = -\frac{\partial \chi}{\partial r'} \tag{2.20}$$

If we now eliminate the pressure between equations (2.15) and (2.16) and neglect terms of $0(\delta)$, we obtain the following equation for χ

$$\frac{\partial}{\partial \tau}\nabla^2\chi - \frac{\epsilon^2}{r'}\frac{\partial(\chi, \nabla^2\chi)}{\partial(r', \psi)} - \frac{2}{r'}\left(r'w'\frac{\partial w'}{\partial r'}\sin\psi\right.$$

$$\left. + w'\frac{\partial w'}{\partial \psi}\cos\psi\right) = \frac{1}{2}\beta^2\nabla^4\chi \tag{2.21}$$

where

$$\nabla^2 \equiv \frac{\partial^2}{\partial r'^2} + \frac{1}{r'}\frac{\partial}{\partial r'} + \frac{1}{r'^2}\frac{\partial^2}{\partial \psi^2} \; ; \quad \frac{\partial(a, b)}{\partial(r', \psi)} \equiv \frac{\partial a}{\partial r'}\frac{\partial b}{\partial \psi} - \frac{\partial a}{\partial \psi}\frac{\partial b}{\partial r'} \tag{2.22}$$

From the expressions (2.5), we find that the component ζ_3 of curl $\underline{u}$ is equal to $-\frac{W^2}{Ra\omega}\nabla^2\chi$. Therefore $-\nabla^2\chi$ is the non-dimensional vorticity of the secondary flow and equation (2.21) is the vorticity equation.

When we neglect terms of $0(\delta)$, equation (2.17) becomes

$$\frac{\partial w'}{\partial \tau} - \frac{\epsilon^2}{r'}\frac{\partial(\chi, w')}{\partial(r', \psi)} = \cos\tau + \frac{1}{2}\beta^2\nabla^2 w' \tag{2.23}$$

The boundary conditions of no slip on the wall of the pipe can be written as

$$\chi = \frac{\partial \chi}{\partial r'} = w' = 0 \quad \text{on } r' = 1 \tag{2.24}$$

These conditions, together with the requirement that the flow field is regular within the pipe, are sufficient for the determination of the solutions to (2.21) and (2.23).

CHAPTER 3

THE LIMIT $\beta \to 0$

In this chapter we shall seek asymptotic solutions to (2.21) and (2.23) which tend to the exact solutions in the limit $\beta \to 0$, R_s fixed; in later chapters we shall study the consequences of taking the further limits $R_s \to 0$ and $R_s \to \infty$.

Because of the nature of the imposed pressure gradient, we shall admit only those solutions which have a harmonic dependence on τ. Any other solution is an eigensolution which determines whether or not the solution described below is stable. Such questions of stability are not our concern here.

The primes will now be dropped from the dimensionless quantities defined in (2.14) for reasons of simplicity, and all variables are now dimensionless unless stated otherwise.

In the Stokes layer, or inner region, we have seen that the relevant length scale is $(2\nu/\omega)^{1/2}$. Therefore, in accord with boundary layer theory, we introduce the following scaled variables for this region,

$$\eta = \beta^{-1}(1-r), \qquad X = \beta^{-1}\chi \tag{3.1}$$

and seek solutions to (2.21) and (2.23) for this inner region of the form

$$w = w_o(\tau, \eta, \psi; R_s) + \beta w_1(\tau, \eta, \psi; R_s) + \beta^2 w_2(\tau, \eta, \psi; R_s) + \cdots \tag{3.2}$$

$$\Xi = \Xi_o(\tau, \eta, \psi; R_s) + \beta \Xi_1(\tau, \eta, \psi; R_s) + \beta^2 \Xi_2(\tau, \eta, \psi; R_s) + \cdots \tag{3.3}$$

subject to the boundary conditions (2.24), which can be written as

$$w_i = \Xi_i = \frac{\partial \Xi_1}{\partial \eta} = 0, \quad \eta = 0 \qquad i = 0, 1, 2, 3, \ldots \tag{3.4}$$

In the outer region, away from the Stokes layer, we look for solutions of the form

$$w = \sin \tau \tag{3.5}$$

$$\chi = \chi_o(\tau, r, \psi; R_s) + \beta \chi_1(\tau, r, \psi; R_s) + \beta^2 \chi_2(\tau, r, \psi; R_s) + \cdots \tag{3.6}$$

and require that these should match with the solutions in the inner region in some suitable way. Equation (3.5) is a direct consequence of (2.23) if we note that no steady part of w may exist as there is no preferential direction for the motion; it can be seen to be just the potential flow solution.

Substituting (3.5) and (3.6) into (2.21) and (2.23), and equating like powers of β, we have:

$$\frac{\partial}{\partial \tau} \nabla^2 \chi_o = 0 \tag{3.7}$$

$$\frac{\partial}{\partial \tau} \nabla^2 \chi_1 = 0 \tag{3.8}$$

$$\frac{\partial}{\partial \tau} \nabla^2 \chi_2 - \frac{R_s}{2r} \frac{\partial(\chi_o, \nabla^2 \chi_o)}{\partial (r, \psi)} = \frac{1}{2} \nabla^4 \chi_o \qquad (3.9)$$

Equation (3.7) implies

$$\nabla^2 \chi_o = g_o(r, \psi ; R_s) \qquad (3.10)$$

and hence

$$\chi_o = \chi_o^{(u)}(r, \psi, \tau ; R_s) + \chi_o^{(s)}(r, \psi ; R_s) \qquad (3.11)$$

where

$$\nabla^2 \chi_o^{(u)} = 0 \qquad (3.12)$$

$$\nabla^2 \chi_o^{(s)} = g_o(r, \psi ; R_s) \qquad (3.13)$$

$\chi_o^{(u)}$ can contain terms proportional to $e^{in\tau}$ ($n = 1$ to ∞), and has zero time average; $\chi_o^{(s)}$ is independent of τ. Similarly, we have

$$\chi_1 = \chi_1^{(u)}(r, \psi, \tau ; R_s) + \chi_1^{(s)}(r, \psi ; R_s) \qquad (3.14)$$

where

$$\nabla^2 \chi_1^{(u)} = 0 \qquad (3.15)$$

$$\nabla^2 \chi_1^{(s)} = g_1(r, \psi ; R_s) \qquad (3.16)$$

When we substitute (3.1), (3.2) and (3.3) into (2.21) and (2.23), and equate like powers of β, we arrive at the following equations for w_o and Ξ_o

$$\left(\frac{\partial}{\partial \tau} - \frac{1}{2} \frac{\partial^2}{\partial \eta^2}\right) w_o = \cos \tau \qquad (3.17)$$

$$\left(\frac{\partial}{\partial \tau} - \frac{1}{2} \frac{\partial^2}{\partial \eta^2}\right) \frac{\partial^2 \Xi_o}{\partial \eta^2} = -2 w_o \frac{\partial w_o}{\partial \eta} \sin \psi \qquad (3.18)$$

The solution of (3.17) satisfying (3.4) and which matches with (3.5) when $\eta \to \infty$, is easily seen to be

$$w_o = \sin\tau - e^{-\eta}\sin(\tau - \eta) \qquad (3.19)$$

Substituting (3.19) into (3.18) and solving, we find the general solution to (3.18) may be written as

$$\Xi_o = \left\{ -\frac{1}{8}e^{-2\eta} - \frac{\sqrt{2}}{2}e^{-\eta}\cos(-\eta+\pi/4) - \frac{\sqrt{2}}{16}e^{-2\eta}\cos(2\tau-2\eta+\pi/4) \right.$$

$$\left. - \frac{\sqrt{2}}{2}e^{-\eta}\cos(2\tau-\eta+\pi/4) \right\} \sin\psi$$

$$+ \Re \sum_{n=1}^{\infty} D_n(\psi)\, e^{-\sqrt{n}(1+i)\eta + in\tau}$$

$$+B(\psi)\eta^3 + C(\psi)\eta^2 + F(\tau,\psi)\eta + G(\tau,\psi) \qquad (3.20)$$

where terms of non-harmonic dependence on τ, and of exponential growth as $\eta \to \infty$, have been excluded. The latter exclusion is necessary to enable the solution in the inner region to match with that in the outer region as $\eta \to \infty$. The symbol $\Re$ means 'real part of'.

To effect the matching, we assume that there is a common region of validity for the inner and outer solutions when $\eta \sim \infty$ and $r \sim 1$ respectively. Thus, if we write the solution for the outer region in terms of the variables of the inner region, we have, for $r \sim 1$

$$\mathbb{K} = \beta^{-1}\left[\chi_o\right]_{r=1} - \eta\left\{\frac{\partial \chi_o}{\partial r}\right]_{r=1} + \left[\chi_1\right]_{r=1}$$

$$+ \beta\left\{\frac{\eta^2}{2}\left[\frac{\partial^2 \chi_o}{\partial r^2}\right]_{r=1} - \eta\left[\frac{\partial \chi_1}{\partial r}\right]_{r=1} + \left[\chi_2\right]_{r=1}\right\}$$

$$+ \beta^2\left\{-\frac{\eta^3}{6}\left[\frac{\partial^3 \chi_o}{\partial r^3}\right]_{r=1} + \frac{\eta^2}{2}\left[\frac{\partial^2 \chi_1}{\partial r^2}\right]_{r=1} - \eta\left[\frac{\partial \chi_2}{\partial r}\right]_{r=1}\right.$$

$$\left. + \left[\chi_3\right]_{r=1}\right\} + O(\beta^3) \qquad (3.21)$$

For this to match with the inner solution when $\eta \sim \infty$, we see from (3.20) that $B(\psi) \equiv C(\psi) \equiv 0$ and

$$\chi_o^{(u)}(1, \psi, \tau; R_s) + \chi_o^{(s)}(1, \psi; R_s) = 0 \qquad (3.22)$$

It may be possible, however, to have B or C non-zero if we rescale χ. We investigate the likelihood of this in appendix A, and though no rigorous proof is established, arguments are put forward to show that B and C are probably zero.

A consequence of (3.22) is that

$$\chi_o^{(u)} = 0 \qquad \text{on } r = 1 \qquad (3.23)$$

and the only regular solution to (3.12) with this boundary condition is

$$\chi_o^{(u)} = 0 \qquad (3.24)$$

Hence $F(\tau, \psi)$ can be seen, from matching (3.20) and (3.21), to be a function of ψ alone ($F(\psi)$).

From the boundary conditions (3.4), we can now deduce

$$D_n(\psi) \equiv 0\,, \quad n \neq 2\,; \quad D_2(\psi) = \frac{5}{8}\sin\psi\, e^{i\pi/4}$$

$$F(\psi) = -\frac{1}{4}\sin\psi\,; \quad G(\tau,\psi) = \frac{(9\sqrt{2}-10)}{16}\cos(2\tau+\pi/4)\sin\psi$$

$$+ 5/8\sin\psi \tag{3.25}$$

Therefore, finally, we have

$$\chi_o = \Big\{ -\frac{1}{4}\eta + \frac{5}{8} - \frac{1}{8}e^{-2\eta} - \frac{\sqrt{2}}{2}e^{-\eta}\cos(-\eta+\pi/4)$$

$$+ \frac{5}{8}e^{-\sqrt{2}\eta}\cos(2\tau-\sqrt{2}\eta+\pi/4) - \frac{\sqrt{2}}{16}e^{-2\eta}\cos(2\tau-2\eta+\pi/4)$$

$$- \frac{\sqrt{2}}{2}e^{-\eta}\cos(2\tau-\eta+\pi/4) + \frac{(9\sqrt{2}-10)}{16}\cos(2\tau+\pi/4)\Big\}\sin\psi$$

(3.26)

Because only harmonic dependence on τ is allowed and (3.24) implies χ_o is independent of τ, equation (3.9) yields the two equations

$$\frac{\partial}{\partial\tau}\nabla^2\chi_2 = 0 \tag{3.27}$$

$$-\frac{1}{r}\frac{\partial(\chi_o, \nabla^2\chi_o)}{\partial(r,\psi)} = \frac{1}{R_s}\nabla^4\chi_o \tag{3.28}$$

We find, therefore, that χ_o satisfies the two-dimensional Navier-Stokes equation, with R_s playing the role of a conventional Reynolds number. From matching (3.21) with (3.26), we see that the boundary conditions on χ_o are

$$\chi_o = 0\,, \quad \frac{\partial\chi_o}{\partial r} = \frac{1}{4}\sin\psi \quad \text{on } r = 1 \tag{3.29}$$

and the condition on $\chi_1^{(u)}$ is

$$\chi_1^{(u)} = \frac{(9\sqrt{2}-10)}{16}\cos(2\tau+\pi/4)\sin\psi \quad \text{on } r = 1 \qquad (3.30)$$

There is one less boundary condition on $\chi_1^{(u)}$ than on χ_o, because the equation it satisfies (3.15) is second order, whereas that satisfied by χ_o (3.28) is fourth order. These conditions are sufficient to enable the equations to be solved, when we demand that the solutions shall be regular everywhere within the pipe.

We easily find now that

$$\chi_1^{(u)} = \frac{(9\sqrt{2}-10)}{16}\, r\cos(2\tau+\pi/4)\sin\psi \qquad (3.31)$$

The equation of $0(\beta^3)$ in the outer region yields the two equations

$$\frac{\partial}{\partial\tau}\nabla^2\chi_3 - \frac{R_s}{2r}\frac{\partial(\chi_1^{(u)}, \nabla^2\chi_o)}{\partial(r,\psi)} = 0 \qquad (3.32)$$

$$-\frac{1}{r}\frac{\partial(\chi_1^{(s)}, \nabla^2\chi_o)}{\partial(r,\psi)} - \frac{1}{r}\frac{\partial(\chi_o, \nabla^2\chi_1^{(s)})}{\partial(r,\psi)} = \frac{1}{R_s}\nabla^4\chi_1^{(s)} \qquad (3.33)$$

In the inner region the equations for w_1 and Ξ_1 are

$$\left(\frac{\partial}{\partial\tau} - \frac{1}{2}\frac{\partial^2}{\partial\eta^2}\right)w_1 = -\frac{1}{2}\frac{\partial w_o}{\partial\eta} \qquad (3.34)$$

$$\left(\frac{\partial}{\partial\tau} - \frac{1}{2}\frac{\partial^2}{\partial\eta^2}\right)\frac{\partial^2\Xi_1}{\partial\eta^2} = \frac{\partial^2\Xi_o}{\partial\tau\,\partial\eta} - \frac{\partial^3\Xi_o}{\partial\eta^3} - 2\frac{\partial(w_o w_1)}{\partial\eta}\sin\psi \qquad (3.35)$$

The solution of (3.34) satisfying (3.4) and matching with (3.5) as $\eta \to \infty$ is easily found to be

$$w_1 = -\frac{1}{2}\eta\, e^{-\eta}\, \sin(\tau - \eta) \qquad (3.36)$$

If we substitute the expressions for w_o (3.19), Ξ_o (3.26) and w_1 (3.36) into (3.35) and solve, we find that the general solution of Ξ_1 can be written as

$$\Xi_1 = \Big\{ -\frac{\sqrt{2}}{16}\eta e^{-2\eta}\cos(2\tau - 2\eta + \pi/4) - \frac{1}{16}e^{-2\eta}\cos(2\tau - 2\eta)$$

$$- \frac{\sqrt{2}}{4}\eta e^{-\eta}\cos(2\tau - \eta + \pi/4) + \frac{1}{4}e^{-\eta}\cos(2\tau - \eta)$$

$$+ \frac{5}{16}\eta e^{-\sqrt{2}\eta}\cos(2\tau - \sqrt{2}\eta + \pi/4) - \frac{\sqrt{2}}{4}\eta e^{-\eta}\cos(-\eta + \pi/4)$$

$$+ \frac{1}{4}e^{-\eta}\cos(-\eta) - \frac{1}{8}\eta e^{-2\eta} - \frac{1}{16}e^{-2\eta}\Big\}\sin\psi$$

$$+ \mathcal{R}\sum_{n=1}^{\infty} J_n(\psi)\, e^{-\sqrt{n}(1+i)\eta + in\tau} + H(\psi)\eta^3$$

$$+ I(\psi)\eta^2 + K(\tau,\psi)\eta + L(\tau,\psi) \qquad (3.37)$$

Terms of exponential growth as $\eta \to \infty$ and of non-harmonic dependence on τ have again been omitted. From (3.21) we see that, for Ξ_1 to be matched with $-\eta\left[\frac{\partial \chi_1^{(u)}}{\partial r}\right]_{r=1}$, we must have

$$K(\tau,\psi) = -\frac{(9\sqrt{2}-10)}{16}\cos(2\tau + \pi/4)\sin\psi + K^{*}(\psi) \qquad (3.38)$$

Also from matching we have

$$H(\psi) \equiv 0 \tag{3.39}$$

If we now apply the boundary conditions (3.4) we find

$$\left.\begin{aligned} &J_n(\psi) \equiv 0, \quad n \neq 2 \; ; \quad J_2(\psi) = -\frac{(16\sqrt{2}-15)}{32}\sin\psi \\ &K^{*}(\psi) = \frac{1}{2}\sin\psi \; ; \quad H(\tau,\psi) = \left[\frac{(16\sqrt{2}-21)}{32}\cos 2\tau - \frac{3}{16}\right]\sin\psi \end{aligned}\right\} \tag{3.40}$$

Hence

$$\begin{aligned} X_1 = \Big\{ &-\frac{\sqrt{2}}{16}\eta e^{-2\eta}\cos(2\tau - 2\eta + \pi/4) - \frac{1}{16}e^{-2\eta}\cos(2\tau - 2\eta) \\ &- \frac{\sqrt{2}}{4}\eta e^{-\eta}\cos(2\tau - \eta + \pi/4) + \frac{1}{4}e^{-\eta}\cos(2\tau - \eta) \\ &+ \frac{5}{16}\eta e^{-\sqrt{2}\eta}\cos(2\tau - \sqrt{2}\eta + \pi/4) - \frac{(16\sqrt{2}-15)}{32}e^{-\sqrt{2}\eta}\cos(2\tau - \sqrt{2}\eta) \\ &- \frac{\sqrt{2}}{4}\eta e^{-\eta}\cos(-\eta + \pi/4) + \frac{1}{4}e^{-\eta}\cos(-\eta) - \frac{1}{8}\eta e^{-2\eta} \\ &- \frac{1}{16}e^{-2\eta} - \frac{(9\sqrt{2}-10)}{16}\eta\cos(2\tau + \pi/4) + \frac{1}{2}\eta + \frac{(16\sqrt{2}-21)}{32}\cos 2\tau \\ &- \frac{3}{16}\Big\}\sin\psi + I(\psi)\eta^2 \end{aligned} \tag{3.41}$$

The coefficient $I(\psi)$ is determined from matching with $\frac{1}{2}\eta^2\left[\frac{\partial^2 \chi_o}{\partial r^2}\right]_{r=1}$ in (3.21).

From matching (3.21) with (3.26) and (3.41) we see that the boundary conditions on $\chi_1^{(s)}$ are

$$\chi_1^{(s)} = 5/8 \sin\psi, \quad -\frac{\partial \chi_1^{(s)}}{\partial r} = \frac{1}{2}\sin\psi \qquad \text{on } r = 1 \tag{3.42}$$

If $\chi_2^{(u)}$ and $\chi_2^{(s)}$ are defined in the same manner as $\chi_o^{(u)}$ and $\chi_o^{(s)}$, we find, in addition, that the boundary condition on $\chi_2^{(u)}$ is

$$\chi_2^{(u)} = \frac{(16\sqrt{2}-21)}{32} \cos 2\tau \sin\psi \qquad \text{on } r = 1 \tag{3.43}$$

The equation for $\chi_2^{(u)}$ is (from 3.27)

$$\nabla^2 \chi_2^{(u)} = 0 \tag{3.44}$$

and the only regular solution of this, satisfying (3.43), is

$$\chi_2^{(u)} = \frac{(16\sqrt{2}-21)}{32} r \cos 2\tau \sin\psi \tag{3.45}$$

The equation of $0(\beta^4)$ in the outer region yields the two equations

$$\frac{\partial}{\partial\tau}\nabla^2\chi_4 - \frac{R_s}{2r}\frac{\partial(\chi_2^{(u)}, \nabla^2\chi_o)}{\partial(r,\psi)} - \frac{R_s}{2r}\frac{\partial(\chi_1^{(u)}, \nabla^2\chi_1^{(s)})}{\partial(r,\psi)} = 0 \tag{3.46}$$

$$-\frac{1}{r}\frac{\partial(\chi_2^{(s)}, \nabla^2\chi_o)}{\partial(r,\psi)} - \frac{1}{r}\frac{\partial(\chi_o, \nabla^2\chi_2^{(s)})}{\partial(r,\psi)} - \frac{1}{r}\frac{\partial(\chi_1^{(s)}, \nabla^2\chi_1^{(s)})}{\partial(r,\psi)} = \frac{1}{R_s}\nabla^4\chi_2^{(s)} \tag{3.47}$$

The equations for w_2 and $\bar{X}_2$ in the inner region are

$$\left(\frac{\partial}{\partial\tau} - \frac{1}{2}\frac{\partial^2}{\partial\eta^2}\right)w_2 = \frac{R_s}{2}\frac{\partial\bar{X}_o}{\partial\psi}\frac{\partial w_o}{\partial\eta} - \frac{1}{2}\frac{\partial w_1}{\partial\eta} - \frac{1}{2}\eta\frac{\partial w_o}{\partial\eta} \tag{3.48}$$

$$\left(\frac{\partial}{\partial\tau} - \frac{1}{2}\frac{\partial^2}{\partial\eta^2}\right)\frac{\partial^2 X_2}{\partial\eta^2} = \frac{R_s}{2}\left\{-\frac{\partial X_0}{\partial\eta}\frac{\partial^3 X_0}{\partial\eta^2\partial\psi} + \frac{\partial X_0}{\partial\psi}\frac{\partial^3 X_0}{\partial\eta^3}\right\}$$

$$- \frac{\partial^3 X_1}{\partial\eta^3} - \eta\frac{\partial^3 X_0}{\partial\eta^3} - \frac{1}{2}\frac{\partial^2 X_0}{\partial\eta^2} + \frac{\partial^4 X_0}{\partial\eta^2\partial\psi^2}$$

$$+ \frac{\partial}{\partial\tau}\left\{\frac{\partial X_1}{\partial\eta} + \eta\frac{\partial X_0}{\partial\eta} - \frac{\partial^2 X_0}{\partial\psi^2}\right\}$$

$$- 2\left\{\frac{\partial}{\partial\eta}(w_0 w_2) + w_1\frac{\partial w_1}{\partial\eta}\right\}\sin\psi \qquad (3.49)$$

The solution of (3.48) satisfying the boundary conditions (3.4) and matching with (3.5) as $\eta \to \infty$ is found to be

$$w_2 = -\frac{3}{8}\eta^2 e^{-\eta}\sin(\tau-\eta) + \frac{\sqrt{2}}{16}\eta e^{-\eta}\cos(\tau-\eta+\pi/4)$$

$$+ R_s\left\{-\frac{1}{16}\eta^2 e^{-\eta}\sin(\tau-\eta) + \frac{1}{32}\eta e^{-\eta}\cos(\tau-\eta)\right.$$

$$+ \frac{9}{32}\eta e^{-\eta}\sin(\tau-\eta) + \frac{3}{320}e^{-3\eta}\cos(\tau-\eta)$$

$$+ \frac{1}{80}e^{-3\eta}\sin(\tau-\eta)$$

$$+ \frac{1}{12}e^{-2\eta}\sin(\tau-2\eta) - \frac{5}{64}e^{-(1+\sqrt{2})\eta}\sin[3\tau-(1+\sqrt{2})\eta]$$

$$+ \frac{5}{64}e^{-(1+\sqrt{2})\eta}\sin[\tau-(\sqrt{2}-1)\eta] + \frac{1}{192}e^{-3\eta}\sin(3\tau-3\eta)$$

$$+ \frac{1}{4}e^{-2\eta}\sin(3\tau-2\eta) - \frac{(5\sqrt{2}-9)}{64}e^{-\eta}\sin(3\tau-\eta)$$

$$\left. - \frac{(5\sqrt{2}-9)}{64}e^{-\eta}\cos(\tau+\eta) + \frac{(25\sqrt{2}-48)}{320}e^{-\eta}\cos(\tau-\eta)\right.$$

$$- \frac{167}{960} e^{-\eta} \sin(\tau - \eta)$$

$$+ \frac{(15\sqrt{2}-61)}{192} e^{-\sqrt{3}\eta} \sin(3\tau - \sqrt{3}\eta) \Big\} \cos\psi \qquad (3.50)$$

When this is substituted into (3.49), together with the expressions for w_o (3.19), X_o (3.26), w_1 (3.36) and X_1 (3.41), the equation can be solved for X_2. Owing to the labour involved only the part of $\frac{\partial X_2}{\partial \eta}$ independent of τ ($\frac{\partial X_2^{(s)}}{\partial \eta}$) has been found, this being sufficient to determine matching conditions on $\chi_2^{(s)}$.

$$\frac{\partial X_2^{(s)}}{\partial \eta} = \Big\{ \frac{1}{4}\eta^2 e^{-2\eta} + \frac{1}{32}\eta e^{-2\eta} + \frac{3}{32} e^{-2\eta} + \frac{3}{8}\eta^2 e^{-\eta} \sin\eta$$

$$- \frac{11}{16}\sqrt{2}\,\eta e^{-\eta} \cos(-\eta + \pi/4) + \frac{1}{4} e^{-\eta} \cos\eta \Big\} \sin\psi$$

$$+ R_s \Big\{ \frac{1}{64}\eta^2 e^{-2\eta} - \frac{7}{128}\eta e^{-2\eta} + \frac{497}{3,840} e^{-2\eta} + \frac{1}{5,120} e^{-4\eta}$$

$$+ \frac{215}{512} e^{-2\sqrt{2}\eta} + \frac{1}{32}\eta^2 e^{-\eta} \sin\eta + \frac{1}{64}\eta e^{-\eta} \cos\eta$$

$$- \frac{9}{64}\eta e^{-\eta} \sin\eta - \frac{83}{640} e^{-\eta} \cos\eta + \frac{167}{1,920} e^{-\eta} \sin\eta$$

$$- \frac{19}{9,600} e^{-3\eta} \cos\eta - \frac{1}{800} e^{-3\eta} \sin\eta - \frac{(5\sqrt{2}-9)}{256} e^{-2\eta} \cos 2\eta$$

$$- \frac{1}{96} e^{-2\eta} \sin 2\eta - \frac{5}{96}\sqrt{2}\, e^{-(\sqrt{2}+1)\eta} \cos(\sqrt{2}-1)\eta$$

$$+\frac{25}{384}e^{-(\sqrt{2}+1)\eta}\sin(\sqrt{2}-1)\eta-\frac{55}{4,608}\sqrt{2}\,e^{-(2+\sqrt{2})\eta}\cos(2-\sqrt{2})\eta$$

$$+\frac{25}{2,304}e^{-(2+\sqrt{2})\eta}\sin(2-\sqrt{2})\eta$$

$$-\frac{(45\sqrt{2}-50)}{512}e^{-\sqrt{2}\eta}\cos\sqrt{2}\eta\Big\}\sin 2\psi$$

$$+M(\psi)\eta^2+N(\psi)\eta+P(\psi) \qquad (3.51)$$

When we apply the boundary condition,

$$\frac{\partial \chi_2^{(s)}}{\partial \eta}=0 \qquad \text{on} \quad \eta=0 \qquad (3.52)$$

which can be deduced from (3.4), we find

$$P(\psi)=-\frac{11}{32}\sin\psi-R_s\left(\frac{13,793}{76,800}-\frac{395}{2,304}\sqrt{2}\right)\sin 2\psi \qquad (3.53)$$

The coefficients $M(\psi)$ and $N(\psi)$ are found from matching with

$$-\frac{1}{2}\eta^2\left[\frac{\partial^3\chi}{\partial r^3}_0\right]_{r=1} \quad \text{and} \quad \eta\left[\frac{\partial^2\chi}{\partial r^2}_1\right]_{r=1} \quad \text{respectively (see 3.21).}$$

From matching (3.21) with (3.41) and (3.51) we see that the boundary conditions on $\chi_2^{(s)}$ are

$$\left.\begin{aligned}\chi_2^{(s)}&=-\frac{3}{16}\sin\psi\\ -\frac{\partial\chi_2^{(s)}}{\partial r}&=-\frac{11}{32}\sin\psi-R_s\left(\frac{13,793}{76,800}-\frac{395}{2,304}\sqrt{2}\right)\sin 2\psi\end{aligned}\right\}\ \text{on } r=1 \qquad (3.54)$$

In order to evaluate the coefficients I, M and N we need to find the solution for the stream function in the outer region. In the next two chapters we study the limiting forms of this solution as $R_s \to 0$ and $R_s \to \infty$.

CHAPTER 4

THE FURTHER LIMIT $R_s \to 0$

We now look for a solution which tends to the exact solution in the further limit $R_s \to 0$.

We try, therefore, a solution to (3.28) of the form

$$\chi_o = \chi_{oo}(r,\psi) + R_s \chi_{o1}(r,\psi) + R_s^2 \chi_{o2}(r,\psi) + \ldots \tag{4.1}$$

The matching conditions (3.29) give us the following boundary conditions on the χ_{oi}

$$\left.\begin{aligned} &\chi_{oo} = 0\,; \quad \frac{\partial \chi_{oo}}{\partial r} = \frac{1}{4}\sin\psi \\ &\chi_{oi} = 0\,; \quad \frac{\partial \chi_{oi}}{\partial r} = 0\,, \quad i \geq 1 \end{aligned}\right\} \quad \text{on } r = 1 \tag{4.2}$$

If we substitute (4.1) into (3.28) and equate like powers of R_s, we find, as our equation for χ_{oo},

$$\nabla^4 \chi_{oo} = 0 \tag{4.3}$$

The solution of (4.3) which is regular and satisfies (4.2) is found to be

$$\chi_{oo} = -\frac{r}{8}(1-r^2)\sin\psi \tag{4.4}$$

The equation of $0(R_s)$ for χ_{o1} is

$$\nabla^4 \chi_{o1} = -\frac{1}{r}\,\frac{\partial(\chi_{oo}, \nabla^2 \chi_{oo})}{\partial(r,\psi)} \tag{4.5}$$

The regular solution of (4.5) which satisfies (4.2) is

$$\chi_{o1} = \frac{-r^2(1-r^2)^2 \sin 2\psi}{3072} \tag{4.6}$$

Similarly, the equation for χ_{o2} is

$$\nabla^4 \chi_{o2} = -\frac{1}{r}\frac{\partial(\chi_{oo}, \nabla^2\chi_{o1})}{\partial(r,\psi)} - \frac{1}{r}\frac{\partial(\chi_{o1}, \nabla^2\chi_{oo})}{\partial(r,\psi)} \tag{4.7}$$

and its regular solution, subject to (4.2), is

$$\chi_{o2} = -\frac{1}{1,474,560}\left\{\frac{1}{2}r(1-r^2)^2(2-7r^2+4r^4)\sin\psi + r^3(1-r^2)^3 \sin 3\psi\right\} \tag{4.8}$$

Matching, we can see from (3.21) that $I(\psi)$ in the expression for χ_1 (3.41) is equal to $\frac{1}{2}\left[\frac{\partial^2\chi_o}{\partial r^2}\right]_{r=1}$.

$$I(\psi) = \frac{3}{8}\sin\psi - \frac{R_s}{768}\sin 2\psi + \frac{R_s^2}{737,280}\sin\psi + 0(R_s^3) \tag{4.9}$$

Likewise, $M(\psi)$ in(3.51), which is equal to $-\frac{1}{2}\left[\frac{\partial^3\chi_o}{\partial r^3}\right]_{r=1}$, can be determined to $0(R_s^2)$.

$$M(\psi) = -\frac{3}{8}\sin\psi + \frac{3}{256}R_s \sin 2\psi - \frac{R_s^2}{61,440}\sin 3\psi + 0(R_s^3) \tag{4.10}$$

We adopt the same procedure for $\chi_1^{(s)}$, writing

$$\chi_1^{(s)} = \chi_{10} + R_s\chi_{11} + R_s^2\chi_{12} + \ldots \tag{4.11}$$

The matching conditions (3.42) now become

$$\left.\begin{aligned} \chi_{10} &= \frac{5}{8}\sin\psi \;;\; \frac{\partial \chi_{10}}{\partial r} = -\frac{1}{2}\sin\psi \\ \chi_{1i} &= 0 \qquad ;\; \frac{\partial \chi_{1i}}{\partial r} = 0\,, \quad i \geq 1 \end{aligned}\right\} \text{on } r = 1 \tag{4.12}$$

Substituting (4.11) into (3.33) we find, as our equation for χ_{10}

$$\nabla^4 \chi_{10} = 0 \tag{4.13}$$

The solution to (4.13), satisfying (4.12), and which is regular, is

$$\chi_{10} = \frac{r}{16}(19 - 9r^2)\sin\psi \tag{4.14}$$

The equation for χ_{11} is

$$\nabla^4 \chi_{11} = -\frac{1}{r}\frac{\partial(\chi_{10},\, \nabla^2 \chi_{00})}{\partial(r,\psi)} - \frac{1}{r}\frac{\partial(\chi_{00},\, \nabla^2\chi_{10})}{\partial(r,\psi)} \tag{4.15}$$

whose regular solution, subject to (4.12), is

$$\chi_{11} = \frac{9}{3072} r^2 (1-r^2)^2 \sin 2\psi \tag{4.16}$$

The equation for χ_{12} is

$$\begin{aligned} \nabla^4 \chi_{12} = &-\frac{1}{r}\frac{\partial(\chi_{11},\, \nabla^2\chi_{00})}{\partial(r,\psi)} - \frac{1}{r}\frac{\partial(\chi_{10},\, \nabla^2\chi_{01})}{\partial(r,\psi)} \\ &- \frac{1}{r}\frac{\partial(\chi_{01},\, \nabla^2\chi_{10})}{\partial(r,\psi)} - \frac{1}{r}\frac{(\chi_{00},\, \nabla^2\chi_{11})}{(r,\psi)} \end{aligned} \tag{4.17}$$

and the solution satisfying (4.12) which is regular is

$$\begin{aligned} \chi_{12} = \frac{1}{3072}\Big\{ &\frac{1}{1920}(154r - 597r^3 + 840r^5 - 505r^7 \\ &+ 108r^9)\sin\psi + \frac{1}{320}(-r^3 - 7r^5 + 17r^7 - 9r^9)\sin 3\psi \Big\} \end{aligned} \tag{4.18}$$

Now $N(\psi)$ in (3.51) can be determined, it being equal to

$$\left[\frac{\partial^2 \chi_1}{\partial r^2}\right]_{r=1}$$

$$N(\psi) = -\frac{27}{8}\sin\psi + \frac{9}{384} R_s \sin 2\psi$$

$$- \frac{R_s^2}{12,288}\left(\frac{9}{20}\sin\psi + \sin 3\psi\right) + 0(R_s^3) \qquad (4.19)$$

We solve equation (3.47) in an analagous manner to that employed above, and we find

$$\chi_2^{(s)} = -\frac{r}{64}(29-17r^2)\sin\psi - \frac{49}{6,144} R_s \left\{\left(\frac{15,018}{1,225} - \frac{1,580}{147}\sqrt{2}\right)r^2 \right.$$

$$\left. + \left(-\frac{16,243}{1,225} + \frac{1,580}{147}\sqrt{2}\right)r^4 + r^6\right\} \sin 2\psi$$

$$+ 0(R_s^2) \qquad (4.20)$$

CHAPTER 5

THE FURTHER LIMIT $R_s \to \infty$

In this chapter we seek a solution to (3.28) which tends to the exact solution for χ_o in the limit $R_s \to \infty$, subject to the matching requirements (3.29).

The problem now under consideration, as described by (3.28) and (3.29) is equivalent to that of steady, two-dimensional flow inside a circle, whose 'wall' has a tangential velocity $v_w = -0.25\varkappa \varkappa(W^2/R\omega) \sin\psi$. For reasons to be discussed later, a thin boundary layer of thickness $0(aR_s^{-1/2})$ will be formed at the wall, in which the velocity of the flow is adjusted to that dictated by the flow in the interior of the circle, which we will refer to as the core. We postulate that in the limit $R_s \to \infty$ no streamlines of the motion in the core enter or leave the boundary layer, thereby causing the core to have uniform vorticity (see Batchelor (1956), Squire (1956) and Prandtl (1927)). This, however, does not determine the core flow uniquely. For instance, the core may be divided into several regions each having uniform vorticity of a strength different from that of its neighbours. As will be seen later, these regions will be separated by boundary layers because of velocity or stress discontinuities between them. We shall choose the simplest possible arrangement of two

vortices in which the vorticity of the core in the semicircle $0 < \psi < \pi$ is equal in magnitude, but of opposite sign, to that in the semicircle $\pi < \psi < 2\pi$ (see Fig. 5.1). This implies a definite velocity distribution at the edge of the core, and if this were identical to the velocity of the wall then there would be no doubt as to the correctness of this model for the core flow. In fact it will be seen that the velocity distribution at the edge of the core flow is, for the most part, quite close to a sinusoidal distribution (Fig. 5.2), and this gives us good grounds on which to argue in favour of the model, as depicted in Fig. 5.1.

Although its property of uniform vorticity is a consequence of small viscosity, the flow in the core is inviscid, and, in order for the tangential velocity at its edge to be adjusted to the velocity of the wall, a balance must be set up between the viscous and inertial terms in equation (3.~~31~~28). In order to achieve this, a thin boundary layer of thickness $0(aR_s^{-1/2})$ must be formed at the wall, and is depicted as part of the shaded region in Fig. 5.1. A boundary layer is also formed along the line of symmetry $\psi = 0, \pi$ because, when the fluid in the boundary layer at the wall, having started at $\psi = \pi$, reaches $\psi = 0$, it meets boundary layer fluid from the other semicircle. The two boundary layers impact, and must continue along the line of symmetry. They retain their boundary layer character because,

although the velocity is continuous across the line of symmetry, the vorticity is not, and Harper (1963) has shown that this itself leads to the formation of a boundary layer of thickness $0(aR_s^{-1/2})$ in which to smooth out the discontinuity.

We first solve for the flow in the core region of the upper semicircle in Fig.5.1. If we refer to the flow in the core by an overbar, the governing equation for $\bar{\chi}_o$ is

$$\nabla^2 \bar{\chi}_o = -\zeta \tag{5.1}$$

where ζ is the non-dimensional vorticity, which we may expect to be negative from the velocity distribution on the wall of the circle. The boundary condition of no flow normal to the boundary of the core is

$$\bar{\chi}_o = 0 \quad \text{on } r = 1 \quad \text{or } \psi = 0, \pi \tag{5.2}$$

The solution of (5.1) subject to (5.2), which is regular everywhere within the semicircle is

$$\bar{\chi}_o = \frac{\zeta}{2\pi} \left\{ \left[1 - \frac{1}{2}\left(r^2 + \frac{1}{r^2}\right) \cos 2\psi \right] \tan^{-1}\left(\frac{2r \sin\psi}{1 - r^2}\right) \right.$$

$$- \frac{1}{4}\left(r^2 - \frac{1}{r^2}\right) \sin 2\psi \cdot \log\left(\frac{1+2r\cos\psi + r^2}{1-2r\cos\psi + r^2}\right)$$

$$\left. + \left(r - \frac{1}{r}\right) \sin\psi - \frac{\pi}{2} r^2 (1 - \cos 2\psi) \right\} \tag{5.3}$$

The method of solution is given in detail for the elliptic pipe in Chapter 8. This gives as our flow velocity at the edge of the core

$$- \left[\frac{\partial \bar{\chi}_o}{\partial r} \right]_{r=1} = \bar{v}_1 = \frac{\zeta}{\pi} (\pi \sin^2\psi - 2 \sin\psi - \sin 2\psi . \log \tan(\psi/2)) \tag{5.4}$$

In the boundary layer adjacent to the circle wall $\frac{\partial}{\partial r} \sim O(R_s^{+1/2})$ and $\chi_o \sim O(R_s^{-1/2})$. Thus, if we retain the leading terms in (3.28) and integrate once with respect to r, we obtain the boundary layer equation

$$v \frac{\partial v}{\partial \psi} + u \frac{\partial v}{\partial r} = \bar{v}_1 \frac{d\bar{v}_1}{d\psi} + R_s^{-1} \frac{\partial^2 v}{\partial r^2} \tag{5.5}$$

The function of integration has been put equal to $\bar{v}_1 \frac{d\bar{v}_1}{d\psi}$ in the normal way, so that at the edge of the boundary layer the equation is satisfied by the core flow to first order in R_s ; this function is just the pressure gradient acting on the fluid in the boundary layer. We now linearise (5.5) in a manner analagous to that employed by Moore (1963) in his study of the stress induced boundary layer at the surface of a spherical air bubble; the subsequent analysis follows closely that of Harper and Moore (1968), who studied the flow associated with a spherical liquid drop. Moore's linearisation is, however, formally justified in the limit $R_s \to \infty$, whereas that employed here is not.

We now assume that the velocity in the boundary layer is a small perturbation of the velocity in the core and write

$$v = \bar{v} + v_p \quad , \quad u = \bar{u} + u_p \tag{5.6}$$

where a suffix p denotes a perturbation quantity. The justification for

this assumption will be discussed later. Substituting (5.6) into (5.5) and neglecting quadratic terms in the perturbation quantities, we have, as our boundary layer equation,

$$\bar{v}_1 \frac{\partial v_p}{\partial \psi} + v_p \frac{d\bar{v}_1}{d\psi} + (1-r)\frac{d\bar{v}_1}{d\psi}\frac{\partial v_p}{\partial r} = R_s^{-1}\frac{\partial^2 v_p}{\partial r^2} \qquad (5.7)$$

noting that $\bar{v} = \bar{v}_1$ and $\bar{u} = (1-r)\dfrac{d\bar{v}_1}{d\psi}$ to a boundary layer approximation. The boundary conditions can now be written as

$$\left.\begin{aligned} &v_p = v'_w - \bar{v}_1 \text{ on the circle wall} \\ &v_p \to 0 \text{ at the edge of the boundary layer} \end{aligned}\right\} \qquad (5.8)$$

where v'_w is the non-dimensional velocity of the circle wall and is equal to $-0.25 \sin\psi$. There will also be some initial condition on v_p at the start of the boundary layer.

We transform (5.7) into the diffusion equation by the use of the following transformations

$$\left.\begin{aligned} y &= -(-\zeta^{-1} R_s)^{1/2} \bar{v}_1 (1-r) \\ x &= -\zeta^{-1} \int_{\pi}^{\psi} \bar{v}_1 \, d\psi \\ \gamma &= \zeta^{-2} \bar{v}_1 v_p \end{aligned}\right\} \qquad (5.9)$$

Equation (5.7) now becomes

$$\frac{\partial \gamma}{\partial x} = \frac{\partial^2 \gamma}{\partial y^2} \qquad (5.10)$$

with the boundary conditions

$$\left.\begin{aligned} \gamma(x, 0) &= \zeta^{-2} (v'_w - \bar{v}_1) \bar{v}_1 \\ \gamma &\to 0 \quad \text{as } y \to \infty \end{aligned}\right\} \tag{5.11}$$

and some initial condition $\gamma(0, y)$ which will be discussed later. The solution of (5.10) subject to these conditions is given in Carslaw and Jaeger (1959).

$$\gamma(x, y) = \frac{1}{2(\pi x)^{1/2}} \int_0^\infty \gamma(0, y') \left\{ e^{-(y-y')^2/4x} - e^{-(y+y')^2/4x} \right\} dy'$$

$$+ \frac{2}{\sqrt{\pi}} \int_{\frac{y}{2\sqrt{x}}}^\infty \gamma(x - y^2/4\mu^2, 0)\, e^{-\mu^2}\, d\mu \tag{5.12}$$

Similarly, the boundary layer equation for the layer along the line of symmetry $\psi = 0, \pi$ can be written as

$$u \frac{\partial u}{\partial s} + v \frac{\partial u}{\partial n} = \bar{u}_1 \frac{d\bar{u}_1}{ds} + R_s^{-1} \frac{\partial^2 u}{\partial n^2} \tag{5.13}$$

where s is the non-dimensional coordinate along the line $\psi = 0, \pi$ and $s = 0$ is $\psi = 0$, and n is the non-dimensional coordinate normal to it and pointing into the semicircle. The non-dimensional velocities associated with the new coordinates are u and v. Thus u is in the direction of s increasing and v is in the direction of n increasing. The non-dimensional velocity of the flow in the core at $n = 0$ is $\bar{u}_1$ and is equal to $-\left[\frac{1}{r} \frac{\partial \bar{\chi}_o}{\partial \psi}\right]_{\psi=0}$ at $s = 1-r$, $\psi = 0$ and $\left[\frac{1}{r} \frac{\partial \bar{\chi}_o}{\partial \psi}\right]_{\psi=\pi}$ at $s = r$,

$\psi = \pi$. Using (5.6) and linearising as before, we have, as our boundary layer equation,

$$\bar{u}_1 \frac{\partial u_p}{\partial s} + u_p \frac{d\bar{u}_1}{ds} - n \frac{d\bar{u}_1}{ds} \frac{\partial u_p}{\partial n} = R_s^{-1} \frac{\partial^2 u_p}{\partial n^2} \tag{5.14}$$

The boundary conditions can be written as

$$\left.\begin{aligned} &\frac{\partial u_p}{\partial n} = -\zeta \quad \text{on } n = 0 \\ &u_p \to 0 \text{ at the edge of the boundary layer} \end{aligned}\right\} \tag{5.15}$$

and there will be some initial condition on u_p at the start of the boundary layer.

Employing the following transformations

$$\left.\begin{aligned} Y &= (-\zeta^{-1} R_s)^{1/2} \bar{u}_1 \, n \\ X &= -\zeta^{-1} \int_0^s \bar{u}_1 \, ds \\ \Gamma' &= \zeta^{-2} \bar{u}_1 \, u_p \end{aligned}\right\} \tag{5.16}$$

we again arrive at the diffusion equation

$$\frac{\partial \Gamma'}{\partial X} = \frac{\partial^2 \Gamma'}{\partial Y^2} \tag{5.17}$$

The perturbation vorticity is, to a boundary layer approximation

$$-\frac{\partial u_p}{\partial n} = +(-\zeta \, R_s)^{1/2} \, \zeta \quad \ominus \tag{5.18}$$

where $\Theta = \frac{\partial \Gamma'}{\partial Y}$, and this also satisfies the diffusion equation

$$\frac{\partial \Theta}{\partial X} = \frac{\partial^2 \Theta}{\partial Y^2} \tag{5.19}$$

This is solved subject to the boundary conditions (5.15) which become

$$\Theta = +(-\zeta R_s)^{-1/2} \quad \text{on } Y = 0$$
$$\Theta \to 0 \quad \text{as } Y \to \infty \tag{5.20}$$

and some initial condition $\Theta(0, Y)$. As before we find

$$\Theta(X, Y) = \frac{1}{2(\pi X)^{1/2}} \int_0^\infty \Theta(0, Y') \left\{ e^{-(Y-Y')^2/4X} - e^{-(Y+Y')^2/4X} \right\} dY' \tag{5.21}$$
$$+(-\zeta R_s)^{-1/2} \operatorname{erf}_c \left(\frac{Y}{2\sqrt{X}}\right)$$

We neglect the term of $0(R_s^{-1/2})$, assuming that this is much smaller than the order of magnitude of the perturbation vorticity. This is certainly true in the limit $R_s \to \infty$. If we integrate equation (5.21) with respect to Y, we obtain, after inverting the order of integration,

$$\Gamma'(X, Y) = \frac{1}{2(\pi X)^{1/2}} \int_0^\infty \Gamma'(0, Y') \left\{ e^{-(Y-Y')^2/4X} + e^{-(Y+Y')^2/4X} \right\} dY' \tag{5.22}$$

where the arbitrary function of integration has been chosen so that as $X \to 0$, $\Gamma'(X, Y) \to \Gamma'(0, Y)$. The inversion in the order of

integration is possible as the integral in (5.21) is absolutely convergent for all values of Y.

Let a suffix e denote the end of each boundary layer. Thus x_e is equivalent to $\psi = 0$ for the layer along the circle wall, and X_e is equivalent to $\psi = \pi$, $r = 1$ for the layer along the line of symmetry. Therefore, using the expressions (5.3) and (5.4), we have

$$\left.\begin{aligned} x_e &= \zeta^{-1} \int_0^{\pi} \bar{v}_1 \, d\psi = \frac{\pi}{2} - \frac{2}{\pi} \\ X_e &= -2\zeta^{-1} \int_0^{1} \frac{1}{r} \left[\frac{\partial \bar{X}_o}{\partial \psi}\right]_{\psi=\pi} dr = \frac{2}{\pi} \end{aligned}\right\} \qquad (5.23)$$

We now assume that as the corners ($r = 1$, $\psi = 0$ or π) are approached from within the boundary layers, $-v_p$ in the layer on the circle wall tends to u_p in the layer along the line of symmetry. That is, the perturbation velocity profile is convected around each corner unchanged. This assumption is discussed later. It can be shown that near the end of the boundary layer on the circle wall ($\psi \sim 0$)

$$\bar{v}_1 \sim -\frac{2\zeta}{\pi} (\psi + \psi \log(\psi/2)) \qquad (5.24)$$

and at the start of the boundary layer along the line of symmetry ($s = 1-r \sim 0$)

$$\bar{u}_1 \sim \frac{2\zeta}{\pi} (s + s \log(s/2)) \qquad (5.25)$$

Thus, in the corner, the assumption made above gives us

$$y \equiv Y$$

$$\gamma(x_e, y) \equiv \Gamma(0, Y) \tag{5.26}$$

Similarly, in the other corner we have

$$y \equiv Y$$

$$\Gamma(X_e, Y) \equiv \gamma(0, y) \tag{5.27}$$

Because of conditions (5.26) and (5.27), (5.12) and (5.22) are a pair of linked integral equations for the velocity perturbation in the boundary layer. If we consider the point x_e and substitute (5.22) into (5.12), using (5.26) and (5.27), we obtain the following integral equation for the profile of γ at x_e

$$\gamma(x_e, y) = \frac{1}{4\pi(x_e X_e)^{1/2}} \int_0^\infty \int_0^\infty \gamma(x_e, y') \left\{ e^{-(y'-y'')^2/4X_e} + e^{-(y'+y'')^2/4X_e} \right\} x$$
$$x \left\{ e^{-(y-y'')^2/4x_e} - e^{-(y+y'')^2/4x_e} \right\} dy'\, dy''$$

$$+ \frac{2}{\sqrt{\pi}} \int_{\frac{y}{2\sqrt{x_e}}}^\infty \gamma(x_e - y^2/4\mu^2, 0) e^{-\mu^2}\, d\mu \tag{5.28}$$

Integrating once with respect to y'', we obtain

$$\gamma(x_e, y) = \frac{1}{2\left[\pi(x_e + X_e)\right]^{1/2}} \int_0^\infty \gamma(x_e, y')\, e^{-\frac{y'^2}{4X_e} - \frac{y^2}{4x_e}} \times$$

$$\times \left\{ e^{\alpha^2} \operatorname{erf} \alpha - e^{\beta^2} \operatorname{erf} \beta \right\} dy' + \frac{2}{\sqrt{\pi}} \int_{\frac{y}{2\sqrt{x_e}}}^\infty \gamma(x_e - y^2/4\mu^2, 0) e^{-\mu^2} d\mu \tag{5.29}$$

where

$$\alpha = \left(\frac{y'}{4X_e} + \frac{y}{4x_e}\right)\left(\frac{4x_e X_e}{x_e + X_e}\right)^{1/2}, \quad \beta = \left(\frac{y'}{4X_e} - \frac{y}{4x_e}\right)\left(\frac{4x_e X_e}{x_e + X_e}\right)^{1/2} \tag{5.30}$$

The second integral in (5.29) may be transformed to

$$\frac{y}{2\sqrt{\pi}} \int_0^{x_e} \frac{\gamma(x, 0)\, e^{-\frac{y^2}{4(x_e - x)}}}{(x_e - x)^{3/2}}\, dx \tag{5.31}$$

and this is equal to

$$\frac{y}{2\sqrt{\pi}} \int_\pi^0 \frac{(-\zeta^{-1})\bar{v}_1\, \gamma(x(\psi), 0)}{(x_e - x(\psi))^{3/2}}\, e^{-\frac{y^2}{4(x_e - x(\psi))}}\, d\psi \tag{5.32}$$

Thus we see, from our definitions of $\gamma(x, 0)$ (5.11), x (5.9) and $\bar{v}_1$ (5.4), that we may write (5.32) as

$$\gamma_o^{\,x}(y) + \zeta^{-1}\, \gamma_1^{\,x}(y) \tag{5.33}$$

where $\gamma_o^{\varkappa}$ and $\gamma_1^{\varkappa}$ are known functions of y. Equation (5.29) may now be written as

$$\gamma(x_e, y) = \int_o^\infty \gamma(x_e, y')\, K(y, y')\, dy' + \gamma_o^{\varkappa}(y) + \zeta^{-1}\, \gamma_1^{\varkappa}(y) \qquad (5.34)$$

If we define

$$\gamma(x_e, y) = \gamma_o(y) + \zeta^{-1}\, \gamma_1(y) \qquad (5.35)$$

equation (5.34) may be written as two integral equations of the Fredholm type.

$$\gamma_i(y) = \int_o^\infty \gamma_i(y')\, K(y, y')\, dy' + \gamma_i^{\varkappa}(y), \qquad i = 0 \text{ or } 1 \qquad (5.36)$$

Equations (5.36) were solved numerically, and the computations are described in appendix B. The strength of the vorticity ζ is determined from (5.35) when we enforce the condition $\gamma(x_e, y) \to 0$ as $y \to \infty$. Thus we see from the appendix that $\zeta = -0.56$ correct to two decimal places.

We may now attempt to justify the linearisation. If we plot $-v'_w$ and $-\bar{v}_1$ against ψ as in Fig. 5.2, we see that their difference, which is a measure of the perturbation velocity, is quite small compared with $\bar{v}_1$ for a significant part of the boundary layer. Of course, the perturbation cannot be small near $\psi = 0$ or π, owing to the logarithmic dependence on $\tan(\psi/2)$ in $\bar{v}_1$ and its absence

in v'_w, but we hope that this does not alter the result significantly.

We return now to the assumption contained in (5.26) and (5.27), which we will attempt to justify using the type of analysis employed by Moore (1963), in his investigation of the flow near the rear stagnation point of a spherical bubble, and of Harper (1963), when he considered the flow near the rear stagnation point behind a bluff body. We take the full non-linear Navier-Stokes equations for flow within the circle:

$$u\frac{\partial u}{\partial r}+\frac{v}{r}\frac{\partial u}{\partial \psi}-\frac{v^2}{r}=-\frac{\partial p}{\partial r}-\frac{1}{R_s r}\frac{\partial}{\partial \psi}\left(\frac{\partial v}{\partial r}+\frac{v}{r}-\frac{1}{r}\frac{\partial u}{\partial \psi}\right) \tag{5.37}$$

$$u\frac{\partial v}{\partial r}+\frac{v}{r}\frac{\partial v}{\partial \psi}+\frac{uv}{r}=-\frac{1}{r}\frac{\partial p}{\partial \psi}+\frac{1}{R_s}\frac{\partial}{\partial r}\left(\frac{\partial v}{\partial r}+\frac{v}{r}-\frac{1}{r}\frac{\partial u}{\partial \psi}\right) \tag{5.38}$$

(c.f. equations (2.15) and (2.16)).

Here u and v are the velocity components in the r and ψ directions respectively. If we write u and v as in (5.6), and remove the terms satisfied identically by the core flow, the equations become

$$\bar{u}\frac{\partial u_p}{\partial r}+u_p\frac{\partial \bar{u}}{\partial r}+u_p\frac{\partial u_p}{\partial r}+\frac{\bar{v}}{r}\frac{\partial u_p}{\partial \psi}+\frac{v_p}{r}\frac{\partial \bar{u}}{\partial \psi}+\frac{v_p}{r}\frac{\partial u_p}{\partial \psi}$$

$$-\frac{2\bar{v}v_p}{r}-\frac{v_p^2}{r}=-\frac{\partial p_p}{\partial r}-\frac{1}{R_s r}\frac{\partial}{\partial \psi}\left(\frac{\partial v_p}{\partial r}+\frac{v_p}{r}-\frac{1}{r}\frac{\partial u_p}{\partial \psi}\right) \tag{5.39}$$

$$\bar{u}\frac{\partial v_p}{\partial r} + u_p\frac{\partial \bar{v}}{\partial r} + u_p\frac{\partial v_p}{\partial r} + \frac{\bar{v}}{r}\frac{\partial v_p}{\partial \psi} + \frac{v_p}{r}\frac{\partial \bar{v}}{\partial \psi} + \frac{v_p}{r}\frac{\partial v_p}{\partial \psi}$$

$$+ \frac{\bar{u}\,v_p}{r} + \frac{u_p\,\bar{v}}{r} + \frac{u_p\,v_p}{r} = -\frac{1}{r}\frac{\partial p_p}{\partial \psi} + \frac{1}{R_s}\frac{\partial}{\partial r}\left(\frac{\partial v_p}{\partial r} + \frac{v_p}{r} - \frac{1}{r}\frac{\partial u_p}{\partial \psi}\right) \quad (5.40)$$

where p_p is the perturbation pressure, i.e. $p = \bar{p} + p_p$.

We may now determine the behaviour of all the terms in the equations as they approach either of the corners from within the boundary layers. If we consider, in particular, the end of the boundary layer along the circle wall, then, because γ and y are $0(1)$ in the layer, we may infer from (5.4) and (5.9) that when $\psi \sim 0$

$$\left.\begin{aligned}
&\frac{\partial}{\partial r} \sim \begin{cases} (-\zeta R_s)^{1/2}\psi\log(\psi/2) \text{ for boundary layer quantities} \\ 1 \text{ for } \bar{v} \end{cases} \\
&\frac{\partial}{\partial \psi} \sim \frac{1}{\psi} \\
&\bar{v} \sim \zeta\psi\log(\psi/2) \\
&\bar{u} \sim \frac{\zeta(-\zeta R_s)^{-1/2}}{\psi} \\
&v_p \sim \frac{\zeta\Delta}{\psi\log(\psi/2)} \\
&u_p \sim \frac{\gamma(-\zeta R_s)^{-1/2}\Delta}{\psi^3(\log(\psi/2))^2}
\end{aligned}\right\} \quad (5.41)$$

where Δ is the magnitude of v_p compared with $\bar{v}$. The order of magnitude of each term in (5.39) and (5.40) is thus

$$\frac{\zeta^2(-\zeta R_s)^{-1/2}\Delta}{\psi^3\log(\psi/2)} + \frac{\zeta^2(-\zeta R_s)^{-1/2}\Delta}{\psi^3\log(\psi/2)} + \frac{\zeta^2(-\zeta R_s)^{-1/2}\Delta^2}{\psi^5(\log(\psi/2))^3} + \frac{\zeta^2(-\zeta R_s)^{-1/2}\Delta}{\psi^3\log(\psi/2)}$$

$$\frac{\zeta^2(-\zeta R_s)^{-1/2}\Delta}{\psi^3\log(\psi/2)} + \frac{\zeta^2(-\zeta R_s)^{-1/2}\Delta^2}{\psi^5(\log(\psi/2))^3} - 2\zeta^2\Delta - \frac{\zeta^2\Delta^2}{\psi^2(\log(\psi/2))^2}$$

$$= -\frac{\partial p_p}{\partial r} - \frac{1}{R_s}\left[\frac{\zeta(-\zeta R_s)^{1/2}\Delta}{\psi} + \frac{\zeta\Delta}{\psi^2\log(\psi/2)} - \frac{\zeta(-\zeta R_s)^{-1/2}}{\psi^5(\log(\psi/2))^2}\right] \quad (5.42)$$

$$\frac{\zeta^2\Delta}{\psi} + \frac{\zeta^2(-\zeta R_s)^{-1/2}\Delta}{\psi^2\log(\psi/2)} + \frac{\zeta^2\Delta^2}{\psi^3(\log(\psi/2))^2} + \frac{\zeta^2\Delta}{\psi} + \frac{\zeta^2\Delta}{\psi}$$

$$+ \frac{\zeta^2\Delta^2}{\psi^3(\log(\psi/2))^2} + \frac{\zeta^2(-\zeta R_s)^{-1/2}\Delta}{\psi^2\log(\psi/2)} + \frac{\zeta^2(-\zeta R_s)^{-1/2}\Delta}{\psi^2\log(\psi/2)} \pm \frac{\zeta^2(-\zeta R_s)^{-1/2}\Delta^2}{\psi^4(\log(\psi/2))^3}$$

$$= -\frac{1}{r}\frac{\partial p_p}{\partial\psi} + \frac{1}{R_c}\left[-\zeta^2 R_s\Delta\psi\log(\psi/2) + \zeta(-\zeta R_s)^{1/2}\Delta + \frac{\zeta\Delta}{\psi^3\log(\psi/2)}\right]$$

(5.43)

Therefore, from (5.42), we see that the perturbation pressure behaves in the following manner when $\psi \sim 0$.

$$p_p - p^{\pi} \sim 0\left[\mathrm{Max}\left(\frac{|\zeta R_s^{-1}\Delta|}{\psi^4(\log(\psi/2))^2}, \frac{|\zeta R_s^{-1}\Delta^2|}{\psi^6(\log(\psi/2))^4}, \frac{|\zeta^2(-\zeta R_s)^{-1/2}\Delta|}{|\psi\log(\psi/2)|}, \right.\right.$$

$$\left.\left.\frac{\zeta^2(-\zeta R_s)^{-1/2}\Delta^2}{|\psi^3(\log(\psi/2))^3|}\right)\right] \quad (5.44)$$

The term p^{π} is a function of ψ only, and is determined from those terms in (5.40) which do not decay to zero at the edge of the boundary

layer, e.g. $u_p \frac{\partial \bar{v}}{\partial r}$. Hence, from (5.43), we can see that our approximate equation (5.7) becomes invalid when

$$\frac{\zeta^2 \Delta}{\psi} \sim 0\left[\mathrm{Max}\left(\frac{|\zeta^2(-\zeta R_s)^{-1/2}\Delta|}{|\psi^2 \log(\psi/2)|}, \frac{\zeta^2\Delta^2}{\psi^3(\log(\psi/2))^2}, \frac{\zeta^2(-\zeta R_s)^{-1/2}\Delta^2|p_p|}{|\psi^4(\log(\psi/2))^3|}, \frac{|p_p|}{\psi}\right)\right] \tag{5.45}$$

or, in other words,

$$\psi \sim 0\left[\mathrm{Max}\left((-\zeta R_s)^{-1/4}, (-\zeta R_s)^{-1/6}|\Delta|^{1/6}, |\Delta|^{1/2}\right)\right] \tag{5.46}$$

at most.

Similarly, we find that the approximation used for the other boundary layer becomes invalid at a distance from its end of the same order of magnitude as ψ in (5.46). If $\Delta \ll 0(1)$ we find that when ψ (or the distance from the end of the boundary layer) $\ll 0(1)$, but greater than the order of magnitude given in (5.46), the viscous terms in (5.39) and (5.40) become much smaller than the inertia terms. Therefore, to a first approximation, the equations become inviscid in a region where the linearised boundary layer equation is still valid. We postulate that the equations remain inviscid as the flow turns either corner, and therefore the stream function must satisfy the equation

$$\nabla^2 \chi_o = -G(R_s^{1/2}\chi_o) - \zeta \tag{5.47}$$

where G is the perturbation vorticity and is determined by matching with the perturbation vorticity profile at the end of the boundary layer.

The coefficient $R_s^{1/2}$ is included so that $R_s^{1/2}\chi_o$ is 0(1) in the boundary layer. This phenomenon of a viscous boundary layer turning a corner inviscidly was first discussed by Stewartson (1957).

We consider, in particular, the corner r = 1, $\psi = \pi$ at the end of the boundary layer along the line of symmetry. In the region of the corner we define a new system of polar coordinates r_1, σ which are depicted in Fig. 5.3. Thus ar_1 is the actual distance from the corner, and σ is the angular coordinate measured from the bisector of the corner. When r_1 is small we may deduce from (5.3) that

$$\bar{\chi}_o \sim -\frac{\zeta}{\pi} r_1^2 \left[\frac{1}{4}\pi + \log\left(\frac{r_1}{2}\right) \cos 2\sigma + \frac{1}{2}\cos 2\sigma - \sigma \sin 2\sigma \right] \qquad (5.48)$$

In the boundary layer $\bar{\chi}_o = 0(R_s^{-1/2})$, thus for the boundary layer fluid turning the corner $r_1 = 0\left[R_s^{-1/4}(\log R_s)^{-1/2}\right]$. This leads us to define the following scaled variables of 0(1) in the boundary layer at the corner

$$r_2 = R_s^{1/4}(\log R_s)^{1/2} r_1 \quad , \quad \phi_o = R_s^{1/2} \chi_o \qquad (5.49)$$

Writing $\phi_o = \bar{\phi}_o + \phi_{op}$, expression (5.48) now becomes

$$\bar{\phi}_o \sim -\frac{\zeta}{\pi}\left\{ -\frac{1}{4} + \frac{1}{2}(\log R_s)^{-1} \log(\log R_s)^{-1} \right\} r_2^2 \cos 2\sigma$$

$$-\frac{1}{4}(\log R_s)^{-1} \frac{\zeta}{\pi} r_2^2 \left\{ \frac{1}{4}\pi + \log\left(\frac{r_2}{2}\right)\cos 2\sigma + \frac{1}{2}\cos 2\sigma - \sigma \sin 2\sigma \right\} \qquad (5.50)$$

and we see that, unless $|\log r_2| \sim 0(\log R_s)$, $\bar{\phi}_o$ is dominated by an irrotational term. Equation (5.47) can now be written as

$$\nabla_2^2 \phi_{op} = - (\log R_s)^{-1} G(\phi_o) \tag{5.51}$$

where

$$\nabla_2^2 \equiv \frac{\partial^2}{\partial r_2^2} + \frac{1}{r_2}\frac{\partial}{\partial r_2} + \frac{1}{r_2^2}\frac{\partial^2}{\partial \sigma^2} \tag{5.52}$$

Now, from (5.16) we see that $(-\zeta)^{-1/2}\,\bar{\phi}_o \equiv Y$ to a boundary layer approximation, and at the beginning of the corner G must equal the perturbation vorticity at the end of the boundary layer. This is $-(-\zeta R_s)^{1/2}\,\zeta$ Θ evaluated at the end of the layer and for large R_s this may be taken to be at $X = X_e$ (see (5.18)). Thus (5.51) may now be written as

$$\nabla_2^2 \phi_{op} = +(\log R_s)^{-1}(-\zeta R_s)^{1/2}\,\zeta \left\{ \Theta\left[X_e, (-\zeta)^{-1/2}\bar{\phi}_o\right] + (-\zeta)^{-1/2}\phi_{op}\frac{\partial \Theta}{\partial Y}\left[X_e, (-\zeta)^{-1/2}(\bar{\phi}_o + \lambda\phi_{op})\right]\right\} \tag{5.53}$$

where $0 \le \lambda \le 1$.

Furthermore, if we write (5.50) as

$\bar{\phi}_o \sim \bar{\phi}_{o1} + (\log R_s)^{-1}\,\bar{\phi}_{o2}$ then Θ in (5.46) may be expanded further to

$$\Theta\left[X_e,\ (-\zeta)^{-1/2}\bar{\phi}_o\right] = \Theta\left[X_e, -(-\zeta)^{-1/2}\bar{\phi}_{o1}\right]$$

$$\bar{\phi}\,(\log R_s)^{-1}(-\zeta)^{-1/2}\,\bar{\phi}_{o2}\frac{\partial \Theta}{\partial Y}\left[X_e, -(-\zeta)^{-1/2}(\bar{\phi}_{o1} + \xi\,(\log R_s)^{-1}\bar{\phi}_{o2})\right] \tag{5.54}$$

where $0 \le \xi \le 1$.

Clearly, for $Y \sim 0(1)$, Θ and $\frac{\partial \Theta}{\partial Y}$ are functions of the same

order of magnitude Δ . As $\phi_{op} = 0(\Delta)$ which is assumed small, a first approximation to (5.51) can be written as

$$\nabla_2^2 \phi_{op} = + (\log R_s)^{-1} (-\zeta R_s)^{1/2} \zeta \quad \Theta\left[X_e, (-\zeta)^{-1/2} \bar{\phi}_{o1} \right] \qquad (5.55)$$

Thus, to a first approximation, the perturbation vorticity is convected around the corner on the streamlines of the irrotational motion described by $\bar{\phi}_{o1}$. As $\bar{\phi}_{o1}(\sigma) = \bar{\phi}_{o1}(-\sigma)$, this means that the perturbation vorticity profile at the end of the corner is the same as that at the beginning of the corner. In other words, the perturbation vorticity profile (and hence the perturbation velocity profile) at the start of the boundary layer along the wall is the same as at the end of the boundary layer along the line of symmetry. This is precisely condition (5.27).

However, when $|\log r_2| \sim 0(\log R_s)$, (5.55) is no longer a first approximation to (5.51) as then $(\log R_s)^{-1} \bar{\phi}_{o2} \sim 0(1)$. Nevertheless, as most streamlines do not pass through the region $|\log r_2| \geq 0(\log R_s)$ we may expect this to have an insignificant effect on the result given above. Similarly, when Y is small, Θ and $\frac{\partial \Theta}{\partial Y}$ may not have the same order of magnitude. It is easy to show that

$$\lim_{Y \to 0} \left| \frac{\partial \Theta}{\partial Y} \right| \leq O\left(\lim_{Y \to o} \left| \frac{\Theta}{Y} \right| \right) \qquad (5.56)$$

and so (5.55) may not be a first approximation to (5.51) when

$$\bar{\phi}_o \sim 0\left[\text{Max} \left((\log R_s)^{-1}, |\Delta| \right) \right] \qquad (5.57)$$

However, this again does not affect most streamlines and so the result

quoted above may still be taken as a first approximation.

In addition, mention should be made of the nascent boundary layer formed within the corner region on the circle wall. We may deduce from (5.50) that the non-dimensional velocity just outside this layer is $0\left[R_s^{-1/4}(\log R_s)^{1/2}\right]$. Thus, noting that $\pi - \psi$ is $0\left[R_s^{-1/4}(\log R_s)^{-1/2}\right]$ in the corner region, we find that for viscous and inertia terms to balance in (5.5), the boundary layer thickness must be $0\left[a R_s^{-1/2}(\log R_s)^{-1/2}\right]$. As the corner region has a dimension $0\left[a R_s^{-1/4}(\log R_s)^{-1/2}\right]$ most streamlines do not pass through this layer, and so once again we are justified in taking the condition (5.27) as a first approximation.

An identical analysis to the above may be performed for the flow in the other corner and this leads to the verification of (5.26).

The argument put forward above is only valid if Δ is small. Indeed, for the linearised boundary layer equation to be valid up to the beginning of the corner, we see from (5.46) that we require $\Delta \leq 0(R_s^{-1/2})$. However a glance at Fig. 5.2 shows this to be improbable for moderately large values of R_s, and, of course, is not true in the limit $R_s \to \infty$. However, we can say that the approximations (5.26) and (5.27) should be no worse than the linearisation and, as we shall see in the next chapter, the results seem to indicate that this itself is quite good.

CHAPTER 6

DISCUSSION OF RESULTS FOR THE CIRCULAR PIPE

As can be seen from the solutions for χ_o, both for small and large values of R_s, the secondary flow in the outer region is steady in the limit $\beta \to 0$, and in the opposite sense to that predicted for a steady pressure gradient along the pipe. (see Dean (1927 and 1928), Barua (1963) and McConalogue and Srivastava (1968)). That is, the motion along the line of symmetry $\psi = 0, \pi$ is from the outer side of the pipe to the inner. The reason seems to be that 'centrifuging' generates motion which is entirely confined to the Stokes layer. The fluid is driven along the wall from the outer side of the bend to the inner under the action of the pressure gradient which, in the Stokes layer, is no longer balanced by the centrifugal force associated with the flow along the pipe; it returns centrifugally within, and at the edge of the Stokes layer only, and in so doing 'drags' the fluid in the outer region around in the manner found. A sketch of the mean first order streamlines in Fig. 6.1 makes this clear.

Let us now formally put β equal to zero. In Fig. 6.2 the secondary velocity profiles are plotted along the line $\psi = \pi/2$ in the outer region for different values of R_s. When $R_s = 0$, 100 and 200 the expansion (4.1) for χ_o is employed truncating it after the term

of $0(R_s^2)$. However, the error involved is $0(\chi_{o4} R_s^4)$ as χ_{o3} (like χ_{o1}) is identically zero along $\psi = \pi/2$. When $R_s = \infty$ the expression (5.3) for χ_o is used. As can be seen the expansion for small R_s seems to be quite convergent in practice for values of R_s up to two hundred, and, indeed, seems to describe the transition of flow from small to large values of R_s fairly well. It is, however, more instructive to plot the vorticity profiles along $\psi = \pi/2$, and this is done in Fig. 6.3. The truncated expansion used for small R_s now only seems to be convergent in practice for values of R_s up to one hundred. Nevertheless, bearing in mind that the error involved is $0(\nabla^2 \chi_{o4} R_s^4)$, the profile for $R_s = 200$ may not be without some significance. It shows clearly the development of a core of uniform vorticity as R_s increases, but perhaps indicates that the magnitude of the vorticity when $R_s \to \infty$ has been over-estimated by our crude linearisation.

In consideration of the last remark it is worth observing that if the wall of the circle in Chapter 5 moves with a velocity $\bar{v}_1$, this being the velocity at the semicircular edge of the core flow, then no boundary layer is formed at the wall of the circle, and any effect due to the vorticity discontinuity along the line of symmetry is $0(R_s^{-1/2})$ which can be neglected. If ζ is now chosen so that the average velocity at the circle wall is the same as for the problem

under consideration i.e.

$$-\frac{1}{4}\int_0^{\pi} \sin\psi\, d\psi = \int_0^{\pi} \bar{v}_1\, d\psi \qquad (6.1)$$

$$= \frac{\zeta}{\pi}\int_0^{\pi} (\pi \sin^2\psi - 2\sin\psi - \sin 2\psi \log\tan(\psi/2))d\psi$$

then we find $\zeta = -0.535$. This figure is reassuringly close to that predicted both by the linearised theory developed in Chapter 5 for large R_s and by the shape of the low R_s vorticity curve for $R_s = 200$.

In addition, a recent paper by Kuwahara and Imai (1969) is in very close agreement to the above calculations. They consider the flow in the circle when the wall moves with a velocity $V \sin\psi$, and thus their Reynolds number Va/ν is equivalent to $R_s/4$. Using an identical expansion to (4.1) of the stream function for low Reynolds number, they conclude that the radius of convergence of such an expansion for the velocity profile along $\psi = \pi/2$ is probably $R_s = 120$. In addition they perform some numerical calculations for higher values of R_s, the most significant feature of which is the confirmation of Batchelor's uniform vorticity model for the flow in the core. As well as confirming the single vortex model for flow in each semi-circle, they deduce that the value of the non-dimensional vorticity in the core for $R_s = 2048$ is $\zeta = -0.54$, and they adopt this as its probable limiting value as $R_s \to \infty$. This gives considerable support

to our value of $\zeta = -0.56$ as $R_s \to \infty$, more so when it is realised that, together with Fig. 6.3, the calculations imply that as R_s increases so does the magnitude of ζ. This gives rise to considerable confidence in the approximate theory of Chapter 5.

It is also of interest to locate the precise position of that stagnation point of the secondary flow in the outer region which represents the vortex centre (r_c, ψ_c). Using the expansion (4.1) for χ_o we find

$$\left.\begin{aligned} r_c &= \sqrt{3}/3 - \sqrt{3}\, R_s^{\,2}/1,658,880 + 0(R_s^{\,4}) \\ \psi_c &= \pi/2 - \sqrt{3}\, R_s/864 + 0(R_s^{\,3}) \end{aligned}\right\} \qquad (6.2)$$

On the other hand, as $R_s \to \infty$ the centre tends to $(0.48, \pi/2)$. Thus the vortex centre moves in the direction of the fluid motion at the semicircular edge of the vortex before inertial effects become dominant and return it to the line $\psi = \pi/2$. Similar results have been obtained by Burggraf (1966) and Kuwahara and Imai (1969).

Let us now formally put R_s equal to zero. In Fig. 6.4 the mean secondary velocity profiles are plotted along the line $\psi = \pi/2$ in the outer region, using the first three terms of the series (3.6) for the stream function. These terms are calculated in Chapter 4. The values of β used are 0.00, 0.04, 0.08 and 0.12, and in order to demonstrate that the series is still a good asymptotic representation of the velocity profile at $\beta = 0.12$, the profile calculated from

the first two terms of (3.6) is included for this value. This is important, for if we had allowed β in this theory to take any value then as $\beta \to \infty$ the Stokes layer would thicken until it occupied the whole of the interior of the pipe, and a steady state solution would then be set up with concomitant positive centrifuging. (In fact the limit $\beta \to \infty$ when R_s is small or finite would be equivalent to Dean's (1927 and 1928) solution as the Dean number K is $2W^2a^3/\nu^2R = 4R_s/\beta^2$ and this is small in Dean's theory). However, for $\beta = 0.12$ (in general $\beta > 0.11$) the mean flow given by these first three terms of the expansion (3.6), when R_s is equal to zero, is wholly from the inside to the outside on the line $\psi = \pi/2$. This shows a tendency towards the solution for the steady problem.

In addition, the profiles of the functions Γ and Ψ, described in Chapter 5 for the outer boundary layer when $R_s \to \infty$, have been calculated at various stations around the semicircle. These are plotted in Figs. 6.5a and 6.5b, and their numerical calculation is described in Appendix B.

Of more immediate interest are the implications for the cardiovascular system, and in particular the aorta. Unfortunately the data available is rather imprecise as yet, but McDonald (1960) quotes the following figures for the ascending aorta in man

$$\left.\begin{aligned} 2a &= 2.3 - 2.45 \text{ cm} \\ \text{Mean systolic velocity} &= 21.3 - 87.4 \text{ cm s}^{-1} \\ \nu &= 0.04 \text{ cm}^2 \text{ s}^{-1} \end{aligned}\right\} \qquad (6.3)$$

Thus if we take $a = 1.5$ cm and $\omega = 2\pi$ rad s^{-1} our parameter β has the value 0.08.

The mean systolic velocity is the average over time of the velocity along the artery whilst the heart is contracting; when the heart is dilating the flow in the aorta is of a much smaller magnitude owing to the closure of the valves leading to it. Thus the flow is essentially pulsatile, and if we approximate this crudely by

$$w = W (1 + \sin \omega t) \qquad (6.4)$$

we may attempt some order of magnitude analysis on the secondary flow. From (6.3) we may conveniently take W equal to 50 cm s^{-1}.

The ratio a/R is of the order of 0.2 for the human aorta and this gives rise to a Dean number $K = 2W^2a^3/R\nu^2$ of $0(10^6)$. Thus we may expect the boundary layer analysis of Barua (1963) to be relevant to this problem. This predicts that a thin boundary layer is formed on the wall of the pipe in which the pressure gradient in the cross-section, induced by centrifugal effects, is balanced by the inertial and viscous terms of the momentum equation. From equation (2.7) we see that this implies $v^2/a \sim W^2/R$ and so the secondary flow v must be $0\left[W(a/R)^{1/2}\right]$ in the boundary layer. Similarly the boundary layer thickness d must be such that $\nu v/d^2 \sim W^2/R$ and thus

d must be $0(aK^{-1/4})$ where K is the Dean number. Barua's model states that the fluid transported by the secondary flow in the boundary layer returns across the interior of the pipe in planes parallel to the plane in which the pipe is coiled. This implies that in the interior of the pipe the secondary flow is $0\left[W(a/R)^{1/2} K^{-1/4}\right]$ from continuity.

If we ignore the interaction that will take place between the secondary flows produced by the steady and oscillatory parts of (6.4), then we may deduce the order of magnitude of their ratio near the wall of the pipe to be

$$\frac{W(a/R)^{1/2}}{W^2/R\omega} = \frac{\omega a}{W}\left(\frac{R}{a}\right)^{1/2} \qquad (6.5)$$

Although, of course, the flows interact strongly, we may expect the above ratio to give an indication of which one predominates, remembering that the secondary flows are in the opposite sense to each other. For the values of W, ω, a and a/R given above the ratio is equal to 0.4, and in addition is smaller by a factor $K^{-1/4}$ in the interior of the pipe.

Thus it seems that the type of secondary flow described in this thesis may well predominate over the flow due to the steady part of the motion along the artery. Certainly there is no clear cut choice between the two and the possibility that one may cancel the other cannot be ruled out. (See Corrigenda)

CHAPTER 7

THE EXPERIMENT

The apparatus consisted of a length of clear plastic tubing bent into one loop of a circular spiral of small pitch and filled with water. A pump, which consisted of a large glass syringe, was attached to one end, and this was driven approximately in simple harmonic motion by an eccentric mounted on the shaft of an electric motor; at the other end of the pipe there was a reservoir. The apparatus is shown by Fig. 7.1 in plan view.

For an indicator dye a 5°/o aqueous solution of aramanth was used, its density being adjusted to that of water by adding a sufficient quantity of alcohol. A streak of dye was injected at A with the apparatus at rest, the streak of dye running from the bottom of the pipe to the top. This was achieved by puncture of the wall of the pipe with the needle of a syringe, which was filled with dye, followed by the drawing out of a streak; after the needle was removed the hole was patched with adhesive tape. A section at A is shown in Fig. 7.2 after the injection of dye.

The apparatus was then set in motion, and the movement of the streak observed. The results are discussed later.

The dimensions of the apparatus were as follows:

Radius of the pipe a = 0.75 cm

Radius of the spiral R = 10.0 cm

Angular frequency of pump $\omega \simeq 4\pi$ rad s^{-1}

Amplitude of pump = 0.5 cm.

Kinematic viscosity of water = 0.01 cm^2 s^{-1}.

Thus the basic parameters had the following values:

$\delta = 0.075$, $\epsilon = 0.18$, $R_s = 24$, $\beta = 0.05$.

From the magnitude of these parameters we should have expected the flow to look like the situation in Fig. 6.1. In fact only the motion in the outer region was observed clearly, but this was not surprising as the inner region was very small.

The photographs in Fig. 7.3 were taken at intervals of approximately three seconds, the camera being positioned at B and above the plane in which the pipe was coiled. It viewed the test section at an angle of approximately 45°, and so the streak of dye was inclined at a similar angle in order to obtain a clearer picture. As can be seen, in the centre of the pipe the streak of dye was observed to move towards the inside of the bend; at the top and bottom, on the other hand, it moved towards the outside, thus agreeing with the predictions for flow in the outer region.

It should be mentioned that what was observed was the path of each particle of fluid, and so we need to consider the mass-transport

velocity of particles in an oscillatory flow. Longuet-Higgins (1953) has shown that in addition to the first order secondary flow calculated in this thesis, there is a contribution to the particle velocity of the same order and whose mean is equal to

$$\overline{\left(\int^{t} \underline{w}\, dt\right) \cdot \operatorname{grad} \underline{w}} \qquad (7.1)$$

where an overbar denotes the average in time over one oscillation and $\underline{w} = (0, 0, W w_o)$ is the dimensional first order velocity vector of the flow. This can be evaluated using the expressions (3.5) and (3.19) for w_o in the interior of the pipe and in the Stokes layer respectively. We find that for small a/R (7.1) is equal to zero in the interior of the pipe and

$$\frac{W^2}{R\omega}\left(\frac{1}{2} e^{-\eta} \sin\eta \cos\psi\,,\ -\frac{1}{2} e^{-\eta} \sin\eta \sin\psi\,,\ 0\right) \qquad (7.2)$$

in the Stokes layer. Thus in the inner region or Stokes layer there is a contribution to the first order mean particle velocity which is parallel to the plane in which the pipe is coiled, and is directed from the inside to the outside of the curve in which the pipe is bent. This contribution decays to zero at the edge of the inner layer, and so its effect was not observed in the experiment.

It should also be noted that the observed flow could not have been that predicted by the present theory, as the experiment was

started from rest. However, we may see from a consideration of the momentum equation (2.1) that near the wall of the pipe, where viscous effects predominate, $\frac{\partial \underline{u}}{\partial t} \sim \nu \frac{\partial^2 \underline{u}}{\partial r^2}$ and thus the flow would have taken a time of $0(d^2/\nu)$ to diffuse a distance d. Thus the Stokes layer of thickness $0(\nu/\omega)^{1/2}$ was formed in a time of $0(\omega^{-1})$, or, in other words, after a few oscillations. This must have produced the same qualitative flow pattern in the interior as predicted in this thesis. Because R_s was small in this experiment, the diffusive process was still the mechanism for setting up the secondary flow in the interior, and this would therefore have taken a time $\tau_s \sim 0(a^2/\nu)$. The streak of dye should have traversed the pipe in a time $\tau_d \sim 0(aR\omega/W^2)$, but because $\tau_s/\tau_d = R_s = 24$ we see that the flow in the interior of the pipe could not have reached that described in Chapter 4. Nevertheless, it should have been similar qualitatively.

In addition to the above, the effect of the entry regions near the pump and reservoir should be mentioned. Intuitively we should have expected that any effect due to these regions should have only been felt at a distance from the pump or reservoir of the order of the amplitude of a fluid particle. More convincingly, we postulate that near the pump or reservoir the boundary layer grew with distance along the pipe at the same rate as does the Blasius boundary

layer formed when a fluid flows over a semi-infinite flat plate. This implies that the thickness of the boundary layer was proportional to $(\nu D/W)^{1/2}$ where D was the distance measured along the pipe from either the pump or reservoir (see for example Jones and Watson (1963)). We argue that the effect of the entry regions ended when the thickness of this Blasius boundary layer became equal to the thickness of the viscous shear-wave layer which exists in our theory, i.e. $(\nu D/W)^{1/2} \sim (\nu/\omega)^{1/2}$, or, in other words, $D \sim W/\omega$. This is restating our intuitive notion that any effect of the entry regions was only felt at a distance from the pump or reservoir of the order of the amplitude of a fluid particle.

CHAPTER 8

THE ELLIPTIC PIPE

1. The Inner Region

We now consider the problem when the pipe has an elliptic cross-section, and, using our knowledge of flow in a circular pipe, we can deduce the first order flow in the cross-section without recourse to the full equations of motion. We first adopt a new coordinate system as depicted in Fig. 8.1. The cylindrical coordinates r, ψ are replaced by the Cartesian coordinates x, y. The origin C is at the centre of the pipe and Cy is parallel to $0z$ and coincides with one of the principal axes of the ellipse. In addition, we let the length of this principal axis in the $0y$ direction be $2b$, and the length of the principal axis in the $0x$ direction be $2a$.

As before we apply a simple sinusoidal pressure gradient

$$-\frac{\partial}{\partial\theta}(p/\rho) = RW\omega\cos\omega t \qquad (8.1.1)$$

along the pipe, and, if viscosity is absent, we can easily deduce that the potential flow solution is

$$\left.\begin{aligned} w &= \frac{RW}{R+x}\sin\omega t \\ p/\rho &= -R\theta W\omega\cos\omega t - \frac{W^2}{2}\left[\left(\frac{R}{R+x}\right)^2 - 1\right]\sin^2\omega t \end{aligned}\right\} \qquad (8.1.2)$$

there being no secondary flow in the cross-section (c.f. (2.11)). Using our knowledge of the flow in the circular pipe, we can say that, when viscosity is present, a Stokes shear-wave layer of thickness $O(\nu/\omega)^{1/2}$ is formed on the wall of the pipe when $\beta = (\omega a^2/2\nu)^{-1/2}$ is small (assuming $b = 0(a)$). In the interior of the pipe the flow field is given to first order in β by the potential flow solution (8.1.2).

We now define the wall of the pipe in terms of the eccentric angle ψ

$$x = a\cos\psi \quad , \quad y = b\sin\psi \tag{8.1.3}$$

and introduce the inner region variable

$$\eta = \beta^{-1} n/a \tag{8.1.4}$$

where n is the inward drawn normal to the wall of the pipe (c.f. (3.1)). Furthermore, we introduce the following non-dimensional notation

$$\delta = a/R \ , \quad w' = w/W \ , \quad v' = v\Big/\frac{W^2}{R\omega}$$

$$\tau = \omega t \ , \quad p' = -\frac{1}{2\delta}\left[\frac{1}{(1+\delta\cos\psi)^2} - 1\right]\sin^2\omega t \tag{8.1.5}$$

where v is the component of the secondary flow parallel to the wall of the pipe within the Stokes layer or inner region (c.f. (2.14)).

If we now write

$$w' = w_o' + \beta w_1' + \ldots \tag{8.1.6}$$

then, by analogy with the theory for the circular pipe, the equation of motion for w_o' in the Stokes layer is easily seen to be

$$\left(\frac{\partial}{\partial \tau} - \frac{1}{2}\frac{\partial^2}{\partial \eta^2}\right) w_o' = \frac{\cos \tau}{1+\delta \cos \psi} \qquad (8.1.7)$$

c.f. (3.17).

The solution of (8.1.7) which satisfies the condition of no slip on the pipe wall and which matches with (8.1.2) as $\eta \to \infty$ is

$$w_o' = \frac{1}{1+\delta \cos \psi} \left\{ \sin \tau - e^{-\eta} \sin(\tau - \eta) \right\} \qquad (8.1.8)$$

c.f. (3.19).

We now write

$$v' = v_o' + \beta v_1' + \ldots \qquad (8.1.9)$$

and again by analogy with the circular pipe, we see that v_o' is driven solely by the pressure gradient generated by the centrifugal force due to the flow along the pipe. Thus, if as is the coordinate measured along the pipe wall in the plane of the cross-section and in the direction of ψ increasing, we may write the momentum equation for v_o' in the Stokes layer as

$$\frac{\partial v_o'}{\partial \tau} + \frac{w_o'^2 \sin \lambda}{1 + \delta \cos \psi} = -\frac{\partial p'}{\partial s} + \frac{1}{2}\frac{\partial^2 v_o'}{\partial \eta^2} \qquad (8.1.10)$$

c.f. (2.16).

The pressure p' is that defined in (~~2.14~~ 8.1.5) and λ is the angle between the tangent to the pipe wall and a line parallel to 0y at the point as on the wall. Thus the second term in (8.1.10) gives the

component of centrifugal force due to the axial flow in the s increasing direction. It is easy to show that

$$\sin\lambda = \frac{a\sin\psi}{(a^2\sin^2\psi + b^2\cos^2\psi)^{1/2}} \quad , \quad \frac{\partial}{\partial s} = \frac{a}{(a^2\sin^2\psi + b^2\cos^2\psi)^{1/2}} \frac{\partial}{\partial\psi} \tag{8.1.11}$$

and when these are substituted into (8.1.10), together with the expressions for p' and w_o', the equation becomes

$$\frac{\partial v_o'}{\partial\tau} + \frac{a\sin\psi}{(a^2\sin^2\psi + b^2\cos^2\psi)^{1/2}} \cdot \frac{[\sin\tau - e^{-\eta}\sin(\tau-\eta)]^2}{(1+\delta\cos\psi)^3}$$

$$= \frac{a\sin\psi}{(a^2\sin^2\psi + b^2\cos^2\psi)^{1/2}} \cdot \frac{\sin^2\tau}{(1+\delta\cos\psi)^3} + \frac{1}{2}\frac{\partial^2 v_o'}{\partial\eta^2} \tag{8.1.12}$$

As well as the condition of no slip on the wall of the pipe, we found from our matching arguments of Chapter 3 that v_o' must remain finite at the edge of the Stokes layer or inner region. Applying these conditions to (8.1.12) we find its solution is

$$v_o' = \frac{a\sin\psi}{(a^2\sin^2\psi + b^2\cos^2\psi)^{1/2}(1+\delta\cos\psi)^3} \left\{ -\frac{1}{4} + \frac{1}{4}e^{-2\eta} \right.$$

$$+ e^{-\eta}\sin\eta - \frac{1}{4}e^{-2\eta}\sin(2\tau - 2\eta) - e^{-\eta}\sin(2\tau - \eta)$$

$$\left. + \frac{5}{4}e^{-\sqrt{2}\eta}\sin(2\tau - \sqrt{2}\eta) \right\} \tag{8.1.13}$$

where terms of non-harmonic dependence on τ have been excluded. It is important to note that the first order solution for flow in the Stokes layer, as described by (8.1.8) and (8.1.13), has been found

without using the assumption that $\delta \ll 1$. However, as before, it is found necessary to ignore terms of $0(\delta)$ in order to proceed further with the solution.

Thus with $\delta \ll 1$ we have at the edge of the Stokes layer or inner region

$$\lim_{\eta \to \infty} v_o' = -\frac{1}{4} \frac{a \sin\psi}{(a^2 \sin^2\psi + b^2 \cos^2\psi)^{1/2}} \qquad (8.1.14)$$

and this gives rise to one of the boundary conditions imposed on the first order flow in the outer region. The other condition is just that there is no flow normal to the wall of the pipe between the inner and outer regions, this being true to first order in β for the circular pipe.

As before we may define a Reynolds number R_s associated with the secondary flow, and in the next two sections we look at the limiting forms of the first order solution in the outer region as $R_s \to 0$ and $R_s \to \infty$. We define

$$R_s = \frac{W^2}{R\omega} \cdot \frac{m}{\nu} \qquad (8.1.15)$$

where m is the semi-major axis of the ellipse and is equal to Max(a,b). From the condition (8.1.14) we may deduce that the solution is steady and that when R_s is small the streamfunction satisfies equation (3.28). When R_s is large a core of uniform vorticity is produced within which the equation (5.1) holds, and this is surrounded by the boundary layer described in Chapter 5.

2. The Limit $R_s \to 0$

We assume that the eccentricity e is small and use the method of conformal transformation as used by Segel (1961). We map the ellipse in the z plane ($z = x + iy$) on to a circle of unit radius centred on the origin in the **Z** plane. A suitable transformation is given in Kober (1952) from which the following forms may be deduced for small values of e. When b is the major axis

$$z = m\,Z\left[1 - \frac{e^2}{4}(1+Z^2) - \frac{1}{16}e^4(3 + Z^2 - 2Z^4) + 0(e^6)\right] \qquad (8.2.1)$$

and if r, Ψ are polar coordinates in the **Z** plane with $\Psi = 0$ coinciding with the real axis, the Jacobian J of the transformation is given by

$$J^{-1} = \frac{1}{m^2}\left|\frac{dz}{dZ}\right|^2 = \left[1 - \frac{e^2}{2}(1 + 3r^2\cos 2\Psi) - \frac{1}{16}e^4(5 - 9r^4 - 20r^4\cos 4\Psi) + 0(e^6)\right] \qquad (8.2.2)$$

When a is the major axis the transformation is

$$z = m\,Z\left[1 - \frac{e^2}{4}(1 - Z^2) - \frac{1}{16}e^4(3 - Z^2 - 2Z^4) + 0(e^6)\right] \qquad (8.2.3)$$

and

$$J^{-1} = \left[1 - \frac{e^2}{2}(1 - 3r^2\cos 2\Psi) - \frac{1}{16}e^4(5 - 9r^4 - 20\,r^4\cos 4\Psi) + 0(e^6)\right] \qquad (8.2.4)$$

The line element ds in these transformed coordinates is

given by

$$ds^2 = m^2 J^{-1} (dr^2 + r^2 d\Psi^2) \tag{8.2.5}$$

and hence we find that the equation of continuity (2.2) becomes

$$\frac{\partial}{\partial r}(r J^{-1/2} u) + \frac{\partial}{\partial \Psi}(J^{-1/2} v) = 0 \tag{8.2.6}$$

where $W^2 u/R\omega$ is the fluid velocity in the r increasing direction and $W^2 v/R\omega$ is the component in the Ψ increasing direction. Accordingly we introduce the stream function χ to satisfy (8.2.6)

$$u = \frac{J^{1/2}}{r}\frac{\partial \chi}{\partial \Psi}, \quad v = -J^{1/2}\frac{\partial \chi}{\partial r} \tag{8.2.7}$$

In addition, if $\underline{u}$ is the vector (u, v), we find that in these transformed coordinates

$$\begin{aligned} -\operatorname{curl} \underline{u} \equiv \nabla^2 \chi &\equiv J\left(\frac{\partial^2}{\partial r^2} + \frac{1}{r}\frac{\partial}{\partial r} + \frac{1}{r^2}\frac{\partial^2}{\partial \Psi^2}\right)\chi \\ &\equiv J\, \mathcal{D}^2 \chi \end{aligned} \tag{8.2.8}$$

and thus equation (3.28) becomes

$$\mathcal{D}^2(J\mathcal{D}^2\chi) = -\frac{R_s}{r}\frac{\partial(\chi, J\mathcal{D}^2\chi)}{\partial(r, \Psi)} \tag{8.2.9}$$

The derivation of this equation is given more fully in Chapter 10.

When b is the major axis we may deduce from (8.2.1) that

$$\sin\psi = \sin\Psi - \frac{e^2}{4}(\sin\Psi + \sin 3\Psi) + O(e^4) \tag{8.2.10}$$

and thus the velocity v at the edge of the ellipse, as given by (8.1.14), becomes in these transformed coordinates

$$v = -\frac{1}{4}\left\{ \sin\Psi - \frac{3}{8}e^2(\sin\Psi + \sin 3\Psi) + O(e^4)\right\} \qquad (8.2.11)$$

Therefore, using (8.2.7), we have

$$\frac{\partial\chi}{\partial r} = \frac{1}{4}\left\{ \sin\Psi - \frac{1}{4}e^2(\sin\Psi + 3\sin 3\Psi) + O(e^4)\right\} \quad \text{on } r=1 \qquad (8.2.12)$$

When a is the major axis we may deduce from (8.2.3) that

$$\left.\begin{aligned} \sin\psi &= \frac{a}{b}\left[\sin\Psi - \frac{e^2}{4}(\sin\Psi - \sin 3\Psi) + O(e^4)\right] \\ &= \sin\Psi + \frac{e^2}{4}(\sin\Psi + \sin 3\Psi) + O(e^4) \end{aligned}\right\} \qquad (8.2.13)$$

and thus the velocity v at the edge of the ellipse is given by

$$v = -\frac{1}{4}\left\{ \sin\Psi + \frac{3}{8}e^2(\sin\Psi + \sin 3\Psi) + O(e^4)\right\} \qquad (8.2.14)$$

Therefore we have

$$\frac{\partial\chi}{\partial r} = \frac{1}{4}\left\{ \sin\Psi - \frac{1}{4}e^2(\sin\Psi - 3\sin 3\Psi) + O(e^4)\right\} \quad \text{on } r=1 \qquad (8.2.15)$$

In addition we have the condition that u = 0 at the edge of the ellipse and so

$$\chi = 0 \quad \text{on } r = 1 \qquad (8.2.16)$$

Expressions (8.2.12), (8.2.15) and (8.2.16) are the boundary conditions to be applied in solving equation (8.2.9) (c.f. (3.29)).

We write

$$\chi = \chi_0 + e^2\chi_2 + e^4\chi_4 + \ldots \qquad (8.2.17)$$

and substituting into (8.2.9) and equating like powers of e^2 we find that, as we should expect, χ_0 must be the solution for the circular

pipe. If b is the major axis we find that the equation for χ_2 is

$$-\frac{R_s}{r}\frac{\partial(\chi_o, \mathcal{D}^2\chi_2)}{\partial(r,\Psi)} - \frac{R_s}{r}\frac{\partial(\chi_2, \mathcal{D}^2\chi_o)}{\partial(r,\Psi)}$$

$$-\frac{R_s}{r}\frac{\partial(\chi_o, \frac{1}{2}(1+3r^2\cos 2\Psi)\mathcal{D}^2\chi_o)}{\partial(r,\Psi)}$$

$$= \mathcal{D}^4\chi_2 + \mathcal{D}^2\left[\frac{1}{2}(1+3r^2\cos 2\Psi)\,\mathcal{D}^2\chi_o\right] \qquad (8.2.18)$$

If we now write

$$\left.\begin{aligned}\chi_o &= \chi_{oo} + R_s\chi_{o1} + R_s^2\chi_{o2} + \dots \\ \chi_2 &= \chi_{2o} + R_s\chi_{21} + R_s^2\chi_{22} + \dots\end{aligned}\right\} \qquad (8.1.19)$$

and substitute into (8.2.18), we find, as our equation for χ_{2o}

$$\mathcal{D}^4\chi_{2o} = -\frac{1}{2}\mathcal{D}^2\left[(1+3r^2\cos 2\Psi)\,\mathcal{D}^2\chi_{oo}\right] \qquad (8.2.20)$$

From our previous work on the circular pipe we know

$$\mathcal{D}^2\chi_{oo} = r\sin\Psi \qquad (8.2.21)$$

and hence

$$\mathcal{D}^4\chi_{2o} = 6r\sin\Psi \qquad (8.2.22)$$

The boundary conditions to be satisfied are, from (8.2.12) and (8.2.16),

$$\chi_{2o} = 0\,,\quad \frac{\partial\chi_{2o}}{\partial r} = -\frac{1}{16}(\sin\Psi + 3\sin 3\Psi) \quad \text{on } r=1 \qquad (8.2.23)$$

and the only regular solution of (8.2.22) satisfying (8.2.23) is found to be

$$\chi_{2o} = \frac{1}{32}(2r - 3r^3 + r^5)\sin\Psi + \frac{3}{32}(r^3 - r^5)\sin 3\Psi \qquad (8.2.24)$$

The non-dimensional vorticity ζ of the flow is equal to $-\nabla^2\chi$ which is $-J\mathcal{D}^2\chi$ in the transformed coordinates. Therefore we have

$$\zeta = -\mathcal{D}^2\chi_o - e^2\left[\mathcal{D}^2\chi_2 + \frac{1}{2}(1+3r^2\cos 2\Psi)\,\mathcal{D}^2\chi_o\right] + O(e^4) \qquad (8.2.25)$$

and on the line $\Psi = \pi/2$, this reduces to

$$\zeta = -\left[\mathcal{D}^2\chi_o\right]_{\Psi=\pi/2} + \frac{1}{4}e^2 r(1-3r^2) + O(e^2 R_s) \qquad (8.2.26.)$$

remembering that $-\mathcal{D}^2\chi_o$ is the vorticity for the circular pipe.

Similarly, when a is the major axis, the equation for χ_{2o} is

$$\mathcal{D}^4\chi_{2o} = -\frac{1}{2}\mathcal{D}^2\left[(1-3r^2\cos 2\Psi)\,\mathcal{D}^2\chi_{oo}\right] \qquad (8.2.27)$$

with the boundary conditions

$$\chi_{2o} = 0, \quad \frac{\partial\chi_{2o}}{\partial r} = -\frac{1}{16}(\sin\Psi - 3\sin 3\Psi) \text{ on } r = 1 \qquad (8.2.28)$$

Hence we find

$$\chi_{2o} = \frac{1}{32}(r^3 - r^5)\sin\Psi - \frac{3}{32}(r^3 - r^5)\sin 3\Psi \qquad (8.2.29)$$

and the vorticity ζ is

$$\zeta = -\mathcal{D}^2\chi_o - e^2\left[\mathcal{D}^2\chi_2 + \frac{1}{2}(1-3r^2\cos 2\psi)\,\mathcal{D}^2\chi_o\right] + O(e^4) \qquad (8.2.30)$$

Hence along the line $\psi = \pi/2$ the vorticity is given by

$$\zeta = -\left[\mathcal{D}^2\chi_o\right]_{\psi=\pi/2} - \frac{3}{4}e^2 r(1-r^2) + O(e^2 R_s) \qquad (8.2.31)$$

3. The Limit $R_s \to \infty$

In order to solve for the flow in the core of uniform vorticity we can use the method of conformal transformation described in the previous section. This, however, is deferred until later as the form of the solution it gives is less suitable for computational purposes than the following. It does have the advantage though, of enabling us to obtain an explicit form for the stream function, as well as serving as a usetul check on the method given below.

Let us consider the coordinate system depicted in Fig. 8.1. Further let us assume that b is the major axis. We define elliptic coordinates ϕ, ψ such that

$$\left.\begin{aligned} &x = d\sinh\phi\cos\psi \quad , \quad y = d\cosh\phi\sin\psi \\ &0 \le \psi < 2\pi \quad , \quad 0 \le \phi \le \phi_o \end{aligned}\right\} \qquad (8.3.1)$$

and we observe that

$$a = d\sinh\phi_o, \quad b = d\cosh\phi_o \text{ and } e = \operatorname{sech}\phi_o \qquad (8.3.2)$$

The line element ds is given by

$$ds^2 = \frac{d^2}{2}(\cosh 2\phi + \cos 2\psi)(d\phi^2 + d\psi^2) \qquad (8.3.3)$$

whence we may deduce that the equation of continuity (2.2) becomes

$$\frac{\partial}{\partial\phi}\left[\frac{d}{\sqrt{2}}(\cosh 2\phi+\cos 2\psi)^{1/2}u\right] + \frac{\partial}{\partial\psi}\left[\frac{d}{\sqrt{2}}(\cosh 2\phi+\cos 2\psi)^{1/2}v\right] = 0 \qquad (8.3.4)$$

where $W^2u/R\omega$ is the velocity component in the ϕ increasing direction, and $W^2v/R\omega$ is the component in the ψ increasing direction.

We therefore define a streamfunction χ such that

$$u = \frac{\sqrt{2}b}{d(\cosh 2\phi+\cos 2\psi)^{1/2}}\frac{\partial\chi}{\partial\psi}, \quad v = \frac{-\sqrt{2}b}{d(\cosh 2\phi+\cos 2\psi)^{1/2}}\frac{\partial\chi}{\partial\phi} \qquad (8.3.5)$$

and if $\underline{u}$ is the vector (u, v), then in the core of the upper semi-ellipse we must have

$$-m^2 \operatorname{curl} \underline{u} = \nabla^2\bar{\chi} = -\zeta \qquad (8.3.6)$$

where ζ is the non-dimensional uniform vorticity of the core and an overbar refers to the flow in the core (c.f. (5.1)). The solution to (8.3.6) must satisfy the condition of no flow across the boundary of the semi-elliptic core, i.e.

$$\bar{\chi} = 0 \text{ on } \phi = \phi_o \text{ or } \psi = 0, \pi \qquad (8.3.7)$$

In these coordinates we find (8.3.6) may be written as

$$\left(\frac{\partial^2}{\partial\phi^2} + \frac{\partial^2}{\partial\psi^2}\right)\bar{\chi} = -\frac{\zeta}{2}\left(\frac{d}{b}\right)^2(\cosh 2\phi + \cos 2\psi) \qquad (8.3.8)$$

remembering that we have assumed $b = m$.

If we seek a Fourier series solution to (8. 3. 8) subject to (8. 3. 7), we find

$$\bar{\chi} = -\frac{4\Im}{\pi}\left(\frac{d}{b}\right)^2 \cosh^2\phi_o \sum_{n=o}^{\infty} \frac{\cosh(2n+1)\phi}{\cosh(2n+1)\phi_o} \cdot \frac{\sin(2n+1)\psi}{(2n-1)(2n+1)(2n+3)}$$

$$-\frac{1}{2}\left(\frac{d}{b}\right)^2 \cosh^2\phi \sin^2\psi \qquad (8.3.9)$$

From this we deduce that

$$-\left[\frac{\partial\bar{\chi}}{\partial\phi}\right]_{\phi=\phi_o} = \frac{4\Im}{\pi}\left(\frac{d}{b}\right)^2 \cosh^2\phi_o \sum_{n=o}^{\infty} \frac{\tanh(2n+1)\phi_o}{(2n-1)(2n+3)} \sin(2n+1)\psi$$

$$+\frac{1}{2}\left(\frac{d}{b}\right)^2 \sinh 2\phi_o \sin^2\psi \qquad (8.3.10)$$

We may use (8. 3. 2) to replace the ϕ_o dependence by expansions in terms of the eccentricity and further we may derive the following identity from Bromwich (1947)

$$\sum_{n=o}^{\infty} \frac{\sin(2n+1)\psi}{(2n-1)(2n+3)} \equiv -\frac{1}{2}\sin\psi - \frac{1}{4}\sin 2\psi \log\tan(\psi/2) \qquad (8.3.11)$$

$$0 < \psi < \pi$$

Hence, expanding in powers of the eccentricity, we find

$$-\left[\frac{\partial\bar{\chi}}{\partial\phi}\right]_{\phi=\phi_o} = \Im\left\{\frac{1}{\pi}(\pi\sin^2\psi - 2\sin\psi - \sin 2\psi \log\tan(\psi/2))\right.$$

$$+ e^2\left(\frac{2}{3\pi}\sin\psi - \frac{1}{2}\sin^2\psi\right) + e^4\left(\frac{1}{6\pi}\sin\psi - \frac{1}{8}\sin^2\psi\right)$$

$$\left. + O(e^6)\right\} \qquad (8.3.12)$$

Therefore the velocity $\bar{v}_1$ at the edge of the core flow is, from (8. 3. 5)

$$\bar{v}_1 = \tau\left\{\frac{1}{\pi}(\pi \sin^2\psi - 2\sin\psi - \sin 2\psi \log\tan(\psi/2))\right.$$

$$+ e^2\left(\frac{2}{3\pi}\sin\psi - \frac{1}{\pi}\sin^3\psi - \frac{1}{2}\sin^2\psi + \frac{1}{2}\sin^4\psi\right.$$

$$\left. - \frac{1}{2\pi}\sin 2\psi \sin^2\psi \log\tan(\psi/2)\right)$$

$$+ e^4\left(\frac{1}{6\pi}\sin\psi + \frac{1}{3\pi}\sin^3\psi - \frac{3}{4\pi}\sin^5\psi - \frac{1}{8}\sin^2\psi\right.$$

$$\left. - \frac{1}{4}\sin^4\psi + \frac{3}{8}\sin^6\psi - \frac{3}{8\pi}\sin 2\psi \sin^4\psi \log\tan(\psi/2)\right)$$

$$\left. + O(e^6)\right\} \qquad (8.3.13)$$

Similarly when b is the minor axis we define elliptic coordinates such that

$$x = d\cosh\phi\cos\psi\,, \quad y = d\sinh\phi\sin\psi$$

$$0 \le \psi < 2\pi\,, \qquad 0 \le \phi \le \phi_o \qquad (8.3.14)$$

and therefore

$$a = d\cosh\phi_o, \quad b = d\sinh\phi_o, \quad e = \operatorname{sech}\phi_o \qquad (8.3.15)$$

The line element in this case is given by

$$ds^2 = \frac{d^2}{2}(\cosh 2\phi - \cos 2\psi)(d\phi^2 + d\psi^2) \qquad (8.3.16)$$

and then the equation of continuity is now

$$\frac{\partial}{\partial\phi}\left[\frac{d}{\sqrt{2}}(\cosh 2\phi - \cos 2\psi)^{1/2}u\right] + \frac{\partial}{\partial\psi}\left[\frac{d}{\sqrt{2}}(\cosh 2\phi - \cos 2\psi)^{1/2}v\right] = 0 \qquad (8.3.17)$$

This leads to the following definition for the stream function χ

$$u = \frac{\sqrt{2}\,a}{d(\cosh 2\phi - \cos 2\psi)^{1/2}} \frac{\partial \chi}{\partial \psi}, \quad v = \frac{-\sqrt{2}\,a}{d(\cosh 2\phi - \cos 2\psi)^{1/2}} \frac{\partial \chi}{\partial \phi} \tag{8.3.18}$$

Thus equation (8.3.6) may now be written as

$$\left(\frac{\partial^2}{\partial \phi^2} + \frac{\partial^2}{\partial \psi^2}\right) \bar{\chi} = -\frac{\zeta}{2} \left(\frac{d}{a}\right)^2 (\cosh 2\phi - \cos 2\psi) \tag{8.3.19}$$

whose solution, subject to (8.3.7) is

$$\bar{\chi} = -\frac{4\zeta}{\pi} \left(\frac{d}{a}\right)^2 \sinh^2 \phi_o \sum_{n=0}^{\infty} \frac{\sinh(2n+1)\,\phi}{\sinh(2n+1)\,\phi_o} \cdot \frac{\sin(2n+1)\,\psi}{(2n-1)(2n+1)(2n+3)}$$

$$- \frac{1}{2} \left(\frac{d}{a}\right)^2 \sinh^2 \phi \sin^2 \psi \tag{8.3.20}$$

Hence, using (8.3.11) and (8.3.15), we find

$$-\left[\frac{\partial \bar{\chi}}{\partial \phi}\right]_{\phi=\phi_o} = \zeta \left\{ \frac{1}{\pi} (\pi \sin^2 \psi - 2 \sin \psi - \sin 2\psi \log \tan(\psi/2)) \right.$$

$$+ e^2 \left(\frac{4}{3\pi} \sin \psi - \frac{1}{2} \sin^2 \psi + \frac{1}{\pi} \sin 2\psi \log \tan(\psi/2)\right)$$

$$\left. + e^4 \left(\frac{1}{6\pi} \sin \psi - \frac{1}{8} \sin^2 \psi\right) + O(e^6) \right\} \tag{8.3.21}$$

and

$$\bar{v}_1 = \zeta \left\{ \frac{1}{\pi} (\pi \sin^2 \psi - 2 \sin \psi - \sin 2\psi \log \tan(\psi/2)) \right.$$

$$+ e^2 \left[\frac{1}{3\pi} \sin \psi + \frac{1}{\pi} \sin^3 \psi - \frac{1}{2} \sin^4 \psi \right.$$

$$\left. + \frac{1}{2\pi} (1 + \sin^2 \psi) \sin 2\psi \log \tan(\psi/2) \right]$$

$$+ e^4 \left[\frac{1}{12\pi} \sin \psi + \frac{5}{6\pi} \sin^3 \psi - \frac{3}{4\pi} \sin^5 \psi \right.$$

$$- \frac{1}{2}\sin^4\psi + \frac{3}{8}\sin^6\psi$$

$$+ \frac{1}{8\pi}(1 + 2\sin^2\psi - 3\sin^4\psi)\sin 2\psi \log\tan(\psi/2)\Big]$$

$$+ O(e^6)\Big\} \qquad (8.3.22)$$

The velocity at the edge of the outer region is given by (8.1.14). Thus, using the notation v'_w for this velocity (see Chapter 5), we have when b is the major axis

$$v'_w = -\frac{1}{4}\left\{1 - \frac{1}{2}e^2\cos^2\psi + e^4\left(\frac{3}{8}\sin^4\psi - \frac{1}{4}\sin^2\psi - \frac{1}{8}\right) + O(e^6)\right\}\sin\psi \qquad (8.3.23)$$

and when b is the minor axis

$$v'_w = -\frac{1}{4}\left\{1 + \frac{1}{2}e^2\cos^2\psi + \frac{3}{8}e^4\cos^4\psi + O(e^6)\right\}\sin\psi \qquad (8.3.24)$$

Using the first three terms of the series developed above for evaluating $\left[\frac{\partial\bar{X}}{\partial\phi}\right]_{\phi=\phi_o}$, $\bar{v}_1$ and v'_w we can solve approximately for the flow in the boundary layers when e is small in precisely the same manner as for a circular pipe.

Let ms be a coordinate measured along the periphery of the ellipse in the ψ increasing direction and at $\psi = \pi$, $s = s_e$. In addition let mn be the inward drawn normal to this periphery. If u is the non-dimensional velocity component in the n increasing direction and v is the component in the s increasing direction, then the boundary layer equation along the curved surface is

$$v\frac{\partial v}{\partial s} + u\frac{\partial v}{\partial n} = \bar{v}_1 \frac{d\bar{v}_1}{ds} + R_s^{-1}\frac{\partial^2 v}{\partial n^2} \qquad (8.3.25)$$

(c.f. 5.5)

We again linearise by putting

$$v = \bar{v} + v_p\,, \quad u = \bar{u} + u_p \qquad (8.3.26)$$

where an overbar denotes core flow and a suffix p denotes a perturbation quantity. Substituting (8.3.26) into (8.3.25) and neglecting squares of perturbation quantities we have

$$\bar{v}_1 \frac{\partial v_p}{\partial s} + v_p \frac{d\bar{v}_1}{ds} - n\frac{d\bar{v}_1}{ds}\frac{\partial v_p}{\partial n} = R_s^{-1}\frac{\partial^2 v_p}{\partial n^2} \qquad (8.3.27)$$

(c.f. 5.7).

We then employ the following transformations

$$\left.\begin{aligned} y &= -(-\zeta^{-1} R_s)^{1/2}\,\bar{v}_1\, n \\ x &= -\zeta^{-1}\int_{s_e}^{s} \bar{v}_1\, ds = \zeta^{-1}\int_{\pi}^{\psi}\left[\frac{\partial\bar{\chi}}{\partial\phi}\right]_{\phi=\phi_o} d\psi \\ \gamma &= \zeta^{-2}\,\bar{v}_1\, v_p \end{aligned}\right\} \qquad (8.3.28)$$

and this reduces equation (8.3.27) to the diffusion equation

$$\frac{\partial\gamma}{\partial x} = \frac{\partial^2\gamma}{\partial y^2} \qquad (8.3.29)$$

(c.f. (5.9) and (5.10)).

For the boundary layer along the line of symmetry $\psi = 0, \pi$

we define coordinates ms along the line and mn normal to it. In addition s = 0 is $\psi = 0$, $\phi = \phi_o$. If u is now the non-dimensional velocity component in the s increasing direction and v is the component in the n increasing direction, then the boundary layer equation is

$$u \frac{\partial u}{\partial s} + v \frac{\partial u}{\partial n} = \bar{u}_1 \frac{d\bar{u}_1}{ds} + R_s^{-1} \frac{\partial^2 u}{\partial n^2} \qquad (8.3.30)$$

where $\bar{u}_1$ is the velocity at the edge of the core (c.f. (5.13)). Using (8.3.26) and linearising, we obtain

$$\bar{u}_1 \frac{\partial u_p}{\partial s} + u_p \frac{d\bar{u}_1}{ds} - n \frac{d\bar{u}_1}{ds} \frac{\partial u_p}{\partial n} = R_s^{-1} \frac{\partial^2 u_p}{\partial n^2} \qquad (8.3.31)$$

(c.f. (5.14)).

If we employ the following transformations

$$\left.\begin{aligned} Y &= (-\zeta^{-1} R_s)^{1/2} \bar{u}_1 \, n \\ X &= -\zeta^{-1} \int_o^s \bar{u}_1 \, ds \\ \Gamma &= \zeta^{-2} \bar{u}_1 \, u_p \end{aligned}\right\} \qquad (8.3.32)$$

then (8.3.31) reduces to

$$\frac{\partial \Gamma}{\partial X} = \frac{\partial^2 \Gamma}{\partial Y^2} \qquad (8.3.33)$$

(c.f. (5.16) and (5.17)).

We may note that for the elliptic pipe

$$\left.\begin{aligned} x_e &= \mathcal{J}^{-1} \int_{\pi}^{0} \left[\frac{\partial \bar{\chi}}{\partial \phi}\right]_{\phi=\phi_o} d\psi \\ X_e &= 2\,\mathcal{J}^{-1} \int_{0}^{\phi_o} \left[\frac{\partial \bar{\chi}}{\partial \psi}\right]_{\psi=0} d\phi \end{aligned}\right\} \qquad (8.3.34)$$

and hence that if b is the major axis

$$\left.\begin{aligned} x_e &= \frac{\pi}{2} - \frac{2}{\pi} + e^2\left(\frac{4}{3\pi} - \frac{\pi}{4}\right) + e^4\left(\frac{1}{3\pi} - \frac{\pi}{16}\right) + 0(e^6) \\ X_e &= \frac{2}{\pi} - \frac{4}{3\pi}e^2 - \frac{1}{3\pi}e^4 + 0(e^6) \end{aligned}\right\} \qquad (8.3.35)$$

and if a is the major axis

$$\left.\begin{aligned} x_e &= \frac{\pi}{2} - \frac{2}{\pi} + e^2\left(\frac{2}{3\pi} - \frac{\pi}{4}\right) + e^4\left(\frac{1}{3\pi} - \frac{\pi}{16}\right) + 0(e^6) \\ X_e &= \frac{2}{\pi} - \frac{2}{3\pi}e^2 - \frac{1}{3\pi}e^4 + 0(e^6) \end{aligned}\right\} \qquad (8.3.36)$$

Neglecting terms of $0(e^6)$ in the expansions for $\left[-\frac{\partial \bar{\chi}}{\partial \phi}\right]_{\phi=\phi_o}$, $\bar{v}_1$, v'_w, x_e and X_e we proceed with the calculations in precisely the same way as in Chapter 5, but noting that (5.32) now becomes

$$\frac{y}{2\sqrt{\pi}} \int_{\pi}^{0} \frac{(-\mathcal{J}^{-1})\left[-\frac{\partial \bar{\chi}}{\partial \phi}\right]_{\phi=\phi_o} \gamma(x,(\psi),0)\, e^{\frac{-y^2}{4(x_e - x(\psi))}}}{(x_e - x(\psi))^{3/2}}\, d\psi \qquad (8.3.37)$$

The computations are described in Appendix B and the values of $\mathcal{J}$ are tabulated in Table 2. A discussion of the results and their

implications is deferred until § 8.4.

We now solve (8.3.6) by the method of conformal transformation as used in § 8.2. Although the form of $\bar{v}_1$ is less suitable for computational purposes, it does enable us to obtain an explicit form for the stream function as well as serving as a useful check on the previous work.

In the transformed coordinate system of § 8.2 equation (8.3.6) becomes

$$\left.\begin{aligned} \mathcal{D}^2\bar{\chi} &= -\,J^{-1}\zeta \\ &= -\zeta\Big\{\,1 - \tfrac{1}{2}e^2(1 \pm 3r^2\cos 2\psi) \\ &\qquad - \tfrac{1}{16}e^4(5 - 9r^4 - 20r^4\cos 4\psi) \\ &\qquad + O(e^6)\,\Big\} \end{aligned}\right\} \tag{8.3.38}$$

where the plus sign is to be taken when b is the major axis. The boundary condition (8.3.7) becomes

$$\bar{\chi} = 0 \qquad \text{on } r = 1 \text{ or } \psi = 0, \pi \tag{8.3.39}$$

If we write

$$\bar{\chi} = \bar{\chi}_o + e^2\bar{\chi}_2 + e^4\bar{\chi}_4 + \ldots \tag{8.3.40}$$

then the equation for $\bar{\chi}_o$ is

$$\mathcal{D}^2\bar{\chi}_o = -\zeta \tag{8.3.41}$$

with the boundary condition

$$\bar{\chi}_o = 0 \qquad \text{on } r = 1 \text{ or } \psi = 0, \pi \tag{8.3.42}$$

We seek a Fourier series solution to (8.3.41) subject to (8.3.42) and we find

$$\bar{\chi}_o = -\frac{4\zeta}{\pi} \sum_{n=o}^{\infty} \frac{r^{2n+1} \sin(2n+1)\psi}{(2n-1)(2n+1)(2n+3)} - \frac{\zeta r^2}{4}(1-\cos 2\psi) \tag{8.3.43}$$

In order to sum this series we make use of the following identities taken from Bromwich (1947)

$$\left.\begin{aligned} \sum_{n=o}^{\infty} \frac{r^{2n+1}\cos(2n+1)\psi}{2n+1} &\equiv \frac{1}{4}\log\left(\frac{1+2r\cos\psi+r^2}{1-2r\cos\psi+r^2}\right) \\ \sum_{n=o}^{\infty} \frac{r^{2n+1}\sin(2n+1)\psi}{(2n+1)} &\equiv \frac{1}{2}\tan^{-1}\left(\frac{2r\sin\psi}{1-r^2}\right) \end{aligned}\right\} \tag{8.3.44}$$

Then splitting each term in (8.3.43) into its partial fractions and summing, we find

$$\begin{aligned} \bar{\chi}_o = \frac{\zeta}{2\pi}\Bigg\{ & \left[1 - \frac{1}{2}\left(r^2 + \frac{1}{r^2}\right)\cos 2\psi\right] \tan^{-1}\left(\frac{2r\sin\psi}{1-r^2}\right) \\ & - \frac{1}{4}\left(r^2 - \frac{1}{r^2}\right)\sin 2\psi \cdot \log\left(\frac{1+2r\cos\psi+r^2}{1-2r\cos\psi+r^2}\right) \\ & + \left(r - \frac{1}{r}\right)\sin\psi - \frac{\pi}{2}r^2(1-\cos 2\psi)\Bigg\} \end{aligned} \tag{8.3.45}$$

(c.f. (5.3)).

If b is the major axis then the equation for $\bar{\chi}_2$ is

$$\mathcal{D}^2 \bar{\chi}_2 = \frac{\zeta}{2}(1 + 3r^2\cos 2\psi) \tag{8.3.46}$$

with the boundary condition

$$\bar{\chi}_2 = 0 \qquad \text{on } r = 1 \text{ or } \psi = 0, \pi \tag{8.3.47}$$

The solution of (8.3.46) subject to (8.3.47) is

$$\bar{\chi}_2 = \frac{8\zeta}{\pi} \sum_{n=0}^{\infty} \frac{r^{2n+1} \sin(2n+1)\psi}{(2n-3)(2n+1)(2n+5)} + \frac{\zeta r^2}{8}(1 - \cos 2\psi) + \frac{\zeta r^4}{8}(\cos 2\psi - \cos 4\psi) \tag{8.3.48}$$

which can be summed, using (8.3.44), to give

$$\bar{\chi}_2 = \frac{\zeta}{4\pi}\left\{\left[\frac{1}{2}\left(r^4 + \frac{1}{r^4}\right) - 1\right] \tan^{-1}\left(\frac{2r\sin\psi}{1-r^2}\right) + \frac{1}{4}\left(r^4 - \frac{1}{r^4}\right)\sin 4\psi \log\left(\frac{1+2r\cos\psi+r^2}{1-2r\cos\psi+r^2}\right) - \left(r^3 - \frac{1}{r^3}\right)\sin 3\psi - \frac{1}{3}\left(r - \frac{1}{r}\right)\sin\psi + \frac{\pi}{2}r^2(1 - \cos 2\psi) + \frac{\pi}{2}r^4(\cos 2\psi - \cos 4\psi)\right\} \tag{8.3.49}$$

If we write the velocity v in the ψ increasing direction as

$$v = v_1 + e^2 v_2 + e^4 v_4 + \ldots \tag{8.3.50}$$

then we may deduce from (8.2.7) that

$$v_2 = -\frac{\partial \bar{\chi}_2}{\partial r} - \frac{1}{4}(1+3r^2\cos 2\psi)\frac{\partial \bar{\chi}_0}{\partial r} \tag{8.3.51}$$

and hence that the value of v_2 at $r = 1$ is

$$[v_2]_{r=1} = \Im\left\{ \frac{14}{3\pi}\sin\Psi - \frac{5}{\pi}\sin^3\Psi - \frac{5}{2}\sin^2\Psi + \frac{5}{2}\sin^4\Psi \right.$$
$$\left. + \frac{1}{2\pi}(2-5\sin^2\Psi)\sin 2\Psi \log\tan(\Psi/2) \right\} \qquad (8.3.52)$$

When the expression (8.3.13) for $\bar{v}_1$ is written in the transformed coordinates using (8.2.10) then the term of $0(e^2)$ is found to be identical with (8.3.52) thus checking the arithmetic of the previous method.

Similarly when b is the minor axis the equation for $\bar{\chi}_2$ is

$$\mathfrak{D}^2\bar{\chi}_2 = \frac{\Im}{2}(1 - 3r^2\cos 2\Psi) \qquad (8.3.53)$$

and the solution of this, subject to (8.3.47), is found to be

$$\bar{\chi}_2 = \frac{\Im}{4\pi}\left\{ \left[-\frac{1}{2}(r^4 + \frac{1}{r^4})\cos 4\Psi + (r^2+\frac{1}{r^2})\cos 2\Psi - 1\right]\tan^{-1}\left(\frac{2r\sin\Psi}{1-r^2}\right)\right.$$
$$- \left[\frac{1}{4}(r^4 - \frac{1}{r^4})\sin 4\Psi - \frac{1}{2}(r^2 - \frac{1}{r^2})\sin 2\Psi\right]\log\left(\frac{1+2r\cos\Psi+r^2}{1-2r\cos\Psi+r^2}\right)$$
$$+ (r^3 - \frac{1}{r^3})\sin 3\Psi - \frac{5}{3}(r - \frac{1}{r})\sin\Psi$$
$$\left. + \frac{\pi}{2}r^2(1-\cos 2\Psi) - \frac{\pi}{2}r^4(\cos 2\Psi - \cos 4\Psi)\right\} \qquad (8.3.54)$$

From this it may be deduced that

$$[v_2]_{r=1} = \Im\left\{ -\frac{11}{3\pi}\sin\Psi + \frac{5}{\pi}\sin^3\Psi + 2\sin^2\Psi - \frac{5}{2}\sin^4\Psi \right.$$
$$\left. - \frac{1}{2\pi}(1 - 5\sin^2\Psi)\sin 2\Psi.\log\tan(\Psi/2)\right\} \qquad (8.3.55)$$

which again checks with the value given by the first method.

The equation for $\bar{\chi}_4$ is (regardless of which is the major axis)

$$\mathcal{D}^2 \bar{\chi}_4 = \zeta \left\{ \frac{5}{16} - \frac{9}{16} r^4 - \frac{5}{4} r^4 \cos 4\psi \right\} \qquad (8.3.56)$$

with the boundary condition

$$\bar{\chi}_4 = 0 \quad \text{on } r = 1 \text{ or } \psi = 0, \pi \qquad (8.3.57)$$

We find that the solution to (8.3.56) subject to (8.3.57) is

$$\bar{\chi}_4 = \frac{\zeta}{32\pi} \left\{ \left[-\frac{5}{2}\left(r^6 + \frac{1}{r^6}\right)\cos 6\psi + 2\left(r^4 + \frac{1}{r^4}\right)\cos 4\psi + \frac{5}{2}\left(r^2 + \frac{1}{r^2}\right)\cos 2\psi - 4 \right] \tan^{-1}\left(\frac{2r\sin\psi}{1-r^2}\right) + \left[-\frac{5}{4}\left(r^6 - \frac{1}{r^6}\right)\sin 6\psi + \left(r^4 - \frac{1}{r^4}\right)\sin 4\psi + \frac{5}{4}\left(r^2 - \frac{1}{r^2}\right)\sin 2\psi \right] \log\left(\frac{1+2r\cos\psi+r^2}{1-2r\cos\psi+r^2}\right) + 5\left(r^5 - \frac{1}{r^5}\right)\sin 5\psi - \frac{7}{3}\left(r^3 - \frac{1}{r^3}\right)\sin 3\psi - \frac{16}{3}\left(r - \frac{1}{r}\right)\sin\psi + \frac{5\pi}{2} r^2 (1 - \cos 2\psi) - \frac{\pi}{2} r^6 (1 + 4\cos 4\psi - 5\cos 6\psi) \right\} \qquad (8.3.58)$$

8.4. Conclusions

As was mentioned in Chapter 1, the reason for considering the elliptic pipe is to see whether the linearisation employed in the calculations for $R_s \to \infty$ may be more convincing. Accordingly the values of the three term expansions for the velocities $\bar{v}_1$ and v'_w are plotted in Figs. 8.2a and 8.2b for values of the eccentricity equal to 0.0, 0.3 and 0.5. The curves produced when b is the major

axis are plotted in the first diagram, and those for the case in which a is the major axis in the second. In addition the vorticity curves along the line $\Psi = \pi/2$ are shown in Figs. 8.3a and 8.3b for $R_s = 200$ and $R_s = \infty$. The expressions (8.2.26) and (8.2.31) are used for $R_s = 200$.

We see that when b is the major axis the results are inconclusive. However, when a is the major axis, we see from Fig. 8.2b that the accuracy of the linearisation should improve as the eccentricity increases. However, Fig. 8.3b implies that as the eccentricity increases the magnitudes of the vorticity for $R_s = 200$ and $R_s = \infty$ increase by similar amounts. That is, although the accuracy of the linearisation improves, the difference between the values of the vorticity in the core, given by the $R_s = 200$ and $R_s = \infty$ curves, remain about the same. This indicates that the linearisation may in fact be very good even for the case of a circular pipe. This reinforces the confidence in our linearisation evoked by the work of Kuwahara and Imai (1969).

PART II

FLOW OVER A WAVY WALL

CHAPTER 9

INTRODUCTION

In the second part of this thesis we consider the steady streaming induced by an oscillating flow over a wavy wall. We assume that far from the wall the velocity vector of the flow is parallel to the mean position of the wall and is equal to $U_\infty \cos \omega t$.

As in Part I a viscous shear-wave or Stokes layer is formed on the wall and has a thickness of $0(2\nu/\omega)^{1/2}$, where ν is the kinematic viscosity of the fluid. If α is the amplitude of the wall and K its wavenumber, then we may form the two dimensionless quantities

$$\left.\begin{aligned} a &= \alpha(2\nu/\omega)^{-1/2} = \frac{\text{amplitude of wall}}{\text{Stokes layer thickness}} \\ k &= K(2\nu/\omega)^{1/2} = \frac{\text{Stokes layer thickness}}{\text{wavelength of wall}} \end{aligned}\right\} \quad (9.1)$$

and in the following chapters we shall only consider the case when $a \ll 1$. If $a \gg 1$ and the wavelength of the wall is much greater than the amplitude of oscillation of a fluid particle far from the wall, then we may apply directly the theory of Schlichting (1932) to find the steady streaming in the Stokes layer. Outside of the Stokes layer Schlichting essentially considered only the case when a Reynolds number associated with the steady streaming was small. His work has since been

extended for large values of this Reynolds number by Riley (1965) and Stuart (1966).

For the present problem we may form the Reynolds number

$$R = \frac{U_\infty}{\nu} \left(\frac{2\nu}{\omega}\right)^{1/2} \tag{9.2}$$

and we shall find that the number kR plays an important role. Because the amplitude of oscillation of a fluid particle far from the wall is the U_∞/ω, we see that kR is

$$kR = \frac{\text{particle oscillation amplitude}}{\text{wavelength of wall}} \tag{9.3}$$

Thus $kR \ll 1$ is the condition necessary for Schlicting's theory to hold when $a \gg 1$.

In Chapter 10 the problem is formulated and, because we assume $a \ll 1$, we seek a power series solution in a, the first order solution being just that if the wall were flat. The solution of 0(a) is found to be governed by an equation which is almost identical to the Orr-Sommerfeld equation encountered in the stability theory of plane parallel flows. Thus when $kR \gg 1$ our theory relies heavily on this work, as well as on that of Brooke Benjamin (1959) who considered steady shearing flow over a wavy wall. This is described in Chapter 12. In Chapter 11 we seek a solution to the problem when $kR \ll 1$ and we develop a solution valid for all k which is similar to

that found by Rayleigh (1884) in an analogous problem. If, further, we assume that $k \ll 1$ then we recover the steady streaming predicted by Schlichting (1932). This implies that no restriction need be placed on the size of a for Schlichting's theory to hold, providing that $k \ll 1$.

As in Part I we may consider the implications of the theory for the cardiovascular system. If we use the data of Chapter 5 for the aorta, and assume that the wavelength of a disturbance on the wall is equal to its radius (1.5 cm), then we may deduce the following values for the physical constants of the problem

$$\left.\begin{aligned} &\omega = 2\pi \text{ rad s}^{-1}, \quad \kappa = 4\pi/3 \text{ cm}^{-1} \\ &\nu = 0.04 \text{ cm}^2 \text{ s}^{-1}, \quad U_\infty = 50 \text{ cm s}^{-1} \end{aligned}\right\} \tag{9.4}$$

These give rise to the following values of the nondimensional parameters

$$k = 0.47, \quad R = 141, \quad kR = 67 \tag{9.5}$$

and hence it would appear that the analysis of Chapter 12 for large kR may be of some relevance. In addition we note the value of the parameter

$$k(kR)^{1/3} = 1.92 \tag{9.6}$$

which we assume to be $0(1)$ in Chapter 12. As can be seen, this assumption is amply justified.

CHAPTER 10

FORMULATION OF THE PROBLEM

Let us consider two-dimensional viscous flow over an infinite wall, the surface of which is defined by

$$y = \alpha \cos \kappa x \tag{10.1}$$

where x, y are rectangular Cartesian coordinates. Thus the wall has a wavelength $2\pi\kappa^{-1}$ and an amplitude α (see Fig. 10.1). Writing $z = x + iy$, we consider the following conformal transformation

$$\zeta = \psi + i\phi = z - i\alpha e^{i\kappa z} \tag{10.2}$$

If α is small, the Jacobian J of this transformation is

$$J = \left| \frac{d\zeta}{dz} \right|^2 = 1 + 2\alpha\kappa e^{-\kappa y} \cos \kappa x + 0(\alpha^2) \tag{10.3}$$

and, equating real and imaginary parts, we have

$$\left.\begin{aligned} \psi &= x + \alpha e^{-\kappa y} \sin \kappa x \\ \phi &= y - \alpha e^{-\kappa y} \cos \kappa x \end{aligned}\right\} \tag{10.4}$$

Hence we obtain

$$J = 1 + 2\alpha\kappa e^{-\kappa \phi} \cos \kappa \psi + 0(\alpha^2) \tag{10.5}$$

The surface of the wall is now defined in these transformed coordinates by $\phi = 0(\alpha^2)$ and, because we shall be neglecting terms of $0(\alpha^2)$ in the following analysis, this may be replaced by $\phi = 0$.

Let $\underline{u} = (u, v)$ be the velocity vector in the transformed

coordinate system. Thus u is the component of velocity in the ψ increasing direction, and v is the component in the ϕ increasing direction. In addition let p denote pressure, ρ the density of the fluid and ν its kinematic viscosity. As in Chapter 2 the momentum equation for the flow is

$$\frac{\partial \underline{u}}{\partial t} + \text{grad}(\tfrac{1}{2}\underline{u}^2) - \underline{u} \wedge \text{curl}\, \underline{u} = -\frac{1}{\rho}\text{grad}\, p - \nu\, \text{curl curl}\, \underline{u} \qquad (10.6)$$

and the equation of continuity is

$$\text{div}\, \underline{u} = 0 \qquad (10.7)$$

Because the transformation is conformal, the line element ds in the transformed coordinates is

$$ds^2 = J^{-1}\,(d\psi^2 + d\phi^2) \qquad (10.8)$$

and so, using the well known expressions for grad, div and curl, we have

$$\begin{aligned} \text{grad} &\equiv \left(J^{1/2}\frac{\partial}{\partial \psi}, J^{1/2}\frac{\partial}{\partial \phi}\right) \\ \text{div}\, \underline{u} &= J\left[\frac{\partial}{\partial \psi}(J^{-1/2}u) + \frac{\partial}{\partial \phi}(J^{-1/2}v)\right] \qquad (10.9) \\ \text{curl}\, \underline{u} &= J\left[\frac{\partial}{\partial \psi}(J^{-1/2}v) - \frac{\partial}{\partial \phi}(J^{-1/2}u)\right]\ \underline{i} \end{aligned}$$

where $\underline{i}$ is the unit vector perpendicular to the ψ, ϕ plane.

In order to satisfy (10.7) we define a stream function χ such that

$$u = J^{1/2}\frac{\partial \chi}{\partial \phi}\ ,\quad v = -J^{1/2}\frac{\partial \chi}{\partial \psi} \qquad (10.10)$$

and so

$$\text{curl } \underline{u} = -J \mathcal{D}^2 \chi \underline{i} \tag{10.11}$$

where

$$\mathcal{D}^2 \equiv \frac{\partial^2}{\partial \psi^2} + \frac{\partial^2}{\partial \phi^2} \tag{10.12}$$

If we now eliminate the pressure p from (10.6) by taking the curl of both sides of the equation, we obtain the following equation for χ

$$\frac{\partial}{\partial t} \mathcal{D}^2 \chi - \frac{\partial(\chi, J\mathcal{D}^2\chi)}{\partial(\psi, \phi)} = \nu \mathcal{D}^2 (J \mathcal{D}^2 \chi) \tag{10.13}$$

The boundary conditions we wish to impose on the problem are the conditions of zero slip on the wall and, as y -> ∞, that of the velocity vector being prescribed to be $U_\infty \cos \omega t$ in the x direction. In the transformed coordinate system these conditions become

$$\left.\begin{aligned} &\chi = \frac{\partial \chi}{\partial \phi} = 0 \qquad \text{on } \phi = 0 \\ &\left.\begin{aligned} &\frac{\partial \chi}{\partial \phi} \to U_\infty \cos \omega t \\ &\frac{\partial \chi}{\partial \psi} \to 0 \end{aligned}\right\} \text{ as } \phi \to \infty \end{aligned}\right\} \tag{10.14}$$

In addition only harmonic dependence on ωt will be allowed.

If the wall were flat i.e. J = 1, then the solution of (10.13) subject to (10.14) would be the well known Stokes shear-wave solution

$$\chi = U_\infty \left\{ \phi \cos \omega t + \left(\frac{\nu}{\omega}\right)^{1/2} \left[e^{-\left(\frac{\omega}{2\nu}\right)^{1/2} \phi} \sin\left(\omega t - \left(\frac{\omega}{2\nu}\right)^{1/2} \phi + \pi/4\right) \right.\right.$$

$$\left.\left. \sin(\omega t + \pi/4) \right] \right\} \tag{10.15}$$

We consider here the case where the amplitude of the wave α is finite but also $\alpha << 0\ (\frac{2\nu}{\omega})^{1/2}$. In other words the amplitude of the wave is much smaller than the thickness of the Stokes layer; then we may expect (10.15) to be a first approximation to the solution. We therefore define the following non-dimensional notation

$$\left.\begin{aligned} \chi' &= \chi\left[U_\infty (\tfrac{2\nu}{\omega})^{1/2}\right]^{-1},\quad \psi' = \psi\,(\tfrac{2\nu}{\omega})^{-1/2} \\ \eta &= \phi(\tfrac{2\nu}{\omega})^{-1/2},\quad \tau = \omega t,\quad a = \alpha\,(\tfrac{2\nu}{\omega})^{-1/2} \\ k &= K\,(\tfrac{2\nu}{\omega})^{1/2},\quad R = \frac{U_\infty \sqrt{2}}{(\nu\omega)^{1/2}} \end{aligned}\right\} \qquad (10.16)$$

Equation (10.13) now becomes

$$2R^{-1}\frac{\partial}{\partial\tau}\mathcal{D}'^2\chi' - \frac{\partial(\chi', J\mathcal{D}'^2\chi')}{\partial(\psi', \eta)} = R^{-1}\mathcal{D}'^2(J\,\mathcal{D}'^2\chi') \qquad (10.17)$$

where

$$\mathcal{D}'^2 \equiv \frac{\partial^2}{\partial\psi'^2} + \frac{\partial^2}{\partial\eta^2} \text{ and } J = 1 + 2ake^{-k\eta}\cos k\psi' + 0(a^2) \qquad (10.18)$$

In addition the boundary conditions (10.14) become

$$\left.\begin{aligned} \chi' = \frac{\partial\chi'}{\partial\eta} &= 0 \quad \text{on} \quad \eta = 0 \\ \left.\begin{aligned} \frac{\partial\chi'}{\partial\eta} &\to \cos\tau \\ \frac{\partial\chi'}{\partial\psi'} &\to 0 \end{aligned}\right\} &\text{ as } \eta \to \infty \end{aligned}\right\} \qquad (10.19)$$

For reasons of simplicity the primes will now be dropped from the dimensionless quantities defined in (10.16) and (10.18) and all variables are now dimensionless unless stated otherwise.

We look for a solution to (10.17) of the form

$$\chi = \chi_o + a\,\chi_1 + a^2\,\chi_2 + \ldots \tag{10.20}$$

remembering that for this problem $a \ll 1$. Substituting (10.20) into (10.17) and equating like powers of a we have, as our equation for χ_o

$$2R^{-1}\frac{\partial}{\partial\tau}\mathcal{D}^2\chi_o - \frac{\partial(\chi_o, \mathcal{D}^2\chi_o)}{\partial(\psi, \eta)} = R^{-1}\mathcal{D}^4\chi_o \tag{10.21}$$

whose solution must satisfy the boundary conditions

$$\left.\begin{aligned} &\chi_o = \frac{\partial\chi_o}{\partial\eta} = 0 \quad \text{on} \quad \eta = 0 \\ &\left.\begin{aligned} &\frac{\partial\chi_o}{\partial\eta} \to \cos\tau \\ &\frac{\partial\chi_o}{\partial\psi} \to 0 \end{aligned}\right\} \text{as } \eta \to \infty \end{aligned}\right\} \tag{10.22}$$

As expected, this is just the Stokes shear-wave solution

$$\chi_o = \eta\cos\tau + \frac{1}{\sqrt{2}}\left[e^{-\eta}\sin(\tau - \eta + \pi/4) - \sin(\tau + \pi/4)\right] \tag{10.23}$$

The equation of 0(a) from (10.17) is

$$2R^{-1}\frac{\partial}{\partial\tau}\mathcal{D}^2\chi_1 - \frac{\partial(\chi_o, \mathcal{D}^2\chi_1)}{\partial(\psi, \eta)} - \frac{\partial(\chi_1, \mathcal{D}^2\chi_o)}{\partial(\psi, \eta)}$$

$$- \frac{\partial(\chi_o, 2ke^{-k\eta}\cos k\psi\ \mathcal{D}^2\chi_o)}{\partial(\psi, \eta)}$$

$$= R^{-1}\left\{\mathcal{D}^4\chi_1 + \mathcal{D}^2(2ke^{-k\eta}\cos k\psi\ \mathcal{D}^2\chi_o)\right\} \qquad (10.24)$$

whose solution must satisfy the boundary conditions

$$\left.\begin{aligned} &\chi_1 = \frac{\partial\chi_1}{\partial\eta} = 0 \quad \text{on} \quad \eta = 0 \\ &\left.\begin{aligned} &\frac{\partial\chi_1}{\partial\eta} \to 0 \\ &\frac{\partial\chi_1}{\partial\psi} \to 0 \end{aligned}\right\} \text{ as } \eta \to \infty \end{aligned}\right\} \qquad (10.25)$$

We define $U(\eta, \tau) = \frac{\partial\chi_o}{\partial\eta}$ i.e.

$$U(\eta, \tau) = \cos\tau - e^{-\eta}\cos(\tau - \eta) \qquad (10.26)$$

Then, following Brooke Benjamin (1959), we write

$$\chi_1 = \mathcal{R}\left\{\left[F(\eta, \tau) + U(\eta, \tau)e^{-k\eta}\right]e^{ik\psi}\right\} \qquad (10.27)$$

where $\mathcal{R}$ denotes 'real part of'. This is equivalent to writing

$$\chi = \chi_o(y, \tau) + aF(\eta, \tau) + \ldots \qquad (10.28)$$

where $\chi_o(y, \tau)$ is just the solution (10.23) with η replaced by $y(\omega/2\gamma)^{1/2}$. This is just the solution which would be valid if the wall were flat and is indicative of the fact that we are seeking

perturbations to this solution. Because of our change of coordinate system contributions from this solution arise in the higher order terms of the perturbation expansion, and this leads to our writing χ_1 in the manner shown in (10.27).

Equation (10.24) now becomes

$$\frac{2}{ikR}\frac{\partial}{\partial \tau}(F''-k^2F) + U(F''-k^2F) - U''F$$

$$= \frac{1}{ikR}(F^{iv} - 2k^2F'' + k^4F) \qquad (10.29)$$

with boundary conditions

$$\left.\begin{array}{l} F = 0, \quad F' = -U' \qquad \text{on } \eta = 0 \\ \left.\begin{array}{l} F' \to 0 \\ F \to 0 \end{array}\right\} \quad \text{as } \eta \to \infty \end{array}\right\} \qquad (10.30)$$

A prime denotes differentiation with respect to η.

Equation (10.29) is almost identical to the Orr-Sommerfeld equation which arises in the theory of stability of plane parallel flows, and when the parameter kR is large we shall make use of this theory in solving the equation.

If we write the nondimensional velocity u in the ψ direction as

$$u = u_o + au_1 + a^2u_2 + \ldots \qquad (10.31)$$

then, as a consequence of (10.10), (10.16) and (10.18), we find that

$$u_o = \frac{\partial \chi_o}{\partial \eta} \ , \ u_1 = ke^{-k\eta}\cos k\psi \frac{\partial \chi_o}{\partial \eta} + \frac{\partial \chi_1}{\partial \eta} \tag{10.32}$$

Hence, using (10.26) and (10.27), we can see that

$$u_o = U(\eta, \tau) \ , \ u_1 = \mathcal{R}\left\{ \frac{\partial F}{\partial \eta} + \frac{\partial U}{\partial \eta} e^{-k\eta} \right\} e^{ik\psi} \tag{10.33}$$

and thus the dominant steady streaming is given by

$$u_1^{(s)} = \mathcal{R} \ \frac{e^{ik\psi}}{2\pi} \int_0^{2\pi} \frac{\partial F}{\partial \eta} \, d\tau \tag{10.34}$$

In the next chapter we shall evaluate this when $kR \ll 1$, and in Chapter 12 when $kR \gg 1$.

CHAPTER 11

THE LIMIT kR -> 0

In this chapter we shall seek an asymptotic solution for $F(\eta, \tau)$ which tends to the exact solution of (10.29) in the limit $kR \to 0$. This implies that the wavelength of the wall is very much greater than the amplitude of oscillation of a fluid particle far from the wall. We therefore look for a solution of the form

$$F(\eta,\tau) = F_o(\eta, \tau) + ikR\, F_1(\eta, \tau) + \ldots \tag{11.1}$$

When this is substituted into (10.29) and like powers of ikR are equated, we obtain the following equation for F_o

$$\left[2\frac{\partial}{\partial\tau} - \left(\frac{\partial^2}{\partial\eta^2} - k^2\right)\right]\left(\frac{\partial^2}{\partial\eta^2} - k^2\right) F_o = 0 \tag{11.2}$$

In addition F_o must satisfy the following boundary conditions deduced from (10.30)

$$\left.\begin{aligned} &F_o = 0, \quad F_o' = -\sqrt{2}\cos(\tau+\pi/4) \quad \text{on} \quad \eta = 0 \\ &\left.\begin{aligned} F_o' &\to 0 \\ F_o &\to 0 \end{aligned}\right\} \text{as} \quad \eta \to \infty \end{aligned}\right\} \tag{11.3}$$

From these conditions and the form of equation (11.2), we see that we may write

$$F_o(\eta,\tau) = f_o(\eta)\, e^{i\tau} + \bar{f}_o(\eta)\, e^{-i\tau} \tag{11.4}$$

where an overbar denotes 'complex conjugate'. The equation for $f_o(\eta)$ is

$$\left[\frac{\partial^2}{\partial\eta^2} - (k^2 + 2i)\right]\left(\frac{\partial^2}{\partial\eta^2} - k^2\right) f_o = 0 \tag{11.5}$$

and its solution which allows F_o to satisfy (11.3) is

$$f_o = \frac{\sqrt{2}\, e^{i\pi/4}}{2(\sigma - k)}\left\{ e^{-\sigma\eta} - e^{-k\eta}\right\} \tag{11.6}$$

where $\sigma^2 = k^2 + 2i$ and σ has a positive real part. Therefore we have

$$F_o = \frac{\sqrt{2}}{2}\left\{\frac{e^{i\tau + i\pi/4}}{\sigma - k}\left[e^{-\sigma\eta} - e^{-k\eta}\right] + \frac{e^{-i\tau - i\pi/4}}{\bar{\sigma} - k}\left[e^{-\bar{\sigma}\eta} - e^{-k\eta}\right]\right\} \tag{11.7}$$

The equation of 0(ikR) obtained when (11.1) is substituted into (10.29) is

$$\left[2\frac{\partial}{\partial\tau} - \left(\frac{\partial^2}{\partial\eta^2} - k^2\right)\right]\left(\frac{\partial^2}{\partial\eta^2} - k^2\right)F_1 = -U(F_o'' - k^2 F_o) + U'' F_o \tag{11.8}$$

Therefore, substituting (10.26) and (11.7) into the right hand side of (11.8), we obtain

$$\left[2\frac{\partial}{\partial\tau} - \left(\frac{\partial^2}{\partial\eta^2} - k^2\right)\right]\left(\frac{\partial^2}{\partial\eta^2} - k^2\right) F_1$$

$$= -\frac{\sqrt{2}}{4}\Big\{(\sigma+k)(1-e^{-\eta(1-i)})e^{-\sigma\eta+i\pi/4}$$

$$-\frac{2i}{\sigma-k}\left(e^{-\sigma\eta} - e^{-k\eta}\right)e^{-\eta(1-i)+i\pi/4}$$

$$+ e^{2i\tau}\Big[(\sigma+k)(1-e^{-\eta(1+i)})e^{-\sigma\eta+i\pi/4}$$

$$+\frac{2i}{\sigma-k}\left(e^{-\sigma\eta} - e^{-k\eta}\right)e^{-\eta(1+i)+i\pi/4}\Big]$$

$$+ \text{complex conjugate}\Big\} \qquad (11.9)$$

The boundary conditions on F_1, deduced from (10.30), are

$$\left.\begin{aligned} &F_1 = F_1' = 0 \quad \text{on } \eta = 0 \\ &\left.\begin{aligned} F_1' &\to 0 \\ F_1 &\to 0 \end{aligned}\right\} \text{ as } \eta \to \infty \end{aligned}\right\} \qquad (11.10)$$

From (11.9) and (11.10) we may deduce that

$$F_1(\eta,\tau) = F_1^{(s)}(\eta) + F_1^{(u)}(\eta,\tau) \qquad (11.11)$$

where $F_1^{(u)}$ has zero time average. Furthermore we may write

$$\left.\begin{aligned} F_1^{(s)}(\eta) &= f_1^{(s)}(\eta) + \bar{f}_1^{(s)}(\eta) \\ F_1^{(u)}(\eta,\tau) &= f_1^{(u)}(\eta)\,e^{2i\tau} + \bar{f}_1^{(u)}(\eta)\,e^{-2i\tau} \end{aligned}\right\} \qquad (11.12)$$

where $f_1^{(s)}$ and $f_1^{(u)}$ satisfy the following equations

$$\left[\frac{d^2}{d\eta^2} - k^2\right]^2 f_1^{(s)} = \frac{\sqrt{2}}{4}\left\{(\sigma+k)(1-e^{-\eta(1-i)})e^{-\sigma\eta+i\pi/4} - \frac{2i}{\sigma-k}(e^{-\sigma\eta}-e^{-k\eta})e^{-\eta(1-i)+i\pi/4}\right\} \tag{11.13}$$

$$\left[\frac{d^2}{d\eta^2} - (k^2+4i)\right]\left[\frac{d^2}{d\eta^2} - k^2\right] f_1^{(u)} = \frac{\sqrt{2}}{4}\left\{(\sigma+k)(1-e^{-\eta(1+i)})e^{-\sigma\eta+i\pi/4} + \frac{2i}{\sigma-k}(e^{-\sigma\eta}-e^{-k\eta})e^{-\eta(1+i)+i\pi/4}\right\} \tag{11.14}$$

The solution of these equations subject to the boundary conditions (11.10) is quite straightforward, but for the sake of brevity we shall consider here only the solution to (11.13), this being the most germane to the present study.

If we write (11.13) as

$$\left[\frac{d^2}{d\eta^2} - k^2\right]^2 f_1^{(s)} = Ae^{-\sigma\eta} + Be^{-\sigma\eta-\eta(1-i)} + Ce^{-k\eta-\eta(1-i)} \tag{11.15}$$

it is easily seen that

$$f_1^{(s)} = A'e^{-\sigma\eta} + B'e^{-\sigma\eta-\eta(1-i)} + C'e^{-k\eta-\eta(1-i)} + D'e^{-k\eta} + E'\eta e^{-k\eta} \tag{11.16}$$

where

$$\left.\begin{aligned} A' &= \frac{A}{(\sigma^2-k^2)^2} = -\frac{1}{4}A, \quad B' = \frac{B}{\left[(\sigma+1-i)^2-k^2\right]^2} = \frac{i}{8\sigma^2}B \\ C' &= \frac{C}{\left[(k+1-i)^2-k^2\right]^2} = -\frac{C}{4\left[1+k(1+i)\right]^2} \\ D' &= -(A'+B'+C'), \quad E' = \sigma A'+(\sigma+1-i)B'+(k+1-i)C'+kD' \end{aligned}\right\} \tag{11.17}$$

It is more instructive to consider the form of (11.16) when k is very large or very small. We first consider the case when $k \gg 1$, i.e. the wavelength of the wall is much smaller than the thickness of the Stokes layer. It can be seen that (11.16) is exponentially small unless $\eta \leq O(1/k)$ and so we define a new scaled variable $\eta' = k\eta$. This implies that the steady streaming associated with $f_1^{(s)}$ is confined to a boundary layer whose thickness is of the order of a wavelength, and this is much smaller than the thickness of the Stokes layer. We find

$$f_1^{(s)} \sim \frac{1}{24k^4}(3\eta'^2+\eta'^3)e^{-\eta'}+\frac{\sqrt{2}i}{96k^5}(15\eta'^2+6\eta'^3+\eta'^4)e^{-\eta'+i\pi/4} + O(\frac{1}{k^6}) \tag{11.18}$$

and

$$\frac{\partial f_1^{(s)}}{\partial \eta} \sim \frac{1}{24k^3}(6\eta'-\eta'^3)e^{-\eta'}+\frac{\sqrt{2}i}{96k^4}(30\eta'+3\eta'^2-2\eta'^3-\eta'^4)e^{-\eta'+i\pi/4} + O(\frac{1}{k^5}) \tag{11.19}$$

We see from (10.34) that the dominant steady streaming when $kR \ll 1$ is given by

$$u_1^{(s)} = \mathcal{R}\left\{ikR\frac{\partial F_1^{(s)}}{\partial \eta}e^{ik\psi}\right\} \tag{11.20}$$

and, therefore, when k is large, we find from (11.12) and (11.19) that

$$u_1^{(s)} \sim -\frac{R}{12k^2}\eta'(6-\eta'^2)e^{-\eta'}\sin k\gamma r + O(\frac{R}{k^3}) \qquad (11.21)$$

This steady streaming is sketched in Fig. 11.1.

Let us now consider the case $k \ll 1$ i.e. the wavelength of the wall is much larger than the thickness of the Stokes layer. We see from (11.16) that $f_1^{(s)}$ now consists of two parts. One of these decays to zero in a length scale of the order of the thickness of the Stokes layer ($\eta \to \infty$), whilst the other decays over a much larger length scale of the order of a wavelength ($\eta' \to \infty$). Thus we may expand $f_1^{(s)}$ in powers of k in two regions: one where $\eta \sim 0(1)$ and the other where $\eta' \sim 0(1)$. These may in fact be regarded as inner and outer regions, and their solutions inner and outer solutions (c.f. Part I).

Thus when $\eta \sim 0(1)$, the solution in the Stokes layer or inner region is

$$f_1^{(s)} \sim k\left\{-\frac{1}{8}\eta e^{-\eta}\sin\eta - \frac{3}{8}e^{-\eta}\cos\eta - \frac{1}{4}e^{-\eta}\sin\eta - \frac{1}{32}e^{-2\eta} + \frac{13}{32} - \frac{3}{16}\eta\right\} + k^2\left\{\frac{1}{16}\eta^2 e^{-\eta}\sin\eta + \frac{11}{32}\eta e^{-\eta}\cos\eta + \frac{7}{32}\eta e^{-\eta}\sin\eta + \frac{11}{16}e^{-\eta}\cos\eta - \frac{1}{4}e^{-\eta}\sin\eta + \frac{1}{64}\eta e^{-2\eta} + \frac{1}{64}e^{-2\eta} - \frac{45}{64} + \frac{39}{64}\eta + \frac{3}{16}\eta^2\right\} + O(k^3) \qquad (11.22)$$

and

$$\frac{\partial f_1^{(s)}}{\partial \eta} \sim k\left\{-\frac{1}{8}\eta e^{-\eta}\cos\eta + \frac{1}{8}\eta e^{-\eta}\sin\eta + \frac{1}{8}e^{-\eta}\cos\eta + \frac{1}{2}e^{-\eta}\sin\eta + \frac{1}{16}e^{-2\eta} - \frac{3}{16}\right\} + k^2\left\{\frac{1}{16}\eta^2 e^{-\eta}\cos\eta - \frac{1}{16}\eta^2 e^{-\eta}\sin\eta - \frac{1}{8}\eta e^{-\eta}\cos\eta - \frac{7}{16}\eta e^{-\eta}\sin\eta - \frac{19}{32}e^{-\eta}\cos\eta - \frac{7}{32}e^{-\eta}\sin\eta - \frac{1}{32}\eta e^{-2\eta} - \frac{1}{64}e^{-2\eta} + \frac{39}{64} + \frac{3}{8}\eta\right\} + O(k^3) \qquad (11.23)$$

Therefore we find that

$$u_1^{(s)} \sim \frac{k^2 R}{2}\left\{\frac{1}{2}\eta e^{-\eta}\cos\eta - \frac{1}{2}\eta e^{-\eta}\sin\eta - \frac{1}{2}e^{-\eta}\cos\eta - 2e^{-\eta}\sin\eta - \frac{1}{4}e^{-2\eta} + \frac{3}{4}\right\}\sin k\psi + O(k^3 R) \qquad (11.24)$$

and it can be shown that this is identical to the steady streaming predicted by the theory of Schlichting (1932) for oscillating flow over a curved boundary. This implies that, if $k \ll 1$ and $kR \ll 1$, no restriction need be placed on the amplitude of the wave α for Schlichting's theory to hold.

When $\eta' \sim O(1)$ then we find that $f_1^{(s)}$ may be written as

$$f_1^{(s)} \sim -\frac{3}{16}\eta' e^{-\eta'} + k\left(\frac{13}{32} + \frac{65}{64}\eta'\right)e^{-\eta'} + O(k^2) \qquad (11.25)$$

and

$$\frac{\partial f_1^{(s)}}{\partial \eta} \sim -\frac{3}{16} k (1-\eta') e^{-\eta'} + k^2 \left(\frac{39}{64} - \frac{65}{64}\eta'\right) e^{-\eta'} + O(k^3) \qquad (11.26)$$

Therefore in the outer region we find that

$$u_1^{(s)} \sim \frac{3k^2 R}{8} (1 - \eta') e^{-\eta'} \sin k\psi + O(k^3 R) \qquad (11.27)$$

and so in this region the steady streaming generated within the Stokes layer decays to zero. The solution (11.27) was found by Schlicting (1932) when solving for flow in the outer region for small values of his steady streaming Reynolds number, but it is due originally to Rayleigh (1884) who studied an analogous problem. In both cases the stream function from which (11.27) is derived, satisfies the biharmonic equation with η' and ψ as independent variables.

The steady streaming predicted by (11.24) and (11.27) is sketched in Fig. 11.2 and we may observe that it is qualitatively similar to the situation for large k depicted in Fig. 11.1.

CHAPTER 12

THE LIMIT kR -> ∞

We now look for an asymptotic solution to (10.29) which tends to the exact solution in the limit kR -> ∞, i.e. the amplitude of a fluid particle oscillation far from the wall is much greater than the wavelength of the wall.

Thus when kR is large, we may expect from (10.29) that the governing equation for the flow, away from any viscous boundary layers, is

$$U(F'' - k^2F) - U''F = 0 \qquad (12.1)$$

and we will refer to this as the inviscid equation and its solutions as inviscid solutions. In stability theory equation (12.1) is often referred to as the Rayleigh equation. We may note that, unlike the similar situation in stability theory, the time variable τ appears only as a parameter in (12.1). This is because of our insistence on periodic solutions which implies that $\frac{\partial}{\partial \tau} \sim 0(1)$ and hence $\frac{2}{ikR}\frac{\partial}{\partial \tau} << 1$ in (10.29). This parametric property of τ is important, for it means that we may make extensive use of the theory of Brooke Benjamin (1959) for the steady problem.

As in stability theory (see for example Stuart (1963)) equation (12.1) has a singular point at any position $\eta = \eta_c$ where

$U = 0$ and consequently its solutions cease to be approximate solutions to the full equation (10.29) even when kR is very large. In fact we find by the method of Frobenius that the formal expansion of one of the solutions to (12.1) involves a term in $(\eta - \eta_c) \log (\eta - \eta_c)$ and so the correct form of the approximate solution is in doubt until the appropriate branch of the logarithm is decided. This ambiguity is resolved from a consideration of the full equation (10.29) in the vicinity of the critical point $\eta = \eta_c$, this necessarily taking into account the effects of viscosity. Tollmien (1929) first demonstrated that if the logarithm is expressed as $\log(\eta - \eta_c)$ when $\eta > \eta_c$, then it is to be replaced by $\log(\eta_c - \eta) - i\pi$ when $\eta < \eta_c$ providing $U_c' > 0$ (a suffix c denotes 'evaluated at $\eta = \eta_c$'). If $U_c' < 0$, then the logarithm is to be replaced by $\log(\eta_c - \eta) + i\pi$ when $\eta < \eta_c$.

In order to solve (12.1) we make the further assumption that $k \ll 1$, i.e. the wavelength of the wall is much greater than the thickness of the Stokes layer. Then, following Brooke Benjamin (1959), we find that the solution to (12.1), which is uniformly valid in η and satisfies the boundary condition (10.30) at infinity, is

$$F = A(\tau)\, U\, e^{-k\eta} \left\{ 1 + k \int_{\eta}^{\infty} \left[\left(\frac{U_\infty}{U} \right)^2 - 1 \right] d\eta + O(k^2) \right\} \qquad (12.2)$$

where U_∞ is the limit of U as $\eta \to \infty$ ($U_\infty = \cos \tau$). This solution is due originally to Lighthill (1957). Although the integral in

(12.2) is generally a second order term, near a critical point $\eta = \eta_c$ it becomes dominant and at $\eta = \eta_c$ exactly the integral is infinite. However, as $\eta \to \eta_c$ the zero in U cancels the singularity in the integral, and the whole expression gives the finite value

$$F_c = Ak \frac{U_\infty^2}{U_c'} e^{-k\eta_c} \tag{12.3}$$

if $U_c' \neq 0$. If in (12.2) there exist η_{c_i}, $i = 1, 2, \ldots, n$ such that $U_{c_i} = 0$ and $\eta < \eta_{c_1} < \eta_{c_2} < \ldots < \eta_{c_n}$, then to obtain a more explicit form of (12.2), we indent the path of integration by circuiting each singularity by a small semicircle, under the real axis if $U_{c_i}' > 0$, above if $U_{c_i}' < 0$. We find that (12.2) now becomes

$$F = AUe^{-k\eta}\left\{1 - i\pi k \sum_{i=1}^{n} \left(\frac{U_\infty}{U_{c_i}'}\right)^2 \frac{U_{c_i}''}{|U_{c_i}'|} + k\mathcal{P}\int_\eta^\infty \left[\left(\frac{U_\infty}{U}\right)^2 - 1\right] d\eta + O(k^2)\right\} \tag{12.4}$$

where $\mathcal{P}$ denotes the 'principal value' of the integral in the sense of Hadamard (1923). This principal value is clearly defined by Mangler (1952). The choice of contour is made so that the appropriate branch of the logarithm is chosen correctly on either side of $\eta = \eta_{c_i}$. If there exists a critical point $\eta = \eta_{c_m}$ where both U_{c_m} and U'_{c_m} are zero (but from (10.26) $U''_{c_m} \neq 0$), then we find that (12.4) now becomes

$$F = A\, U e^{-k\eta} \left\{ 1 - i\pi k \sum_{\substack{i=1 \\ i\neq m}}^{n} \left(\frac{U_\infty}{U'_{c_i}} \right)^2 \frac{U''_{c_i}}{\left| U'_{c_i} \right|} \right.$$

$$\pm i\pi k \; \frac{2}{3} \left(\frac{U_\infty}{U''_{c_m}} \right)^2 \left[\frac{U'''_{c_m} \, U^{iv}_{c_m}}{U''^2_{c_m}} - \frac{8}{9} \left(\frac{U'''_{c_m}}{U''_{c_m}} \right)^3 \right]$$

$$\left. + k \, \mathcal{P} \int_{\eta}^{\infty} \left[\left(\frac{U_\infty}{U} \right)^2 - 1 \right] d\eta + 0(k^2) \right\} \qquad (12.5)$$

where the plus sign is taken if the contour is indented below the singularity, the minus sign if indented above. In order to decide which of the contours to take, we would need to consider the solution of the full equation (10.29) near $\eta = \eta_{c_m}$. This is not examined here as we shall not, in fact, require the information. We note that F is singular at $\eta = \eta_{c_m}$ as the differential equation (12.1) implies.

Near $\eta = \eta_c$, and keeping τ constant, it is possible to expand (12.4) in the following Taylor series

$$F \sim A \left[(\eta - \eta_c)(U'_c + \frac{(\eta - \eta_c)^2}{2} U''_c + 0(\eta - \eta_c)^3 \right] e^{-k\eta_c}$$

$$+ Ak \frac{U_\infty^2}{U'_c} \left\{ 1 + \frac{U''_c}{U'_c} (\eta - \eta_c) \log(\eta - \eta_c) + C(\eta - \eta_c) \right.$$

$$\left. + 0\left[(\eta - \eta_c)^2 \log(\eta - \eta_c) \right] \right\} e^{-k\eta_c}$$

$$+ 0(k^2) \qquad (12.6)$$

where C depends on τ and whose evaluation depends on the behaviour of the integrand in (12.4) over the whole of the range of integration and not just locally as with the other terms. It is not evaluated here and is included solely to demonstrate the procedure whereby (12.6) is matched onto a solution valid at the critical point $\eta = \eta_c$. As mentioned before, when $\eta < \eta_c$, $\log(\eta - \eta_c)$ is replaced by $\log(\eta_c - \eta) - i\pi$ if $U_c' > 0$, and by $\log(\eta_c - \eta) + i\pi$ if $U_c' < 0$.

Following Reid (1965), we introduce the small parameter

$$\left.\begin{aligned} \varepsilon &= \left[ikR\, U_c'\right]^{-1/3} \\ \arg \varepsilon &= -\pi/6 \,, \quad U_c' > 0 \\ \arg \varepsilon &= 5\pi/6 \,, \quad U_c' < 0 \end{aligned}\right\} \qquad (12.7)$$

and introduce the new scaled variables for the neighbourhood of $\eta = \eta_c$

$$\lambda = (\eta - \eta_c)\,\varepsilon^{-1}, \quad G = F\,\varepsilon^{-1} \qquad (12.8)$$

Although there is no reason to scale F from the equation (10.29), the boundary conditions for the viscous layer on the wall (10.30) imply the scaling (12.8) so that $G \sim 0(1)$ in the layer. When these are substituted into (10.29) the singularity which is present in (12.1) no longer exists, for now the highest derivative is not lost but is of the same order as a retained non-linear term (see (12.10)). In

addition, we may notice that τ again appears only as a parameter, this being essential to the subsequent analysis, for, in deriving equations (12.10) to (12.12), we expand U as a Taylor series around $\eta = \eta_c$ keeping τ fixed. Thus the viscous effects associated with the critical points η_c are confined to thin layers of thickness $0\left[\varepsilon\,(2\nu/\omega)^{1/2}\right]$.

We expand G in the following manner

$$G = G_{oo} + (\varepsilon \log|\varepsilon|)\,G_{10} + \varepsilon\, G_{11} + 0(\varepsilon \log|\varepsilon|)^2 \qquad (12.9)$$

where the G_{ij} are functions of λ and τ. If we substitute (12.9) into (10.29), and expand U in a Taylor series around $\eta = \eta_c$ keeping τ fixed, then we obtain the following equations for the G_{ij} on equating like powers of ε etc.

$$\left(\frac{\partial^2}{\partial\lambda^2} - \lambda\right)\frac{\partial^2 G_{oo}}{\partial\lambda^2} = 0 \qquad (12.10)$$

$$\left(\frac{\partial^2}{\partial\lambda^2} - \lambda\right)\frac{\partial^2 G_{10}}{\partial\lambda^2} = 0 \qquad (12.11)$$

$$\left(\frac{\partial^2}{\partial\lambda^2} - \lambda\right)\frac{\partial^2 G_{11}}{\partial\lambda^2} = \frac{U_c''}{2U_c'}\left(\lambda^2\frac{\partial^2 G_{oo}}{\partial\lambda^2} - 2\,G_{oo}\right) \qquad (12.12)$$

We will now focus attention onto the viscous layer formed on the wall i.e. $\eta_c = 0$. This will enable us to determine the function $A(\tau)$ in (12.2) and (12.4). Therefore, in what follows, wherever a suffix c would have occurred we now use a suffix o to emphasise that

we are considering this layer. We may deduce the boundary conditions to be imposed on equations (12.10) to (12.12) from (10.30), and these are

$$\left.\begin{aligned} G_{oo} &= 0\,, \quad \frac{\partial G_{oo}}{\partial \lambda} = -U_o' \\ G_{ij} &= \frac{\partial G_{ij}}{\partial \lambda} = 0 \qquad j = 0, 1, \end{aligned}\right\} \text{ on } \lambda = 0 \tag{12.13}$$

together with the requirement that G should match onto the inviscid solution F, assuming a common region of validity.

Following Reid (1965), we may write the general solutions to (12.10) and (12.11) as

$$G_{io} = a_{io} + b_{io}\lambda + c_{io}\int_{\infty_1}^{\lambda} d\lambda \int_{\infty_1}^{\lambda} Ai(\lambda)d\lambda$$

$$+ d_{io}\int_{\infty_2}^{\lambda} d\lambda \int_{\infty_2}^{\lambda} Ai(\lambda e^{2i\pi/3})\, d\lambda$$

$$i = 0, 1 \tag{12.14}$$

where the a_{io} etc. are functions of τ which are chosen to satisfy the boundary and matching conditions. The function $Ai(\lambda)$ is the well known Airy function and a property of this is that it is exponentially small at ∞ for $|\arg \lambda| < \pi/3$, this being the sector in which ∞_1 lies. It is exponentially large elsewhere except on the lines $|\arg \lambda| = \pi/3$ and $\arg \lambda = -\pi$. Thus $Ai(\lambda e^{2i\pi/3})$ is exponentially small for

$-\pi < \arg\lambda < -\pi/3$, this being the sector in which ∞_2 lies. Thus we see from (12.7) and (12.8) that, when $U_o' > 0$, $\arg\lambda = \pi/6$ for $\eta > 0$, and hence we must insist that $d_{io} \equiv 0$ in order that the solution may not be exponentially large at infinity and therefore impossible to match with the inviscid solution. In the same way we see that, when $U_o' < 0$, $\arg\lambda = -5\pi/6$, and hence we must then insist that $c_{io} \equiv 0$.

Making use of the fact that $Ai(\lambda)$ satisfies Airy's equation

$$\left(\frac{d^2}{d\lambda^2} - \lambda\right) Ai(\lambda) = 0 \qquad (12.15)$$

we may, by means of a partial integration, reduce the double integrals in (12.14) to forms involving only a single integration.

e.g.

$$\int_{\infty_1}^{\lambda} d\lambda \int_{\infty_1}^{\lambda} Ai(\lambda)d\lambda = \lambda \int_{\infty_1}^{\lambda} Ai(\lambda)d\lambda - \frac{d}{d\lambda} Ai(\lambda) \qquad (12.16)$$

Hence, noting the values of the following quantities,

$$\left.\begin{aligned} \left[\frac{d}{d\lambda} Ai(\lambda)\right]_{\lambda=0} &= -\frac{3^{1/6}\,\Gamma(2/3)}{2\pi} \\ \int_0^{\infty_1} Ai(\lambda)\, d\lambda &= 1/3 \end{aligned}\right\} \qquad (12.17)$$

We may deduce that, when $U_o' > 0$, the boundary conditions (12.13) are satisfied by G_{oo} and G_{1o} if

$$\left.\begin{aligned} \frac{b_{oo} + U_o'}{a_{oo}} &= \frac{-2\pi}{3^{7/6}\,\Gamma(2/3)} \\ \frac{b_{1o}}{a_{1o}} &= \frac{-2\pi}{3^{7/6}\,\Gamma(2/3)} \end{aligned}\right\} \qquad (12.18)$$

where $\Gamma(x)$ is the Gamma Function c.f. Brooke Benjamin (1959). Similarly we may show that, when $U_o' < 0$, the boundary conditions (12.13) are satisfied by G_{oo} and G_{1o} if

$$\left.\begin{aligned} \frac{b_{oo} + U_o'}{a_{oo}} &= \frac{-2\pi\, e^{2i\pi/3}}{3^{7/6}\,\Gamma(2/3)} \\ \frac{b_{1o}}{a_{1o}} &= \frac{-2\pi\, e^{2i\pi/3}}{3^{7/6}\,\Gamma(2/3)} \end{aligned}\right\} \qquad (12.19)$$

The general solution to (12.12) can be written as

$$G_{11} = \frac{U_o''}{2U_o'}\left[\, 2a_{oo} e^{i\pi/6}\, N(\lambda e^{-i\pi/6}) + b_{oo}\lambda^2 \,\right] \qquad (12.20)$$

$$+ a_{11} + b_{11}\lambda + \text{exponentially decaying terms.}$$

where $N(x)$ is just the function referred to by Stuart (1963), who reproduces a table of its values due to Holstein (1950). This function is regular at the origin and has the following behaviour as $|\lambda| \to \infty$

$$\left.\begin{aligned} N(\lambda e^{-i\pi/6}) &\sim |\lambda| \log(|\lambda|); \quad \arg\lambda = \pi/6 \\ N(\lambda e^{-i\pi/6}) &\sim -|\lambda| \log(|\lambda|) + \pi i|\lambda|; \quad \arg\lambda = -5\pi/6 \end{aligned}\right\} \qquad (12.21)$$

In order to make a meaningful match between these viscous solutions and the inviscid solution (12.4), we need to specify the size of k more carefully. In fact we assume that

$$k = \varepsilon \quad k' \tag{12.22}$$

where $|k'| \sim 0(1)$. We see from (9.6) that this is a reasonable assumption for a typical physiological situation. Thus (12.$\frac{4}{5}$) gives the solution to the inviscid equation correct to $o(\varepsilon^2)$. We may also note that the full solution to (12.1) would give the solution to (10.29) correct to $o(\varepsilon^3)$.

We therefore expand $A(\tau)$ in (12.4) as

$$A(\tau) = A_{oo}(\tau) + (\varepsilon \log|\varepsilon|)A_{10}(\tau) + \varepsilon A_{11}(\tau) + O(\varepsilon^2 \log|\varepsilon|)^2 \tag{12.23}$$

and hence, writing (12.6) in terms of the viscous layer variables (12.8) and using (12.22), we have that as $\eta \to 0$ the inviscid solution behaves like

$$\begin{aligned} G \sim A_{oo}\left\{k' \frac{U_\infty^2}{U_o'} + \lambda U_o'\right\} + \varepsilon \log|\varepsilon| \Bigg\{ & A_{10}\left(k' \frac{U_\infty^2}{U_o'} + \lambda U_o'\right) \\ & + A_{oo} k' \frac{U_\infty^2}{U_o'} \cdot \frac{U_o''}{U_o'} \lambda \Bigg\} + \varepsilon \Bigg\{ A_{11}\left(k' \frac{U_\infty^2}{U_o'} + \lambda U_o'\right) \\ & + A_{oo} \frac{\lambda^2}{2} U_o'' + A_{oo} k' \frac{U_\infty^2}{U_o'} C\lambda \\ & + A_{oo} k' \frac{U_\infty^2}{U_o'} \cdot \frac{U_o''}{U_o'} \lambda \log(|\lambda|) \Bigg\} + O(\varepsilon \log|\varepsilon|)^2 \end{aligned} \tag{12.24}$$

Therefore, in order that the $0(\varepsilon^0)$ term should match with G_{oo} as $\lambda \to \infty$ we have that

$$\left.\begin{aligned} a_{oo} &= A_{oo}\, k' \frac{U_\infty^{\,2}}{U_o'} \\ b_{oo} &= A_{oo}\, U_o' \end{aligned}\right\} \qquad (12.25)$$

Similarly, in order that the $0(\varepsilon \log|\varepsilon|)$ term should match with G_{1o}, we have that

$$\left.\begin{aligned} a_{1o} &= A_{1o}\, k' \frac{U_\infty^{\,2}}{U_o'} \\ b_{1o} &= A_{1o}\, U_o' + A_{oo}\, k' \frac{U_\infty^{\,2}}{U_o'} \cdot \frac{U_o''}{U_o'} \end{aligned}\right\} \qquad (12.26)$$

In addition, we may see that in the $0(\varepsilon)$ term of (12.24) the terms involving $\log(|\lambda|)$ and λ^2 are automatically matched by the solution for G_{11} (12.20) when the property (12.21) is utilised. Also we have

$$\left.\begin{aligned} a_{11} &= A_{11}\, k' \frac{U_\infty^{\,2}}{U_o'} \\ b_{11} &= A_{11}\, U_o' + A_{oo}\, k' \frac{U_\infty^{\,2}}{U_o'} C \end{aligned}\right\} \qquad (12.27)$$

and the matching may be continued to higher order in ε if desired.

Combining (12.18) and (12.25) and (12.20) we find that if $U_o' > 0$

$$\left.\begin{aligned} A_{oo} &= -1\Big/\left[1+\frac{2\pi}{3^{7/6}\Gamma(2/3)}\,k'\left(\frac{U_\infty}{U_o'}\right)^2\right] \\ A_{1o} &= k'\left(\frac{U_\infty}{U_o'}\right)^2\frac{U_o''}{U_o'}\Big/\left[1+\frac{2\pi}{3^{7/6}\Gamma(2/3)}\,k'\left(\frac{U_\infty}{U_o'}\right)^2\right]^2 \end{aligned}\right\} \qquad (12.28)$$

Similarly, if $U_o' < 0$ we see from (12.19) and (12.25) that

$$\left.\begin{aligned} A_{oo} &= -1\Big/\left[1+\frac{2\pi e^{2i\pi/3}}{3^{7/6}\Gamma(2/3)}\,k'\left(\frac{U_\infty}{U_o'}\right)^2\right] \\ A_{1o} &= k'\left(\frac{U_\infty}{U_o'}\right)^2\frac{U_o''}{U_o'}\Big/\left[1+\frac{2\pi e^{2i\pi/3}}{3^{7/6}\Gamma(2/3)}\,k'\left(\frac{U_\infty}{U_o'}\right)^2\right]^2 \end{aligned}\right\} \qquad (12.29)$$

Hence, using (12.22) and (12.7), we see that

$$\left.\begin{aligned} A_{oo} &= -1\Big/\left[1\pm\frac{2\pi\,k(kR)^{1/3}}{3^{7/6}\Gamma(2/3)}\cdot\frac{U_\infty^{\,2}e^{\pm i\pi/6}}{(U_o')^{5/3}}\right] \\ A_{1o} &= k(kR)^{1/3}\frac{U_\infty^{\,2}U_o''e^{i\pi/6}}{(U_o')^{8/3}}\Big/\left[1\pm\frac{2\pi\,k(kR)^{1/3}}{3^{7/6}\Gamma(2/3)}\cdot\frac{U_\infty^{\,2}}{(U_o')^{5/3}}e^{\pm i\pi/6}\right]^2 \end{aligned}\right\} \qquad (12.30)$$

where the plus sign is taken if $U_o' > 0$, and the minus sign is taken if $U_o' < 0$.

We now consider what happens in the viscous layer near a point $\tau = \tau_o$ when $U_o' = 0$. Near such a point

$$U \sim \eta(\tau-\tau_o)\left[\frac{\partial U_o'}{\partial\tau}\right]_{\tau=\tau_o} + \frac{1}{2}\eta^2\left[U_o''\right]_{\tau=\tau_o} + \ldots \qquad (12.31)$$

and, in order to create a balance between the inertial and viscous terms in (10.29), we are led to the following scalings on $\tau - \tau_o$ and η

$$\gamma = \eta\,\delta^{-1}, \quad H = F\,\delta^{-1}, \quad T = (\tau - \tau_o)\,\delta^{-1} \tag{12.32}$$

where δ is a small parameter defined by

$$\left.\begin{aligned} \delta &= \left\{ ikR \left[U_o''\right]_{\tau=\tau_o} \right\}^{-1/4} \\ \arg\delta &= -\pi/8\,, \quad \left[U_o''\right]_{\tau=\tau_o} > 0 \\ \arg\delta &= +\pi/8\,, \quad \left[U_o''\right]_{\tau=\tau_o} < 0 \end{aligned}\right\} \tag{12.33}$$

Substituting (12.32), (12.33) and (12.31) into (10.29) the equation becomes

$$\frac{\partial^4 H}{\partial\gamma^4} + (T\gamma - \tfrac{1}{2}\gamma^2)\frac{\partial^2 H}{\partial\gamma^2} + H = 0(\delta) \tag{12.34}$$

noting that from our definition of U (10.26)

$$\left[\frac{\partial U_o'}{\partial\tau} \Big/ U_o''\right]_{\tau=\tau_o} = -1 \tag{12.35}$$

In addition, the boundary conditions to be satisfied on the wall become, from (10.30)

$$H = 0\,, \quad \frac{\partial H}{\partial\gamma} = -\delta T\left[\frac{\partial U_o'}{\partial\tau}\right]_{\tau=\tau_o} + 0(\delta^2) \tag{12.36}$$

The first order equation for H is obtained by putting the righthand side of (12.34) equal to zero and we again note the important feature that the time variable T occurs only as a parameter. Four independent solutions to this equation are found in Appendix C in the form of contour integrals, but these are not needed for our purposes here. We observe that one solution of (12.34) is

$$H_1 = h(T)\left[T\gamma - \frac{1}{2}\gamma^2 \right] \tag{12.37}$$

We may infer from (12.34) that the other three solutions are regular at $\gamma = 0$, and, by assuming the following behaviour of H as $|\gamma| \to \infty$

$$H \sim \gamma^{\sigma} e^{h_1\gamma + h_2\gamma^2} \left\{ a_o + a_1/\gamma + \ldots \right\} \tag{12.38}$$

we may show that they have the following asymptotic forms

$$H_2 \sim \gamma^{-1} \left\{ b_o + b_1/\gamma + \ldots \right\} \tag{12.39}$$

$$H_3 \sim \gamma^{-(5-T^2/\sqrt{2})/2} e^{+(T\gamma - \gamma^2/2)/\sqrt{2}} \left\{ c_o + c_1/\gamma + \ldots \right\} \tag{12.40}$$

$$H_4 \sim \gamma^{-(5-T^2/\sqrt{2})/2} e^{-(T\gamma - \gamma^2/2)/\sqrt{2}} \left\{ d_o + d_1/\gamma + \ldots \right\} \tag{12.41}$$

where the a_i etc. are functions of T.

Because $\eta > 0$ we see from (12.32) and (12.33) that, for $T \sim 0(1)$, then $d_i \equiv 0$ in order that H may not be exponentially large and therefore impossible to match with the inviscid solution. That the function H does match naturally onto the inviscid solution F may be seen by expanding (12.5) at $\tau = \tau_o$ for small η

$$F \sim A\Bigg\{ \frac{2kU_\infty^2}{3U_o''}\Bigg[\frac{1}{\eta} - \frac{2}{3}\frac{U_o'''}{U_o''} + \Bigg\{\frac{2}{3}\Big(\frac{U_o'''}{U_o''}\Big)^2 - \frac{5}{12}\frac{U_o^{iv}}{U_o''}\Bigg\}\eta$$

$$+\Bigg\{\frac{4}{9}\Big(\frac{U_o'''}{U_o''}\Big)^2 - \frac{1}{2}\frac{U_o'''U_o^{iv}}{U_o''^2}\Bigg\}\eta^2 \log \eta\Bigg]$$

$$+ O(\eta^2) + O(k^2)\Bigg\} \qquad (12.42)$$

Writing this in the scaled variables (12.32) we have when $\eta \sim 0$

$$H \sim O(Ak\delta^{-2}/\gamma) \qquad (12.43)$$

The expression (12.22) implies that k is $O(\delta^{4/3})$ and, since the boundary conditions (12.36) imply that H is $O(\delta)$, we therefore require that

$$A = O(\delta^{5/3}) \qquad (12.44)$$

in order that the inviscid solution should match onto H_2 in (12.39). However, when $U_o' \sim -\delta T U_o''$ (see (12.35)), we see from (12.30) that

$$A_{oo} = O(\delta^{5/3}) \qquad (12.45)$$

Thus the leading term in an expansion for A in terms of the small parameter δ near $\tau = \tau_o$ is of the same order of magnitude as that predicted by the leading term in an expansion in terms of ε elsewhere. This fact is of particular significance when we come to evaluate the steady streaming associated with this flow.

The expression (12.44) also implies that the function H_1

of (12.37) must be of $0(\delta^{8/3})$ in order that it may match onto the dominant term in η^2 of (12.42). (F is expanded at $\tau = \tau_o$ in (12.42) and so T = 0 in the expression for H_1). Thus H_1 is not present in the first order solution. The two remaining functions H_2 (12.39) and H_3 (12.40) (H_4 was dismissed because it was exponentially large at infinity) can now be made to satisfy the boundary conditions (12.36), and this gives rise to the value of the leading term in an expansion for A.

We may also see how this first order solution for H matches onto the viscous solution G_{oo} as $|T| \to \infty$. If we use the W.K.B. method and assume that for arg $\gamma = -\pi/8$ ($U_o'' < 0$) and arg $T = -\pi/8$ ($\tau > \tau_o$)

$$H \sim g(T)\, e^{\sqrt{T}\,\phi(\gamma)} \left\{ f_o(\gamma) + \frac{1}{\sqrt{T}} f_1(\gamma) + \dots \right\} \qquad (12.46)$$

then we find that

$$H \sim g_1 + g_2\gamma + g_3\gamma^{-5/4} \exp\left(-\frac{2}{3}|T\gamma^{3/2}|\, e^{i\pi/4}\right)$$

$$+ g_4\gamma^{-5/4} \exp\left(+\frac{2}{3}|T\gamma^{3/2}|\, e^{i\pi/4}\right) \qquad (12.47)$$

where the g_i are functions of T. We may see immediately that $g_4 \equiv 0$ otherwise H would be exponentially large. If we write the expression for G_{oo} (12.14) in terms of the scaled variables (12.32), then we find that, for $U_o' \sim -\delta T U_o'' > 0$

$$H \sim 0(\delta) + 0(\delta^{8/3})\,\gamma + 0(\delta) \int_{\infty_1}^{|\gamma T^{1/3}|e^{i\pi/6}} d\lambda \int_{\infty_1}^{\lambda} Ai(\lambda)\, d\lambda \qquad (12.48)$$

and we may show that for large T the double integral gives rise to the following asymptotic representation

$$H \sim 0(\delta) + 0(\delta^{8/3})\,\gamma + 0(\delta)\gamma^{-5/4} \exp(-\tfrac{2}{3}\,|T\gamma^{3/2}|\,e^{i\pi/4}) \qquad (12.49)$$

(see Reid (1965)).

Thus as well as ensuring a match with (12.47) we see that it is also consistent with H being $0(\delta)$. In addition the $0(\delta^{8/3})\gamma$ term again demonstrates the order of magnitude of H_1 with which it must match, and this agrees with the order of magnitude found previously. We may perform similar analyses when either $U_o' > 0$ or $\tau < \tau_o$ (or both) and we find again that the functions match onto each other consistently.

Thus this first order solution for H, though not found explicitly, satisfies all our requirements: it satisfies the boundary conditions on the wall and matches onto both the inviscid solution F and the viscous solution G_{co}. It also enables us to find the leading term in an expansion for the function A in (12.4) when $\tau \sim \tau_o$ and, as mentioned before, the important feature of this is that its order of magnitude is the same as that predicted by the leading term in an expansion elsewhere.

The physical significance of this region of thickness $0\left[\delta(2\nu/\omega)^{1/2}\right]$ near $\tau = \tau_o$ is that it represents the creation of another viscous layer of thickness $0\left[\varepsilon(2\nu/\omega)^{1/2}\right]$. This breaks away from the viscous layer on the wall and propagates into the inviscid region moving with the point $\eta = \eta_{c_1}(\tau)$ where $U_{c_1} = 0$. After a certain length of time a point is reached where U_{c_1}' is again zero and now the viscous layer combines with another layer at $\eta = \eta_{c_2}$ and they both disappear. They reappear later as the two layers at $\eta = \eta_{c_2}$ and η_{c_3} respectively. It should be noted that during part of the period of oscillation there are no viscous layers away from the wall, whilst at other times there may be several. Indeed, when $U_\infty = 0$ there are an infinite number although their effect decays exponentially away from the wall. In connection with this it should be mentioned that whilst the solution (12.4) does not exist at $\tau = \tau_\infty$ where $U_\infty = 0$, the limit $\tau \to \tau_\infty$ does. Reference to the sketch of the profiles of $U(\eta, \tau)$ at different stages in a period of oscillation in Fig. 12.1 should make this structure clear.

We may easily see from matching with (12.6) that the viscous solutions G_{ij} given in (12.14) and (12.20) are immediately applicable for the solution of (12.10) - (12.12) in the viscous layers away from the wall. As we should expect, we find that the Airy function solutions are not required. If one had existed and decayed

exponentially for $\eta > \eta_c$, then it would have increased exponentially for $\eta < \eta_c$ and this would have been intolerable. Similarly the first order solution H_2 (12.39) to the equation (12.34) is directly applicable in the regions where the viscous layers are either emerging or disappearing. As before, at the inception of such a region H_2 is matched to the first order viscous solution G_{oo}, but at its conclusion it now has to be matched onto the inviscid solution F. However, on closer investigation using (12.14), (12.25) and (12.24), we see that these are now identical to first order in ε, and thus the matching is, in fact, unaffected. Because A_{oo} is now 0(1) near such a region, we see from matching that H_2 must be $0(\delta^{-2/3})$ and this is $0(\delta^{-5/3})$ greater than in the equivalent region on the wall.

We now concentrate on the evaluation of the steady streaming associated with this flow away from the viscous layer on the wall. From (10.34) we may see that if there were no viscous layers then the contribution of 0(a) would be given by

$$u_1^{(s)} = \mathbb{R}\left\{\frac{e^{ik\psi}}{2\pi}\int_0^{2\pi}\frac{\partial F}{\partial \eta}\,d\tau\right\} \qquad (12.50)$$

F being the inviscid solution and $\mathbb{R}$ denoting 'Real part of'. However, as mentioned in the previous paragraph, near the viscous layer at a point $\eta = \eta_c$, the inviscid solution is identical to the viscous solution to first order in ε. Therefore, using (12.45) and (12.23), we

find that the dominant contribution to the steady streaming is

$$u_1^{(s)} = \mathcal{R}\left\{\frac{e^{-k\eta + ik\psi}}{2\pi}\int_0^{2\pi} A_{oo}\frac{\partial U}{\partial \eta}\, d\tau\right\} \qquad (12.51)$$

the neglected terms being of $0(kR)^{-1/3}$. Strictly, we do not know the value of the leading term for A in a region near the time τ_o when $U_o' = 0$, but we inferred from (12.44) and (12.45) that it was the same order of magnitude as that predicted by A_{oo}. More explicitly it is of $0(\delta^{5/3})$ and, because such a region exists for a time of $0(\delta)$, then the error incurred from this source when using (12.51) is of $0(\delta^{8/3})$. This is $0(kR)^{-2/3}$ and is much smaller than the effect of the neglected terms. Should, however, the integration pass through a region where $U_c' \sim 0$ then the use of (12.51) must involve an error of $0(\delta H)$. We saw from the matching conditions outlined above that H is $0(\delta^{-2/3})$ and so the error is $0(\delta^{1/3})$. Because this is $0(kR)^{-1/12}$ it is very much larger than the error of $0(kR)^{-1/3}$ from the neglected terms. Nevertheless, in the limit $kR \to \infty$, it is still vanishingly small compared to (12.51).

Using (10.26) and (12.30) we find that we can write (12.51) as

$$u_1^{(s)} = \Re\left\{-\frac{\sqrt{2}}{2\pi}e^{-(1+k)\eta+ik\psi}\left[\int_{-\frac{3\pi}{4}}^{\frac{\pi}{4}} \frac{\cos(\tau-\eta+\pi/4)\cos^{5/3}(\tau+\pi/4)}{\cos^{5/3}(\tau+\pi/4)+2\Delta e^{i\pi/6}\cos^2\tau}\,d\tau + \int_{\frac{\pi}{4}}^{\frac{5\pi}{4}} \frac{\cos(\tau-\eta+\pi/4)\cos^{5/3}(\tau+\pi/4)}{\cos^{5/3}(\tau+\pi/4)-2\Delta e^{-i\pi/6}\cos^2\tau}\,d\tau\right]\right\} \quad (12.52)$$

where

$$\Delta = \frac{\pi k (kR)^{1/3}}{2^{5/6}\,3^{7/6}\,\Gamma(2/3)} \quad (12.53)$$

This may be rearranged into the following form

$$u_1^{(s)} = -\frac{\sqrt{2}}{\pi}\Delta\sin(\pi/6)e^{-(1+k)\eta}\sin k\psi \;\; x$$

$$x\left\{\int_{-\frac{\pi}{2}}^{\frac{\pi}{2}} \frac{\cos(t-\eta)\cos^{5/3}t\,(1+\sin 2t)}{\cos^{10/3}t+2\Delta\cos^{5/3}t(1+\sin 2t)\cos(\pi/6)+\Delta^2(1+\sin 2t)^2}\,dt\right\} \quad (12.54)$$

or more graphically

$$u_1^{(s)} = -k\,(kR)^{1/3}e^{-(1+k)\eta}\left\{I_1\cos\eta + I_2\sin\eta\right\}\sin k\psi \quad (12.55)$$

The integrals I_1 and I_2 have been evaluated numerically using an integration routine available on the Imperial College IBM 7094 computer. The results are given for different values of $k(kR)^{1/3}$ in Table 4.

From Chapter 9 it would appear that $k(kR)^{1/3}$ is generally

on the small side for physiological applications, and so the limiting values of I_1 and I_2 as $k(kR)^{1/3}$ or $\Delta \to 0$ are of some interest. We therefore consider the following integrals.

$$J_1 = \int_{-\frac{\pi}{2}}^{\frac{\pi}{2}} \frac{\cos^{8/3} t\,(1+\sin 2t)}{\cos^{10/3} t + 2\Delta \cos^{5/3} t (1+\sin 2t)\cos(\pi/6) + \Delta^2 (1+\sin 2t)^2}\, dt \tag{12.56}$$

and

$$J_2 = \int_{-\frac{\pi}{2}}^{\frac{\pi}{2}} \frac{\sin t \cos^{5/3} t\,(1+\sin 2t)}{\cos^{10/3} t + 2\Delta \cos^{5/3} t (1+\sin 2t)\cos(\pi/6) + \Delta^2 (1+\sin 2t)^2}\, dt \tag{12.57}$$

We may write J_1 as

$$J_1 = \int_{-\frac{\pi}{2}}^{\frac{\pi}{2}} \frac{\cos^{8/3} t\,(1+\sin 2t)}{\cos^{10/3} t + 2\Delta \cos^{5/3} t \cos(\pi/6) + \Delta^2} \left\{ 1 + \right.$$

$$\left. + \sum_{n=1}^{\infty} \frac{(-1)^n \Delta^n \sin^n 2t \left[2\Delta + \Delta \sin 2t - 2\cos^{5/3} t \cos(\pi/6) \right]^n}{\left[\cos^{10/3} t + 2\Delta \cos^{5/3} t \cos(\pi/6) + \Delta^2 \right]^n} \right\} dt \tag{12.58}$$

and because the order of magnitude of each term in the series is $\leq 0(\Delta^{3n/5})$ throughout the range of integration, the error involved in neglecting these will be $\leq 0(\Delta^{3/5})$ times the remaining integral. Therefore we consider

$$J_1 = \int_{-\frac{\pi}{2}}^{\frac{\pi}{2}} \frac{\cos^{8/3} t\,(1+\sin 2t)}{\cos^{10/3} t + 2\Delta \cos^{5/3} t \cos(\pi/6) + \Delta^2}\, dt$$

$$= 2 \int_0^{\frac{\pi}{2}} \frac{\cos^{8/3} t}{\cos^{10/3} t + 2\Delta \cos^{5/3} t \cos(\pi/6) + \Delta^2}\, dt \qquad (12.59)$$

and if we use the substitution $y^3 = \cos t$ then J_1 becomes

$$J_1 = 6 \int_0^1 \frac{y^{10}}{(1-y^6)^{1/2}(y^{10} + 2\Delta y^5 \cos(\pi/6) + \Delta^2)}\, dy \qquad (12.60)$$

We now split up the range of integration into two parts in the following manner

$$J_1 = 6(J_p + J) \qquad (12.61)$$

where

$$\left.\begin{aligned} J_p &= \int_0^p \frac{y^{10}}{(1-y^6)^{1/2}(y^{10} + 2\Delta y^5 \cos(\pi/6) + \Delta^2)}\, dt \\ J &= \int_p^1 \frac{y^{10}}{(1-y^6)^{1/2}(y^{10} + 2\Delta y^5 \cos(\pi/6) + \Delta^2)}\, dt \end{aligned}\right\} \qquad (12.62)$$

We may expand the integrand of J in the following manner

$$J = \int_p^1 \frac{1}{(1-y^6)^{1/2}} \left\{ 1 + \sum_{n=1}^{\infty} a_n \left(\frac{\Delta}{y^5}\right)^n \right\} dy \qquad (12.63)$$

if $\Delta \ll p^5$. The error incurred by replacing the full expression for

J by

$$J = \int_p^1 \frac{1}{(1-y^6)^{1/2}}\, dy \tag{12.64}$$

will therefore be given by the order of magnitude of

$$\int_p^1 \frac{\Delta}{(1-y^6)^{1/2} y^5}\, dy \tag{12.65}$$

which is

$$\leq \Delta \int_p^{1/2} \frac{A}{y^5}\, dy + \Delta \int_{1/2}^1 \frac{B}{(1-y^6)^{1/2}}\, dy \tag{12.66}$$

$$= 0(\Delta / p^4)$$

the constants A and B being of 0(1). Because of the condition $\Delta \ll p^5$ the error in using the expression (12.64) for J is therefore $0(\Delta^{1/5})$.

We now write J as

$$J = \int_0^1 \frac{1}{(1-y^6)^{1/2}}\, dy - \int_0^p \frac{1}{(1-y^6)^{1/2}}\, dy \tag{12.67}$$

and so $J_p + J$ becomes

$$J_p + J = - \int_0^p \frac{2\Delta y^5 \cos(\pi/6) + \Delta^2}{(1-y^6)^{1/2}(y^{10} + 2\Delta y^5 \cos(\pi/6) + \Delta^2)}\, dy \tag{12.68}$$

See Corrigenda

We again expand the integrand so that

$$J_p + J = -\int_0^p \frac{2\Delta y^5 \cos(\pi/6) + \Delta^2}{(y^{10} + 2\Delta y^5 \cos(\pi/6) + \Delta^2)} \left\{1 + \frac{1}{2} y^6 + \ldots\right\} dy \tag{12.69}$$

and the order of magnitude of the integral is given by the first term providing $p^6 \ll 1$. Thus the value of p is such that $\Delta^{1/5} \ll p \ll 1$. Using the substitution $y = \Delta^{1/5}\eta$ the first term in the expansion (12.69) becomes

$$-\Delta^{1/5} \int_0^{p/\Delta^{1/5}} \frac{2\eta^5 \cos(\pi/6) + \Delta^2}{\eta^{10} + 2\eta^5 \cos(\pi/6) + 1} d\eta \tag{12.70}$$

$$= 0(\Delta^{1/5})$$

Therefore, from (12.61), we finally have

$$J_1 = 6 \int_0^1 \frac{1}{(1-y^6)^{1/2}} dy + 0(\Delta^{1/5}) \tag{12.71}$$

which becomes, using the substitution $x = y^6$,

$$J_1 = \int_0^1 (1-x)^{-1/2} x^{-5/6} dx + 0(\Delta^{1/5})$$

$$= B(\tfrac{1}{6}, \tfrac{1}{2}) + 0(\Delta^{1/5}) \tag{12.72}$$

where B is the well known Beta Function.

In a similar way we can show that

$$J_2 = \frac{3}{2} B(\frac{1}{6}, \frac{1}{2}) + 0(\Delta^{1/5}) \tag{12.73}$$

and since

$$B(\frac{1}{6}, \frac{1}{2}) = \frac{\Gamma(1/6)\,\Gamma(1/2)}{\Gamma(2/3)} = \sqrt{\pi}\,\frac{\Gamma(1/6)}{\Gamma(2/3)} \tag{12.74}$$

the expression (12.55) becomes, using (12.53)

$$u_1^{(s)} = -\frac{\pi^{1/2}\Gamma(1/6)k(kR)^{1/3}}{2^{4/3}3^{7/6}\left[\Gamma(2/3)\right]^2}\left[\cos\eta + \frac{3}{2}\sin\eta\right]e^{-(1+k)\eta}\sin k\psi + 0\left[k(kR)^{1/3}\right]^{4/5} \tag{12.75}$$

and this gives

$$u_1^{(s)} = -0.5927\,k(kR)^{1/3}\left[\cos\eta + \frac{3}{2}\sin\eta\right]e^{-(1+k)\eta}\sin k\psi + 0\left[k(kR)^{1/3}\right]^{4/5} \tag{12.76}$$

In Fig. 12.2 we plot the values of $\log(0.5927 - I_1)$ and $\log(0.8890 - I_2)$ against $\log\left[k(kR)^{1/3}\right]$ for values of $k(kR)^{1/3}$ from 0.001 to ~~0.005~~ 0.010 inclusive (see Table 4). As can be seen, the resulting curves are straight lines with gradients of 1/5, and this verifies that the error in (12.76) is $0\left[k(kR)^{1/3}\right]^{1/5}$.

To summarise, the dominant steady streaming is of 0(a), and, if we assume $k \sim 0(kR)^{-1/3}$ then, away from the viscous layer on the wall, it is given by (12.55) in the limit $kR \to \infty$. The error in (12.55) is $0(kR)^{-1/3}$ almost everywhere, but, if η is within a distance $0(kR)^{-1/4}$ from a point where, at some time during a cycle, both U and U' are zero, then the error is of $0(kR)^{-1/12}$. This may

be quite considerable even for very large values of kR. Should we take the further limit $k(kR)^{1/3} \to 0$ then the steady streaming is given by (12.76). Because the error is $0\left[k(kR)^{1/3}\right]^{1/5}$, this too may be quite large for very small values of $k(kR)^{1/3}$. A sketch of the steady streaming predicted by (12.55) is given in Fig. 12.3. This consists of a peculiar stacked structure of regions of recirculation, but, because of the exponential decay away from the wall, only the first few regions are of importance. In this respect it is not dissimilar to the steady streaming depicted in Figs. 11.1 and 11.2 for small kR.

REFERENCES

Barua, S.N., 1963, Quart. J. Mech. Appl. Math. 16, 61.

Batchelor, G.K., 1956, J. Fluid Mech. 1, 177.

Bromwich, T.J.I'a, 1947, Introduction to the Theory of Infinite Series, 2ndEd. Macmillan.

Brooke Benjamin, T., 1959, J. Fluid Mech. 6, 161.

Burggraf, O.R., 1966, J. Fluid Mech. 24, 113.

Carslaw, H.S. and Jaeger, J.C. 1959, Conduction of Heat in Solids, 2nd Ed. Oxford University Press.

Dean, W.R., 1927, Phil. Mag. (7), 4, 208.

Dean, W.R., 1928, Phil. Mag. (7), 5, 673.

Hadamard, J., 1923, Lectures on Cauchy's Problem in Linear Partial Differential Equations. Newhaven - London.

Harper, J.F., 1963, J. Fluid Mech, 17, 141.

Harper, J.F. and Moore, D.W., 1968, J. Fluid Mech. 32, 367.

Holstein, H., 1950, Z. angew. Math. Mech. 30, 25.

Jones, A.F. and Rosenblat, S., 1969, J. Fluid Mech. 37, 337.

Jones, C.W. and Watson, E.J., 1963, Laminar Boundary Layers (Ed. Rosenhead). Chapter 5. Oxford.

Kober, H., 1952, Dictionary of Conformal Representations. Dover.

Kuwahara, K. and Imai, I., 1969, Phys. Fluids Supplement II, 12, 94.

Lighthill, M. J., 1957, J. Fluid Mech. 3, 113.

Longuet-Higgins, M. S., 1953, Phil. Trans. (A) 245, 535.

Mangler, K. W., 1952, Improper Integrals in Theoretical Aerodynamics, Aero. Res. Coun., C. P. No. 94.

McConalogue, D. J. and Srivastava, R. S., 1968, Proc. Roy. Soc. (A), 307, 37.

McDonald, D. A., 1960, Blood Flow in Arteries, London, Arnold.

Moore, D. W., 1963, J. Fluid Mech. 16, 161.

Prandtl, L., 1927, Vier Abhandlugen zur Hydrodynamik und Aerodynamik, Gottingen, English translation in N. A. C. A. Tech. Memo. No. 452.

Rayleigh, Lord., 1884, Phil. Trans. (A), 175, 1.

Reid, W. H., 1965, The Stability of Parallel Flows, Basic Developments in Fluid Dynamics (Ed. Holt) Vol. 1, Academic Press.

Riley, N., 1965, Mathematika, 12, 161.

Riley, N., 1967, J. Inst. Maths. Applics. 3, 419.

Rosenblat, S., 1960, J. Fluid Mech. 8, 388.

Schlichting, H., 1932, Phys. Z. 33, 327.

Segel, L. A., 1961, Quart. Appl. Math. 18, 335.

Squire, H. B., 1956, J. Roy. Aero. Soc. 60, 203.

Stewartson, K., 1957, Proc. Symp. Boundary Layer Res., Int. Union Theoret. Appl. Mech. Freiburg i. Br. (Springer (1968), 59).

Stuart, J. T., 1963, Laminar Boundary Layers (Ed. Rosenhead), Chapter 9, Oxford.

Stuart, J. T., 1966, J. Fluid Mech. 24, 673.

Tollmien, W., 1929, W. Nachr. Ges. Wiss. Gottingen, 1, 21, English translation in Nat. Adv. Comm. Aero., Wash., Mem. No. 909.

Whitham, G. B., 1963, Laminar Boundary Layers (Ed. Rosenhead), Chapter 3, Oxford.

APPENDICES

APPENDIX A

TO SHOW THAT B AND C ARE IDENTICALLY ZERO IN (3.20)

Suppose that in (3.20) B is not identically zero and so in the Stokes layer $\chi_o \sim B\eta^3$ as $\eta \to \infty$. As only harmonic dependence on time is allowed, and the first order flow in the interior must match with χ_o, we may drop the time derivative from (2.21) for our purposes here. Then, using (3.5), this equation for flow in the outer region becomes

$$-\frac{1}{r}\frac{\partial(\chi, \nabla^2\chi)}{\partial(r,\psi)} = \frac{1}{R_s}\nabla^4\chi \qquad (A.1)$$

Writing (3.20) in terms of the variables for the outer region we find that as $\eta \to \infty$

$$\chi \sim B\beta^{-2}(1-r)^3 + O(\beta^{-1}) \qquad (A.2)$$

This leads to our writing χ as

$$\chi = \beta^{-2}\chi_o + \beta^{-1}\chi_o + \ldots \qquad (A.3)$$

where, from (A.2), χ_o must satisfy the boundary conditions

$$\chi_o = \frac{\partial\chi_o}{\partial r} = 0 \qquad \text{on } r = 1 \qquad (A.4)$$

Because of (A.3) the effective Reynolds number in (A.1) is $\beta^{-2}R_s$ and this is large for small β. In addition (A.4) implies that no streamlines associated with χ_o enter or leave the Stokes layer,

and therefore the first order flow in the outer region must have uniform vorticity (Batchelor (1956)). As pointed out in Chapter 5, this does not specify the flow uniquely as the outer region could consist of several regions each having uniform vorticity of a strength different from that of its neighbour. However, having decided on one such configuration, this does imply a definite non-zero velocity distribution at the edge of the outer region as only one solution of the vorticity equation

$$\nabla^2 \chi_o = - \zeta \qquad (A.5)$$

is regular within a closed area. (ζ is the vorticity which is uniform in each region of the configuration.) But (A.4) implies that this velocity distribution must be identically zero and hence $\zeta = \chi_o \equiv 0$. This leads directly to the conclusion that $B \equiv 0$.

We now consider the possibility of a boundary layer being formed at the edge of the outer region. If this has a thickness $0(\sigma)$ then in order to balance inertial and viscous terms in (A.1) we require that $\sigma \chi \sim R_s^{-1}$. But to match with χ_o we require that $\chi \sim \beta^{-2}\sigma^3$ and this leads to the conclusion that $\sigma \sim \beta^{1/2} R_s^{-1/4}$ and $\chi \sim \beta^{-1/2} R_s^{-3/4}$. We therefore define the following boundary layer variables

$$\chi^* = \beta^{1/2} R_s^{3/4} \chi, \quad \eta^* = \beta^{-1/2} R_s^{1/4} (1-r) \qquad (A.6)$$

and then if

$$\chi^{*} = \chi_o^{*} + \delta(\beta)\,\chi_1^{*} + \ldots \qquad (A.7)$$

where $\delta(\beta) \to 0$ as $\beta \to 0$, the equation for χ_o^{*} may be deduced from (A.1) to be

$$\frac{\partial \chi_o^{*}}{\partial \eta^{*}} \frac{\partial^3 \chi_o^{*}}{\partial \eta^{*2} \partial \psi} - \frac{\partial \chi_o^{*}}{\partial \psi} \frac{\partial^3 \chi_o^{*}}{\partial \eta^{*3}} = \frac{\partial^4 \chi_o^{*}}{\partial \eta^{*4}} \qquad (A.8)$$

The boundary conditions (A.4) become

$$\chi_o^{*} = \frac{\partial \chi_o^{*}}{\partial \eta^{*}} = 0 \qquad \text{on } \eta^{*} = 0 \qquad (A.9)$$

The asymptotic form of the solution to (A.9) as $\eta^{*} \to \infty$ can be shown to be

$$\chi_o^{*} \sim a(\psi)\,\eta^{*} + b(\psi) \qquad (A.10)$$

leaving out terms of exponential growth. If $a \equiv 0$ then (A.10) implies that $\frac{\partial \chi_o^{*}}{\partial \eta^{*}} \to 0$ as $\eta^{*} \to \infty$, and Riley (1965) has shown that, with boundary conditions (A.9), this leads to the conclusion that $\chi_o^{*} \equiv 0$. Hence we again find that χ_o and therefore B are identically zero. If $a \not\equiv 0$, then writing (A.10) in the original variables, we have as $\eta^{*} \to \infty$

$$\chi \sim \beta^{-1} R_s^{1/2} (1-r) + \ldots \qquad (A.11)$$

Therefore we introduce the scaled stream function $\bar{\chi} = \beta R_s^{1/2} \chi$ in the interior or core of the pipe. The effective Reynolds number for flow in the core is now $\beta^{-1} R_s^{1/2}$ which is again large for small β. The relation (A.11) also implies that no first order streamlines of

the core flow enter or leave the boundary layer, and thus the first order flow in the core $\bar{\chi}_o$ has uniform vorticity. Therefore we once more have a definite prescribed velocity at the edge of the core and a configuration of regions of uniform vorticity similar to that described previously. However, our experience in Chapter 5 implies that, having decided on one such configuration, the problem can be solved uniquely by applying the condition of recirculation of the boundary layers, including those formed between regions of different vorticities. That is, the problem can be solved completely with only the two boundary conditions (A.9) specified at the edge of the outer region. Because these two conditions are those of no flow, we may therefore deduce that there is no flow throughout the outer region. This again leads to the conclusion that χ_o and hence B are identically zero.

In a similar way we can show that $C \equiv 0$, thus justifying our analysis of Chapter 3. We may note that, if in (A.1), the effective Reynolds number were small, then the boundary conditions (A.4) must imply no flow in the interior, if we expand the solution in powers of the Reynolds number as in Chapter 4. This would again determine B and C to be identically zero.

APPENDIX B

THE NUMERICAL SOLUTION OF (5.36)

The integral equation (5.36) was solved on the Imperial College IBM 7094 machine. An iteration procedure was used whereby an approximate profile for $\gamma_i(y)$ was used to evaluate the right hand side, thus giving an improved estimate for the profile on the left hand side. This in turn was used to evaluate the right hand side and the process continued until the input and output profiles differed by a small enough amount. Infinity was taken to be at $y = 10$ and this was found to be more than adequate.

However, in order to evaluate γ_i up to $y = 10$ on the left hand side, it was necessary to extrapolate for the values of γ_i when $10 < y \leq 20$ to evaluate the right hand side. This was because the maximum contribution to the integral on the right hand side came from the vicinity of $y = y'$, and it was therefore necessary to extend the range of integration until the kernel $K(y, y')$ of the integrand became negligibly small ($< 10^{-6}$). This led to our choice of $y = 20$ for the upper limit of integration. The extrapolation was easily accomplished, the constant profile for γ_i as $y \to \infty$ being anticipated by putting $\gamma_i\ (y > 10) = \gamma_1\ (y = 10)$.

The starting profile used was that of γ_i^{H} this being

evaluated for $y > 0$ from the integral in (5.32) using Simpson's rule with a step length of $\pi/200$. The value of $\gamma_i^{\pi}(0)$ was $\gamma_i(0)$ which we knew exactly to be zero. Similarly the integral on the right hand side of (5.36) was evaluated using Simpson's rule with a step length of 0.1. The errors associated with these integrations will be discussed later.

The iterations were continued until the value of γ_i at each station $y_n = 0.1 \times n$ differed by less than 0.00001 from the value given by the previous iterate. It was, however, found necessary to devise a way of speeding the convergence of the iterations when y was large. This was accomplished by anticipating the behaviour $\gamma_i \to$ constant as $y \to \infty$, and noting that the value of this constant value was approached from above by the iterations. Thus after each evaluation of the profile on the left hand side $\gamma_i^{(1)}$, a new profile $\gamma_i^{(2)}$ was deduced by putting

$$\left.\begin{aligned} \gamma_i^{(2)}(y_n) &= \gamma_i^{(1)}(y_n) \qquad n \leq N \\ \gamma_i^{(2)}(y_n) &= \gamma_i^{(1)}(y_{N+1}) \qquad n \geq N+1 \end{aligned}\right\} \qquad \text{(B.1)}$$

where N was determined from the following conditions

$$\left.\begin{aligned} &\gamma_i^{(1)}(y_N) \leq \gamma_i^{(1)}(y_{100}) - 0.00001 \\ &\gamma_i^{(1)}(y_{100}) - 0.00001 < \gamma_i^{(1)}(y_n) \leq \gamma_i^{(1)}(y_{100}), \quad N < n \leq 100 \end{aligned}\right\} \qquad \text{(B.2)}$$

The profile $\gamma_i^{(2)}$ was then used to obtain the next iterate for γ_i. If,

however, the conditions (B.2) could not be satisfied, or if $\gamma_i^{(2)}(y_{100})$ of the previous iterate were less than the subsequent $\gamma_i^{(1)}(y_{100})$ (indicating that the constant value had been overshot), then the iteration was continued without recourse to the above device. This accelerated the convergence considerably, but it was still found necessary to continue for fifty iterations after the condition for convergence had first been satisfied, in order to guarantee that the resulting profile was correct. If the value $\gamma_i(y_n)$ of one of these fifty profiles was not within 0.00001 of the value due to another, then the iterations were continued.

If h were the step length, then the error associated with using Simpson's rule for the numerical evaluation of the integrals would normally have been $0(h^4)$, provided that the first four derivatives of the integrand existed and were bounded. However it could be shown that, when $y \sim 0$, $\gamma_o'' \sim$, and hence $\gamma_o \sim y \log y$, and that the error was now $0(h^2)$. Therefore, in order to check the accuracy of the integrations, use was made of the following device. If I were the true value of the integral in (B.36) and I_1 and I_2 the values obtained by using Simpson's rule with step lengths of h and 2h respectively, then, for the γ_o profile,

$$I = I_2 + 4Eh^2 = I_1 + Eh^2 \qquad (B.3)$$

and hence

$$I = I_1 + \frac{I_1 - I_2}{3} \qquad (B.4)$$

E being some constant. When the calculations were performed using step lengths of 0.2 and 0.1, the maximum difference between the resulting profiles for γ_0 was found to be 0.00011. Thus (B.4) assured that the profile was given correct to three decimal places when the step length was 0.1. The magnitude of the error associated with the integration of γ_1 was the normal $0(h^4)$, and a similar analysis to that given above showed that, with a step length of 0.1, γ_1 was given correct to at least the four decimal places ensured by the condition for convergence of the iterations. Similarly it could be shown that the γ_i^H were given correct to five decimal places when evaluated from the integral (5.32) using a step length of $\pi/200$.

The profiles for the γ_i^H and γ_i are given in Table 1, and we deduce from (5.35) that, for $\gamma(x_e, y) \to 0$ as $y \to \infty$,

$$\zeta = - \frac{\gamma_1(\infty)}{\gamma_0(\infty)} \qquad (B.5)$$

Therefore, we find that $\zeta = -0.56$ correct to two decimal places. The equation for the elliptic pipe was solved in precisely the same way, and the values of ζ for different values of the eccentricity are given in Table 2.

In addition the profiles of γ and Γ were evaluated at different positions around the semicircle. Having derived the profile

of $\gamma(x_e, y)$, the property (5.26) enabled Γ to be evaluated along the line of symmetry from equation (5.22). Then, having obtained $\Gamma(X_e, Y)$, the property (5.27) was utilised to evaluate γ along the curved boundary from (5.12). The integrals of γ and Γ were again evaluated by Simpson's rule with a step length of 0.1, but, in order to evaluate the second integral on the right hand side of (5.12), the step length had to be shortened considerably for small y from the value used previously. This integral corresponded to $\gamma^{H} = \gamma_o^{H} + \zeta^{-1}\gamma_1^{H}$ evaluated at the position under consideration, $\psi = \Psi$ say. Thus for $y > 0$ it was evaluated from an integral identical to (5.32) except that x_e was replaced by $x(\Psi)$ and the upper limit by Ψ. However, for $\Psi \neq 0$, the integrand had a sharp peak near $y = 0$ and this necessitated the successive shortening of the step length from the value $\pi/200$ used above until the desired accuracy of three decimal places had been achieved. In fact, to conserve computing time, it was finally found necessary to interpolate the value of the integral at $y = 0.1$ from the values at $y = 0.0$, 0.1 and 0.2. The value of the integral at $y = 0.0$ was again known exactly, and was equal to $\gamma(x(\Psi), 0)$ which can be found from the boundary conditions (5.11).

The resulting profiles of Γ and γ correct to three decimal places are tabulated in Tables 3a and 3b respectively, and they are also depicted in Figs. 6.5a and 6.5b.

APPENDIX C

THE FUNCTION H(γ, T)

In this appendix we seek solutions to the following equation derived from (12.34)

$$\frac{\partial^4 H}{\partial \gamma^4} + (T\gamma - \frac{1}{2}\gamma^2)\frac{\partial^2 H}{\partial \gamma^2} + H = 0 \qquad (C.1)$$

We may integrate this once to give

$$\frac{\partial^3 H}{\partial \gamma^3} + (T\gamma - \frac{1}{2}\gamma^2)\frac{\partial H}{\partial \gamma} + (\gamma - T)H = S(T) \qquad (C.2)$$

where S is an arbitrary function of T. Thus three of the solutions to (C.1) also satisfy the homogeneous equation obtained by putting $S \equiv 0$ in (C.2). The other solution is given by a particular integral of (C.2) when $S \not\equiv 0$.

We use the following substitution

$$x = (\gamma - T)^2 \qquad (C.3)$$

and this transforms (C.2) into

$$8x\frac{\partial^3 H}{\partial x^3} + 12\frac{\partial^2 H}{\partial x^2} + (T^2 - x)\frac{\partial H}{\partial x} + H = \frac{S}{x^{1/2}} \qquad (C.4)$$

We now look for a solution of the form

$$H = \int_a^b e^{-px}\,\phi(p)\,dp \qquad (C.5)$$

where the limits a and b are to be chosen in some suitable manner. We also assume for the present that $S \equiv 0$. Equation (C. 4) now becomes

$$\left[(8p^2-1)p\, e^{-px}\phi\right]_a^b + \int_a^b \left[p(1-8p^2)\frac{d\phi}{dp} + (2-T^2p-12p^2)\phi\right] e^{-px}dp = 0 \tag{C. 6}$$

We see that if the limits a and b are chosen so that the expression in squared brackets in (C. 6) is zero, then the equation is satisfied if

$$p(1-8p^2)\frac{d\phi}{dp} + (2-T^2p - 12p^2)\,\phi = 0 \tag{C. 7}$$

and this gives rise to the following expression for ϕ

$$\phi = p^{-2}(1-2\sqrt{2}p)^{(1-T^2/\sqrt{2})/4}(1+2\sqrt{2}p)^{(1+T^2/\sqrt{2})/4} \tag{C. 8}$$

We observe that, when this is substituted into (C. 5), the integrand has a pole at $p = 0$ and branch points at $p = \pm 1/2\sqrt{2}$. Because of this we choose the limits a and b to be at infinity and $|\arg(ax, bx)| < \pi/2$. More explicitly, if we assume that $U_o'' > 0$ and therefore $\arg x = \pi/4$ (see (12. 32)), then we find that the most suitable value of a or b for our purposes is ∞^{π}, where $\arg \infty^{\pi} = -\pi/4$. Thus the three solutions to (C. 4) when $S \equiv 0$ are given by the following integrals

$$I_i = \int_{C_i} \frac{e^{-px}}{p^2}\,(1-2\sqrt{2}p)^{(1-T^2/\sqrt{2})/4}(1+2\sqrt{2}p)^{(1+T^2/\sqrt{2})/4}dp$$

$$i = 1, 2, 3. \tag{C. 9}$$

where the contours C_i start and finish at ∞^{π}, and branch cuts are made from $p = \pm 1/2\sqrt{2}$ to ∞^{π} as shown in Fig. C.1.

The integral I_1 around the contour C_1 is easily calculated from the value of its residue at $p = 0$. Thus we have

$$\begin{aligned} I_1 &= 2\pi i\,(T^2 - x) \\ &= 2\pi i\,(2\gamma T - \gamma^2) \end{aligned} \tag{C.10}$$

and this is just the solution H_1 of (12.37)

If we write

$$p = 1/2\sqrt{2} + re^{i\theta} \tag{C.11}$$

then the integral I_2 around C_2 becomes

$$I_2 = \int_{\infty}^{\delta} \frac{\exp\left[-(1/2\sqrt{2} + re^{-i\pi/4})x\right]}{\left[1/2\sqrt{2} + re^{-i\pi/4}\right]^2} \quad x$$

$$x \left[-2\ /2re^{-i\pi/4}\right]^{(1-T^2/\sqrt{2})/4} \left[2+2\sqrt{2}re^{-i\pi/4}\right]^{(1+T^2/\sqrt{2})/4} e^{-i\pi/4} dr$$

$$+ \int_{\delta}^{\infty} \frac{\exp\left[-(1/2\sqrt{2} + re^{7i\pi/4})x\right]}{\left[1/2\sqrt{2} + re^{7i\pi/4}\right]^2} \quad x$$

$$x \left[-2\sqrt{2}re^{7i\pi/4}\right]^{(1-T^2/\sqrt{2})/4} \left[2+2\sqrt{2}re^{7i\pi/4}\right]^{(1+T^2/\sqrt{2})/4} e^{7i\pi/4} dr$$

$$+ \int_{-\pi/4}^{7\pi/4} \frac{\exp\left[-(1/2\sqrt{2} + \delta e^{i\theta})x\right]}{\left[1/2\sqrt{2} + \delta e^{i\theta}\right]^2} \quad x$$

$$x \left[-2\sqrt{2}\delta e^{i\theta}\right]^{(1-T^2/\sqrt{2})/4} \left[2+2\sqrt{2}\delta e^{i\theta}\right]^{(1+T^2/\sqrt{2})/4} i\delta e^{i\theta} d\theta$$

(C.12)

where δ is the radius of the circle enclosing the branch point $p = 1/2\sqrt{2}$. If $|T^2| < 10$ then the last integral in (C. 12) vanishes as $\delta \to 0$, and, writing $t = r|x|$, we may show that for large $|x|$

$$I_2 \sim 8(-2\ /2)^{(1-T^2/\sqrt{2})/4}\,2^{(1+T^2/\sqrt{2})/4}\left[e^{7i\pi(1-T^2/\sqrt{2})/16}\right.$$
$$\left. - e^{-i\pi(1-T^2/\sqrt{2})/16}\ e^{-x/2\sqrt{2}}\,x^{-(5-T^2/\sqrt{2})/4}\int_0^\infty e^{-t}\,t^{(1-T^2/\sqrt{2})/4}\,dt\right] \qquad \text{(C. 13)}$$

The integral is a complex Gamma Function and is $0(1)$. Thus we see that for large γ

$$I_2 \sim R(T)\ \gamma^{-(5-T^2/\sqrt{2})/2}\ e^{+(\gamma T-\gamma^2/2)/\sqrt{2}} \qquad \text{(C. 14)}$$

where R is some function of T. Although the above asymptotic analysis is only valid if $|T^2| < 10$, we may deduce from (C. 14) that I_2 corresponds to the solution H_3 of (12. 40). In a similar way we can show that the integral I_3 around C_3 corresponds to the solution H_4 of (12. 41). We may treat the case $U_o'' < 0$ in the same way, the only difference being that, since $\arg x = -\pi/4$, we choose $\arg \infty^{\frac{1}{2}} = \pi/4$.

If $S \not\equiv 0$ in (C. 3), then it can be shown that

$$\frac{1}{x^{1/2}} = -\frac{1}{2\sqrt{\pi}} \int_{C_1} \frac{e^{-px}}{p^{1/2}}\,dp \qquad \text{(C. 15)}$$

and hence that equation (C. 4) is satisfied by (C. 5) if

$$p(1-8p^2)\frac{d\phi}{dp} + (2-T^2p - 12p^2)\,\phi = -\frac{1}{2\sqrt{\pi}\,p^{1/2}} \qquad (C.16)$$

We have chosen S = 1 with no loss of generality. This gives rise to the following expression for a particular integral of ϕ

$$\phi = -\frac{1}{2\sqrt{\pi}p^2}(1-2\sqrt{2}p)^{(1-T^2/\sqrt{2})/4}(1+2\sqrt{2}p)^{(1+T^2/\sqrt{2})/4} \times$$

$$\times \int_0^p p^{1/2}(1-2\sqrt{2}p)^{-(5-T^2/\sqrt{2})/4}(1+2\sqrt{2}p)^{-(5+T^2/\sqrt{2})/4}dp \qquad (C.17)$$

which leads to the following integral as a solution of (C. 1)

$$I_4 = \int_{C_1} e^{-px}\,\phi(p)\,dp \qquad (C.18)$$

$\phi(p)$ being that defined in (C. 17). For small p (C. 17) becomes

$$\phi \sim -\frac{1}{3\sqrt{\pi}}\,p^{-1/2}\,(1 + 0(p)) \qquad (C.19)$$

and so if we again assume $U_o'' > 0$, and therefore arg $\infty^{\frac{1}{2}} = -\pi/4$, and let the radius of the circle enclosing the branch point p = 0 tend to zero, we find (C. 18) assumes the form

$$I_4 = \int_\infty^0 e^{-r|x|}\,\phi(re^{-i\pi/4})\,dr\,e^{-i\pi/4}$$

$$+ \int_0^\infty e^{-r|x|}\,\phi(re^{7i\pi/4})dr\,e^{7i\pi/4} \qquad (C.20)$$

We again write $t = r|x|$ and (C. 20) now becomes

$$I_4 = \int_{\infty}^{0} e^{-t}\, \phi\left(\frac{t}{|x|}\, e^{-i\pi/4}\right) dr\, e^{-i\pi/4} + \int_{0}^{\infty} e^{-t}\, \phi\left(\frac{t}{|x|}\, e^{7i\pi/4}\right) dr\, e^{7i\pi/4} \qquad (C.21)$$

Thus, for large $|x|$ we find, using (C. 19)

$$I_4 \sim \frac{2}{3\sqrt{\pi}} \frac{e^{-i\pi/8}}{|x|^{1/2}} \int_{c}^{\infty} \frac{e^{-t}}{t^{1/2}}\, dt \qquad (C.22)$$

$$\sim \frac{2}{3} x^{-1/2}$$

Therefore for large γ

$$I_4 \sim \frac{2}{3} \gamma^{-1} \qquad (C.23)$$

and hence we see that I_4 corresponds to the solution H_2 of (12.39).

TABLES

TABLE 1: The functions y_i^{**} and y_i.

y	$-y_0^{**}$	$-y_1^{**}$	$-y_0$	$-y_1$
0.0	0.0	0.0	0.0	0.0
0.1	0.03286	0.01242	0.038	0.0154
0.2	0.05037	0.02144	0.061	0.0273
0.3	0.05997	0.02774	0.076	0.0365
0.4	0.06466	0.03184	0.086	0.0435
0.5	0.06611	0.03419	0.092	0.0486
0.6	0.06538	0.03515	0.096	0.0523
0.7	0.06318	0.03503	0.099	0.0549
0.8	0.05999	0.03410	0.100	0.0565
0.9	0.05619	0.03257	0.101	0.0574
1.0	0.05204	0.03063	0.101	0.0578
1.1	0.04772	0.02842	0.101	0.0578
1.2	0.04339	0.02606	0.100	0.0576
1.3	0.03914	0.02366	0.099	0.0572
1.4	0.03506	0.02127	0.099	0.0567
1.5	0.03119	0.01896	0.098	0.0561
1.6	0.02758	0.01677	0.097	0.0555
1.7	0.02424	0.01471	0.096	0.0549
1.8	0.02118	0.01282	0.096	0.0544
1.9	0.01840	0.01110	0.095	0.0539
2.0	0.01590	0.00954	0.095	0.0535
2.1	0.01366	0.00815	0.094	0.0532
2.2	0.01168	0.00693	0.094	0.0529
2.3	0.00993	0.00585	0.094	0.0526
2.4	0.00841	0.00491	0.094	0.0524
2.5	0.00707	0.00410	0.093	0.0523
2.6	0.00592	0.00340	--	0.0521
2.7	0.00494	0.00281	--	0.0521
2.8	0.00409	0.00231	--	0.0520
2.9	0.00338	0.00188	0.093	0.0520

y	$-y_0^*$	$-y_1^*$	$-y_0$	$-y_1$
3.0	0.00277	0.00153	0.093	0.0520
3.1	0.00226	0.00124	--	0.0520
3.2	0.00184	0.00100	--	0.0520
3.3	0.00149	0.00080	--	0.0520
3.4	0.00120	0.00063	--	0.0520
3.5	0.00096	0.00050	--	0.0520
3.6	0.00076	0.00040	--	0.0521
3.7	0.00061	0.00031	--	0.0521
3.8	0.00048	0.00024	--	0.0521
3.9	0.00037	0.00019	--	0.0521
4.0	0.00029	0.00014	--	0.0522
4.1	0.00023	0.00011	--	--
4.2	0.00018	0.00008	--	--
4.3	0.00014	0.00006	--	--
4.4	0.00010	0.00005	--	--
4.5	0.00008	0.00004	--	--
4.6	0.00006	0.00003	--	--
4.7	0.00005	0.00002	--	--
4.8	0.00003	0.00001	--	--
4.9	0.00003	0.00001	--	--
5.0	0.00002	0.00001	--	--
5.1	0.00001	0.00000	--	--
5.2	0.00001	--	--	--
5.3	0.00001	--	--	--
5.4	0.00001	--	--	--
5.5	0.00000	0.00000	0.093	0.0522

TABLE 2: The vorticity ζ of the core in the upper semi-ellipse when $R_s \to \infty$.

Minor axis of ellipse in plane of coil

Eccentricity	0.0	0.1	0.2	0.3	0.4	0.5
ζ	-0.56	-0.56	-0.56	-0.55	-0.55	-0.54

Major axis of ellipse in plane of coil

Eccentricity	0.0	0.1	0.2	0.3	0.4	0.5
ζ	-0.56	-0.56	-0.57	-0.59	-0.62	-0.66

TABLE 3: The profiles of Γ and y around the semicircle.

(a) The profiles of Γ along the line of symmetry $\psi=0,\pi$

y	Γ				
	$\psi=0$			$\psi=\pi$	
	r=1.0	r=0.5	r=0.0	r=0.5	r=1.0
0.0	0.000	-0.007	-0.004	-0.003	-0.003
0.1	-0.011	-0.007	-0.004	-0.003	-0.003
0.2	-0.012	-0.006	-0.004	-0.003	-0.003
0.3	-0.011	-0.006	-0.004	-0.003	-0.003
0.4	-0.008	-0.005	-0.004	-0.003	-0.002
0.5	-0.005	-0.004	-0.003	-0.003	-0.002
0.6	-0.003	-0.003	-0.003	-0.002	-0.002
0.7	-0.001	-0.003	-0.003	-0.002	-0.002
0.8	0.001	-0.002	-0.002	-0.002	-0.002
0.9	0.002	-0.001	-0.002	-0.002	-0.002
1.0	0.002	0.000	-0.001	-0.002	-0.002
1.1	0.003	0.000	-0.001	-0.001	-0.001
1.2	0.003	0.001	-0.001	-0.001	-0.001
1.3	0.003	0.001	0.000	-0.001	-0.001
1.4	0.003	0.001	0.000	-0.001	-0.001
1.5	0.002	0.001	0.000	0.000	-0.001
1.6	0.002	0.001	0.000	—	-0.001
1.7	0.002	0.001	0.000	—	0.000
1.8	0.001	0.001	0.000	—	—
1.9	0.001	0.001	0.001	—	—
2.0	0.001	0.001	0.001	—	—
2.1	0.001	0.001	0.001	—	—
2.2	0.000	0.001	0.001	—	—
2.3	—	0.001	0.001	—	—
2.4	0.000	0.000	0.000	0.000	0.000

(b) The profiles of γ along the curved boundary r=1

y	γ				
	$\psi=\pi$	$\psi=3\pi/4$	$\psi=\pi/2$	$\psi=\pi/4$	$\psi=0$
0.0	-0.003	-0.005	0.030	-0.005	0.000
0.1	-0.003	-0.008	0.025	0.001	-0.011
0.2	-0.003	-0.010	0.020	0.005	-0.012
0.3	-0.003	-0.010	0.016	0.007	-0.011
0.4	-0.002	-0.010	0.012	0.008	-0.008
0.5	-0.002	-0.009	0.009	0.009	-0.005
0.6	-0.002	-0.008	0.006	0.009	-0.003
0.7	-0.002	-0.006	0.004	0.008	-0.001
0.8	-0.002	-0.005	0.002	0.008	0.001
0.9	-0.002	-0.004	0.001	0.007	0.002
1.0	-0.002	-0.003	0.000	0.006	0.002
1.1	-0.001	-0.003	-0.001	0.005	0.003
1.2	-0.001	-0.002	-0.001	0.004	0.003
1.3	-0.001	-0.002	-0.002	0.003	0.003
1.4	-0.001	-0.001	-0.002	0.002	0.003
1.5	-0.001	-0.001	-0.002	0.002	0.002
1.6	-0.001	-0.001	-0.002	0.001	0.002
1.7	0.000	-0.001	-0.001	0.001	0.002
1.8	--	-0.001	-0.001	0.000	0.001
1.9	--	0.000	-0.001	--	0.001
2.0	--	--	-0.001	--	0.001
2.1	--	--	-0.001	--	0.001
2.2	--	--	-0.001	--	0.000
2.3	--	--	-0.001	--	--
2.4	0.000	0.000	0.000	0.000	0.000

TABLE 4: The integrals I_1 and I_2.

$k(kR)^{\frac{1}{3}}$	I_1	I_2	$k(kR)^{\frac{1}{3}}$	I_1	I_2
0.1	0.27377	0.22255	2.6	0.03326	0.00124
0.2	0.22331	0.15717	2.7	0.03118	0.00063
0.3	0.19225	0.12233	2.8	0.02925	0.00010
0.4	0.16999	0.09960	2.9	0.02746	-0.00036
0.5	0.15276	0.08318	3.0	0.02579	-0.00075
0.6	0.13875	0.07054	3.1	0.02423	-0.00108
0.7	0.12697	0.06039	3.2	0.02279	-0.00135
0.8	0.11681	0.05200	3.3	0.02144	-0.00159
0.9	0.10789	0.04491	3.4	0.02019	-0.00178
1.0	0.09993	0.03883	3.5	0.01903	-0.00194
1.1	0.09276	0.03357	3.6	0.01794	-0.00207
1.2	0.08624	0.02897	3.7	0.01693	-0.00217
1.3	0.08027	0.02495	3.8	0.01598	-0.00226
1.4	0.07479	0.02141	3.9	0.01510	-0.00232
1.5	0.06973	0.01830	4.0	0.01428	-0.00237
1.6	0.06505	0.01555	4.1	0.01351	-0.00240
1.7	0.06072	0.01314	4.2	0.01279	-0.00242
1.8	0.05669	0.01102	4.3	0.01212	-0.00242
1.9	0.05296	0.00915	4.4	0.01149	-0.00242
2.0	0.04949	0.00751	4.5	0.01090	-0.00241
2.1	0.04627	0.00608	4.6	0.01035	-0.00240
2.2	0.04323	0.00483	4.7	0.00983	-0.00238
2.3	0.04049	0.00373	4.8	0.00935	-0.00235
2.4	0.03790	0.00278	4.9	0.00889	-0.00232
2.5	0.03549	0.00196	5.0	0.00846	-0.00229

TABLE 4(cont.):

$k(kR)^{\frac{1}{3}}$	I_1	I_2
0.001	0.473	0.603
0.002	0.455	0.561
0.003	0.443	0.534
0.004	0.433	0.514
0.005	0.426	0.497
0.006	0.419	0.483
0.007	0.414	0.471
0.008	0.409	0.460
0.009	0.404	0.450
0.010	0.400	0.441

$\log[k(kR)^{\frac{1}{3}}]$	$\log[0.5927-I_1]$	$\log[0.8890-I_2]$
-6.908	-2.123	-1.252
-6.215	-1.983	-1.115
-5.809	-1.899	-1.036
-5.521	-1.834	-0.981
-5.298	-1.792	-0.936
-5.116	-1.750	-0.901
-4.962	-1.722	-0.872
-4.828	-1.694	-0.846
-4.711	-1.668	-0.823
-4.605	-1.647	-0.803

FIGURES

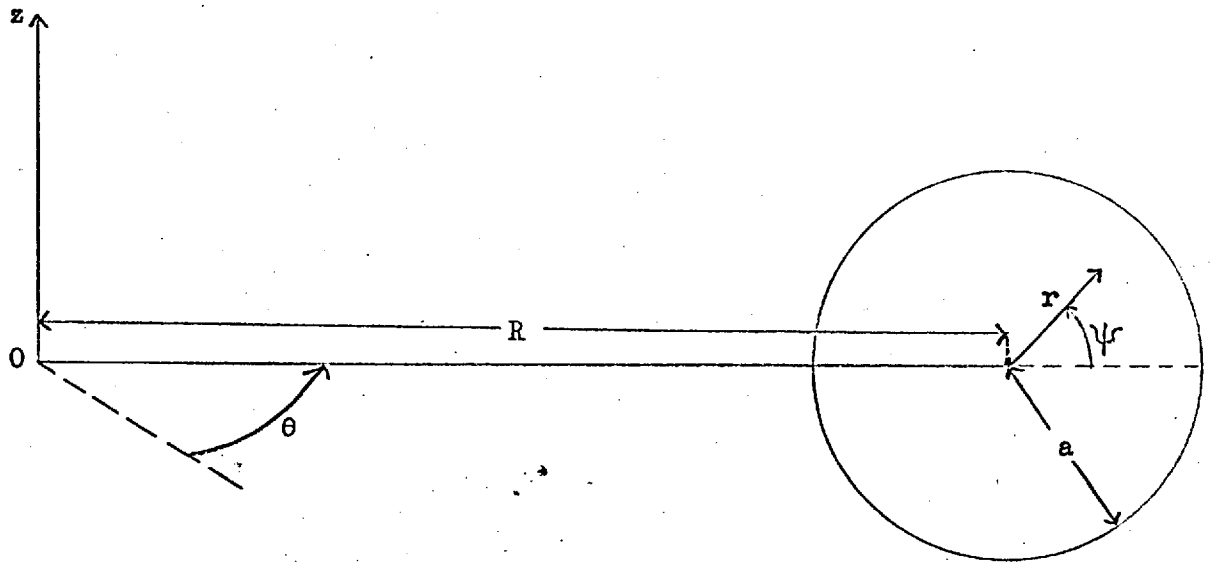

Fig. 2.1: The co-ordinate system for the circular pipe.

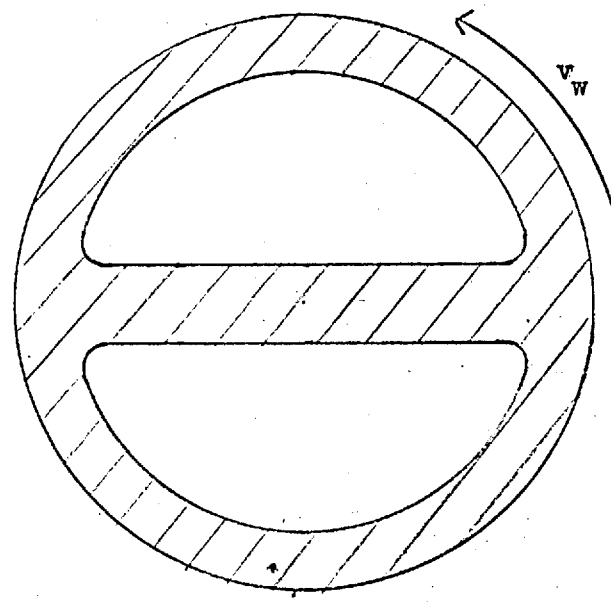

Fig. 5.1: Model for flow in the outer region when $R_s \to \infty$. Shaded regions denote boundary layers; unshaded regions have uniform vortioity.

$v_w = -0.25(W^2/R\omega)\sin\psi$

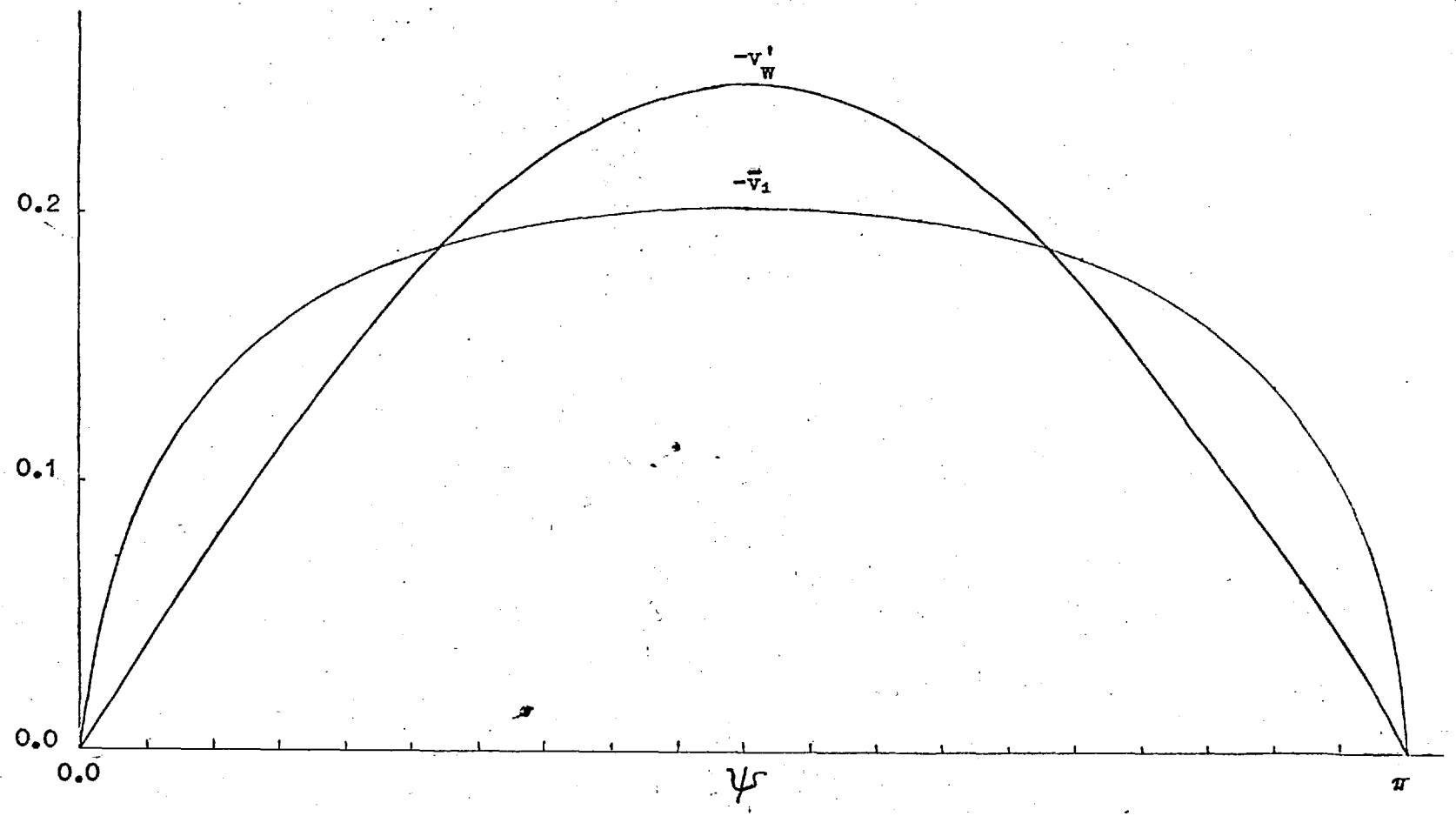

Fig. 5.2: Comparison of the velocity distribution at the edge of the core flow ($\bar{v}_1$) with the distribution on the wall of the circle (v'_w).

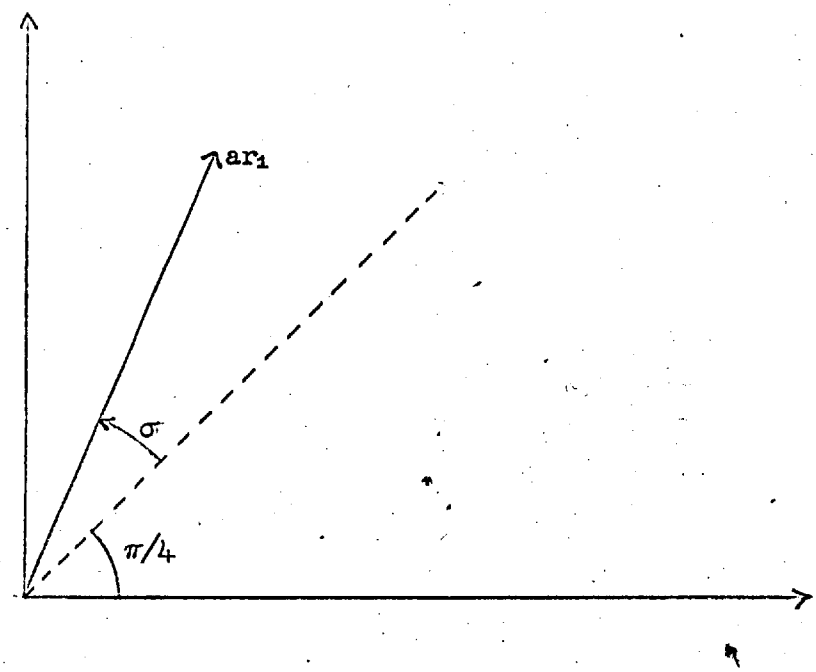

Fig. 5.3: The co-ordinate system in the corner $r=1, \psi=\pi$.

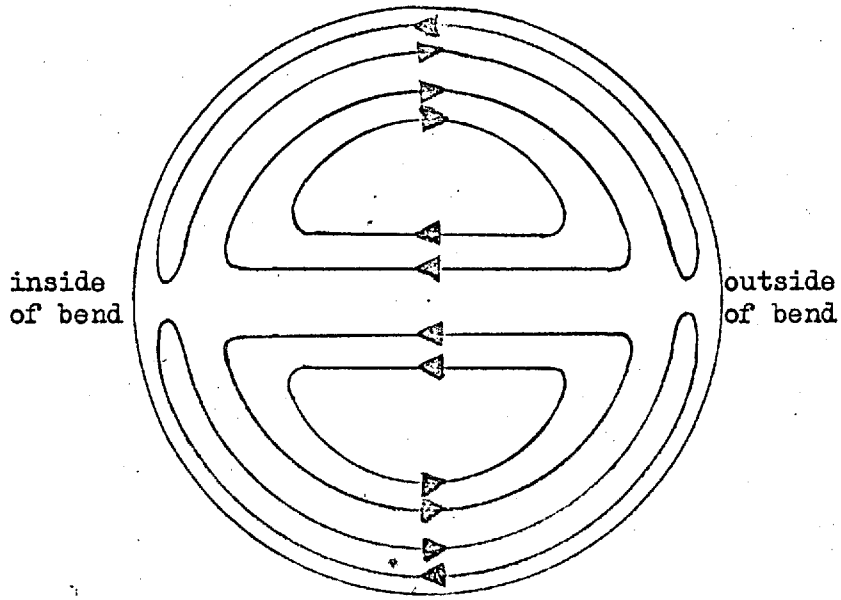

Fig. 6.1: Sketoh of the streamlines in the plane of the cross-section for small β.

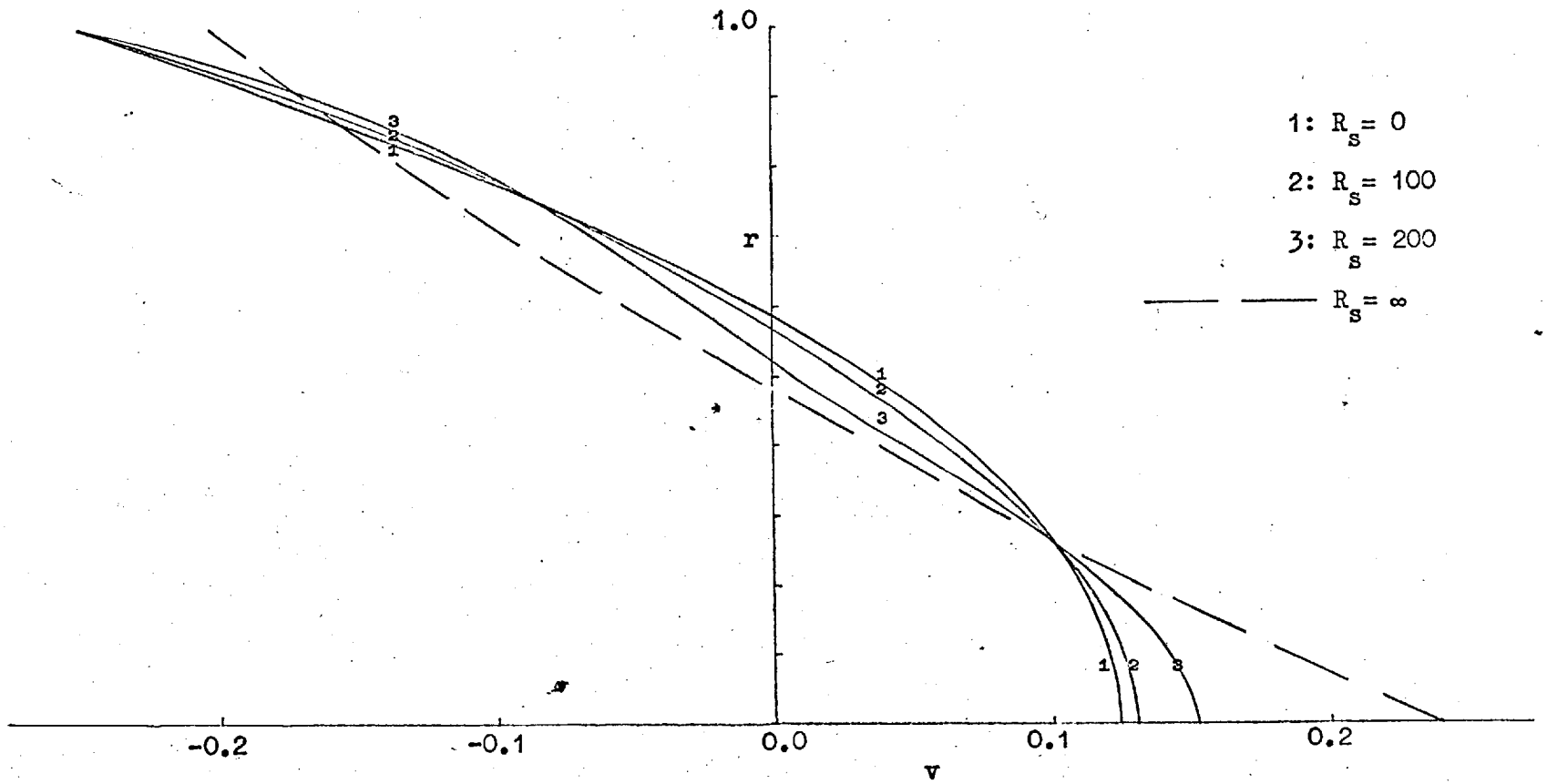

Fig. 6.2: The profiles of the secondary flow's velocity in the outer region along $\psi=\pi/2$ when $\beta=0$.

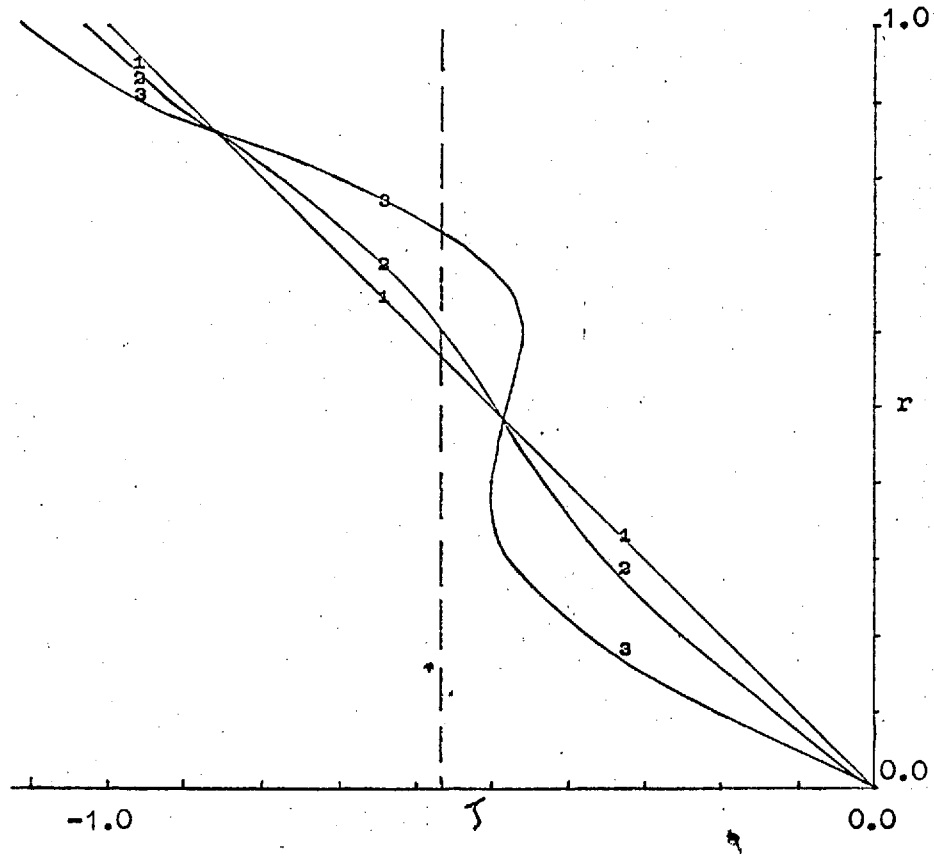

Fig 6.3: The profiles of the secondary flow's vorticity in the outer region along $\psi=\pi/2$ when $\beta=0$.

1: $R_s = 0$

2: $R_s = 100$

3: $R_s = 200$

—— —— $R_s = \infty$

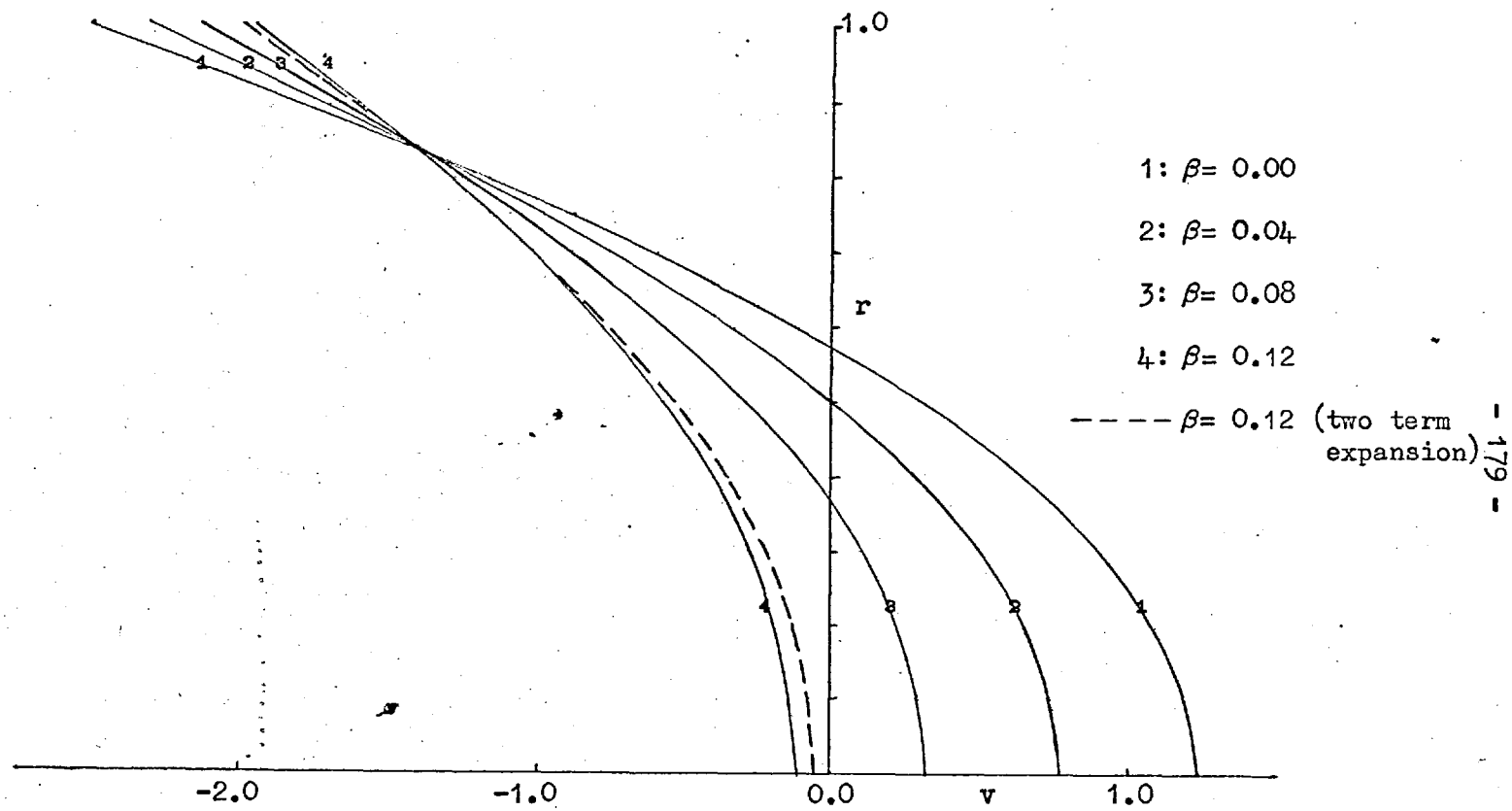

Fig. 6.4: The profiles of the secondary flow's mean velocity in the outer region along $\psi=\pi/2$ when $R_s = 0$.

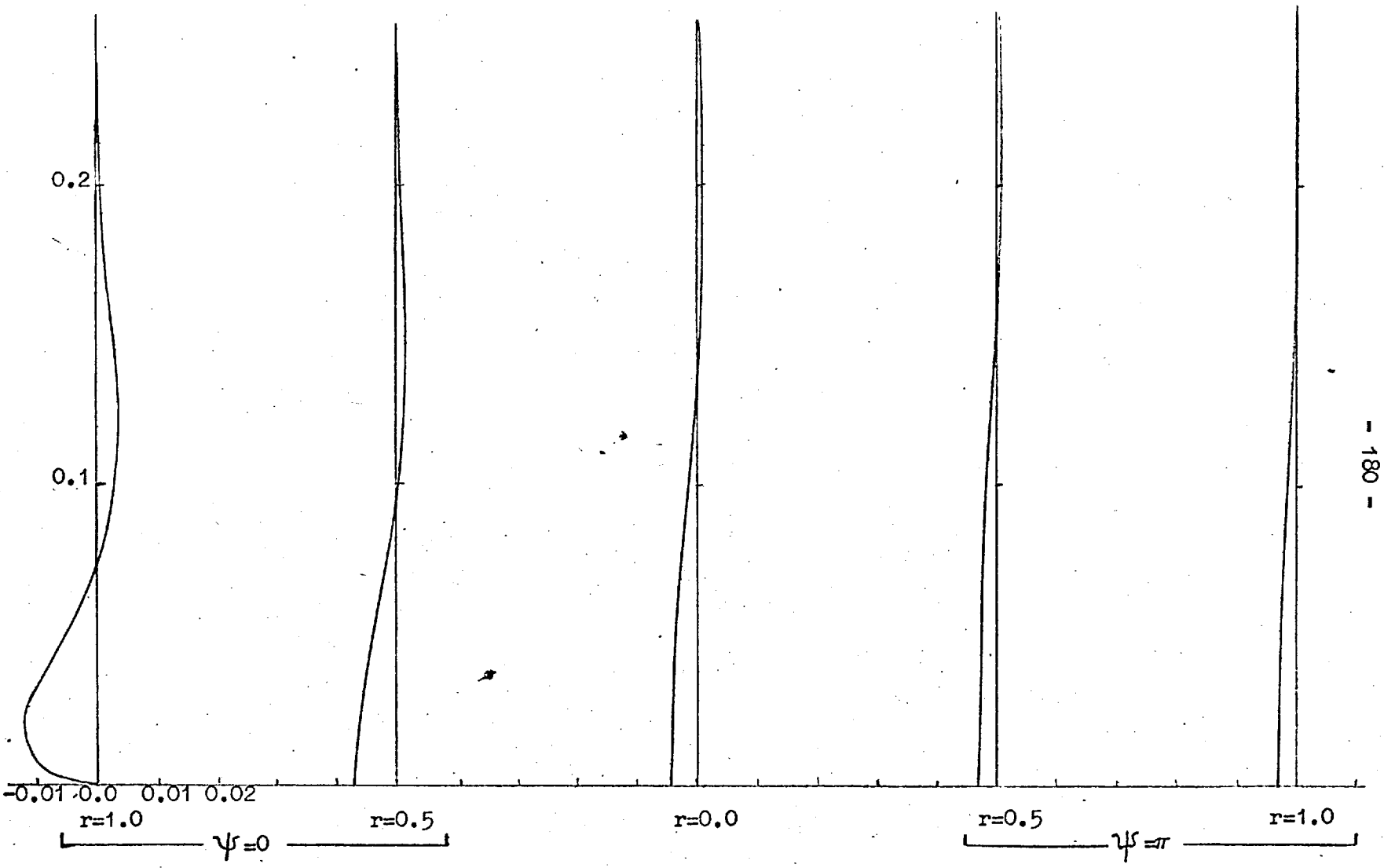

Fig. 6.5a: The profiles of Γ along the line of symmetry $\psi = 0, \pi$.

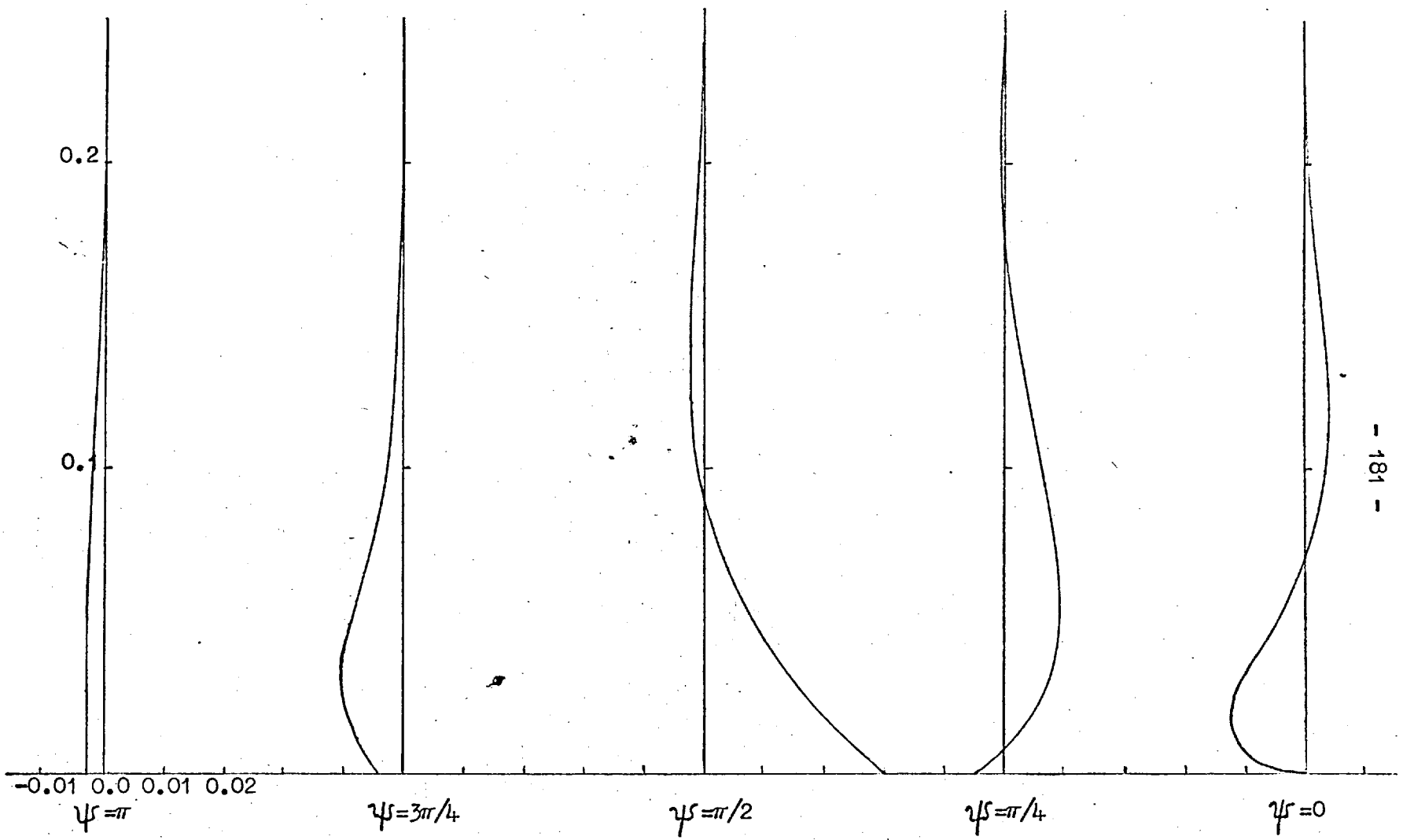

Fig. 6.5b The profiles of y along the curved boundary r= 1.

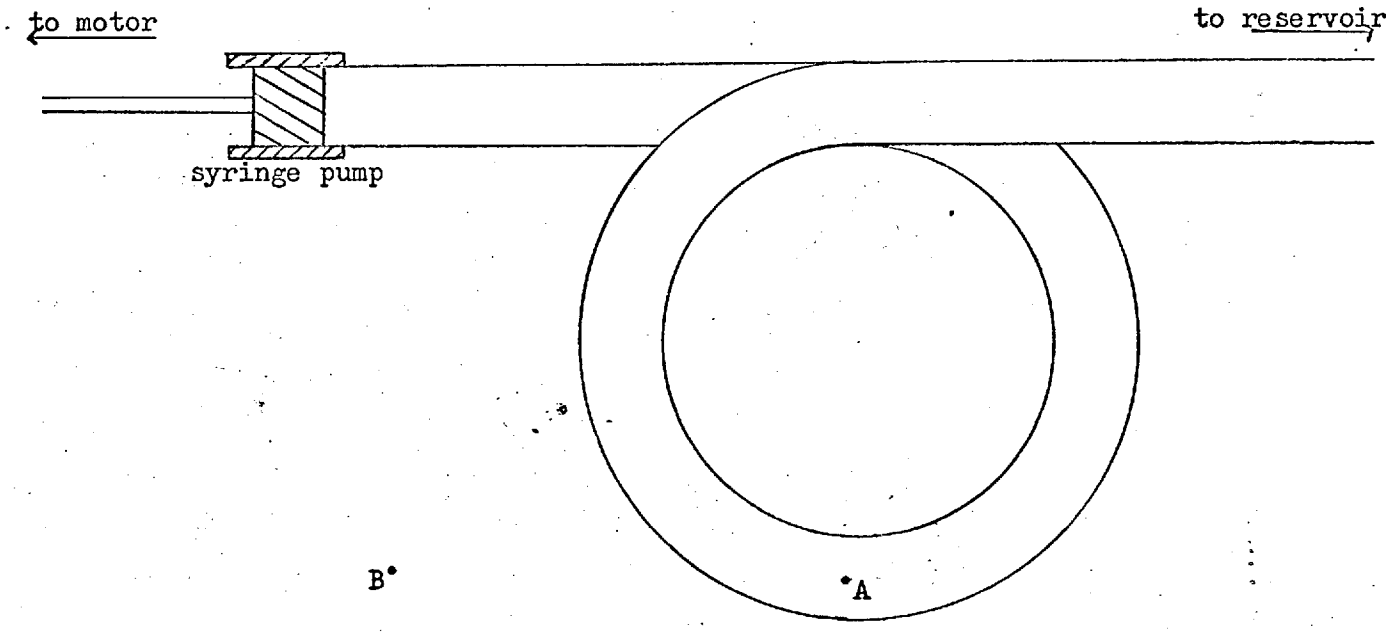

Fig. 7.1: The experimental apparatus.

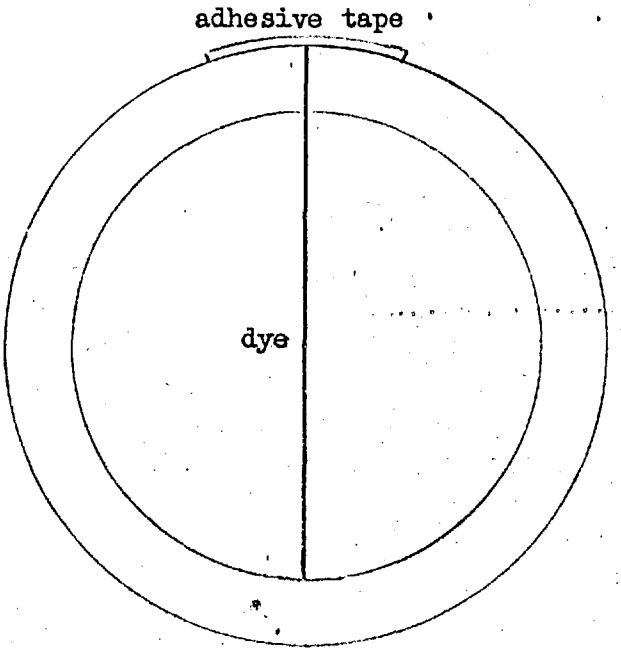

Fig. 7.2: Cross-section of pipe after injection of dye.

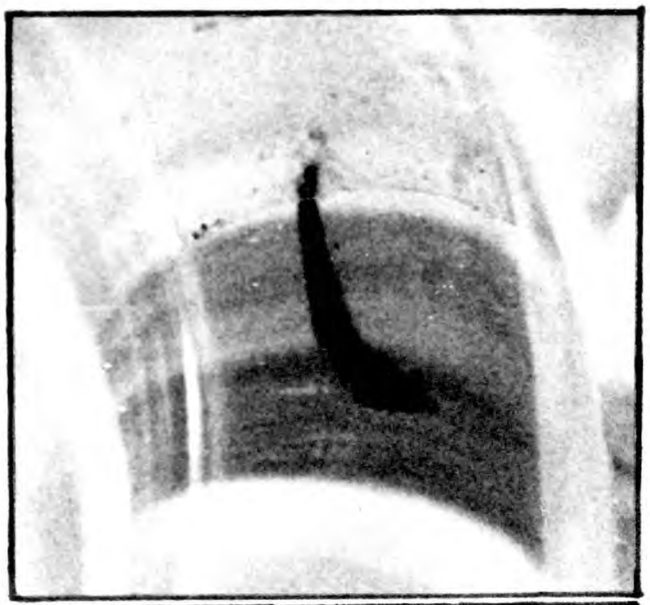

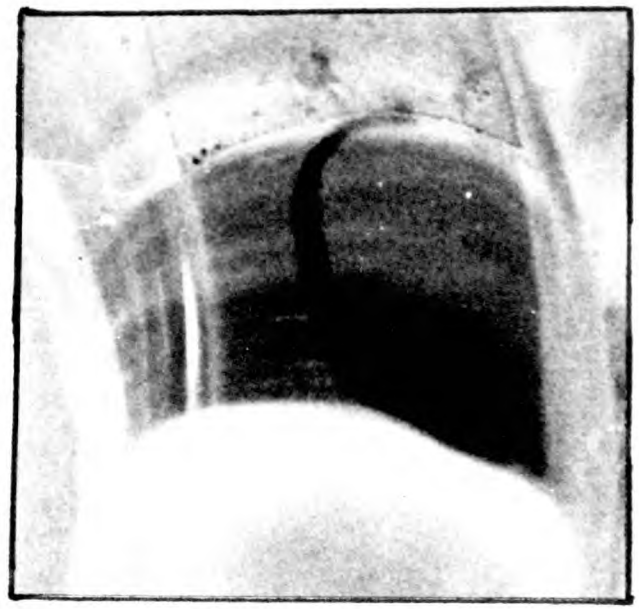

Fig. 7.3. Photographs of test section taken at intervals of approximately three seconds.

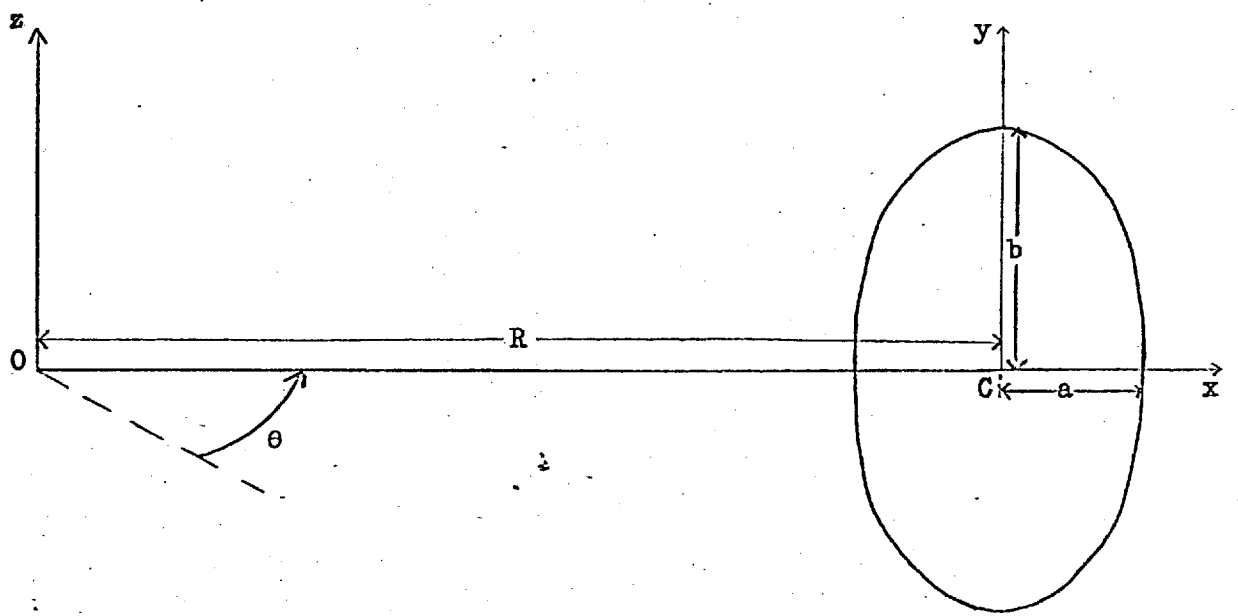

Fig. 8.1 The co-ordinate system for the elliptic pipe.

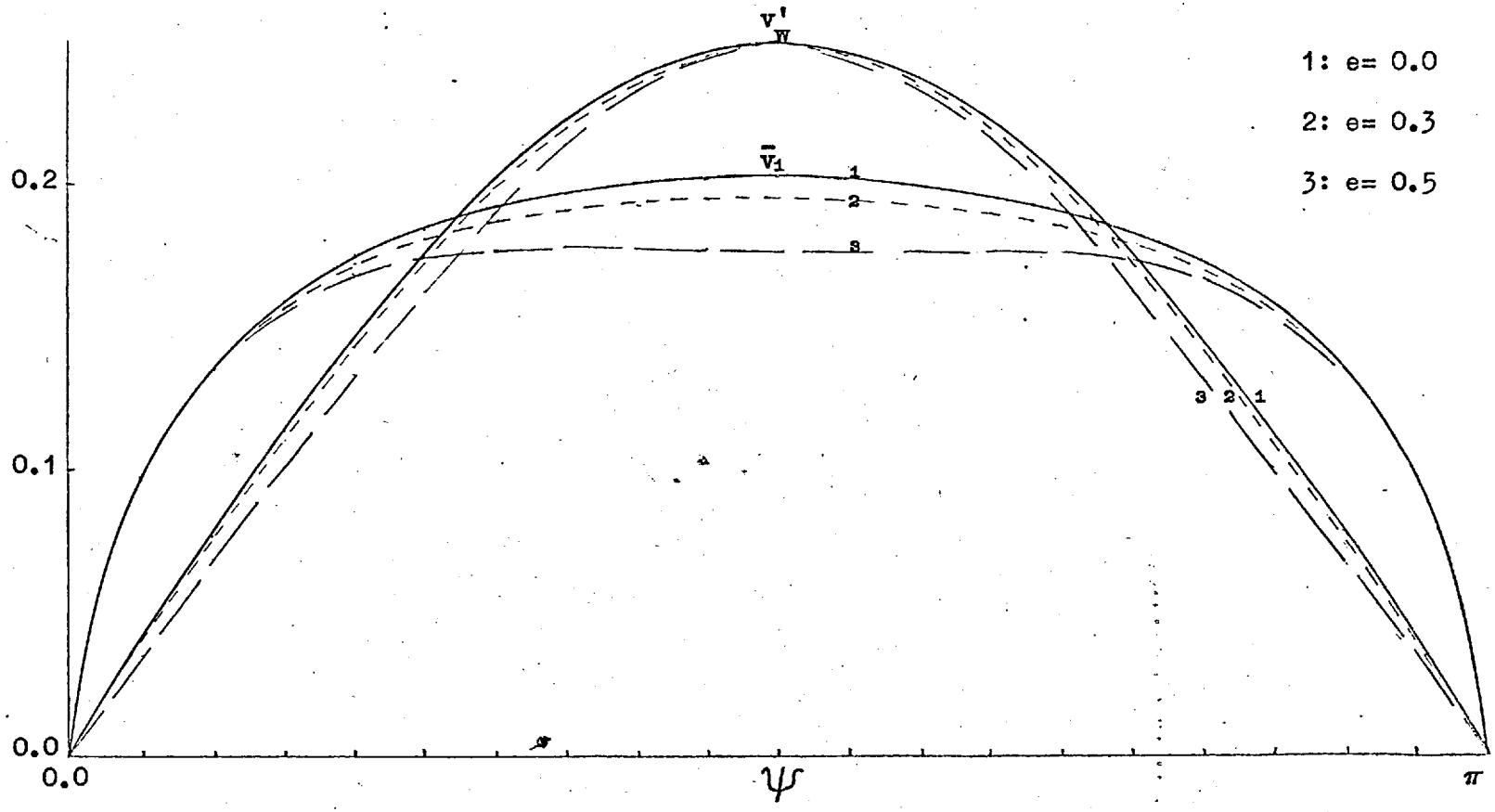

Fig. 8.2a: Comparison of $\bar{v}_1$ with v'_w when the minor axis of the ellipse lies in the plane in which the pipe is coiled.

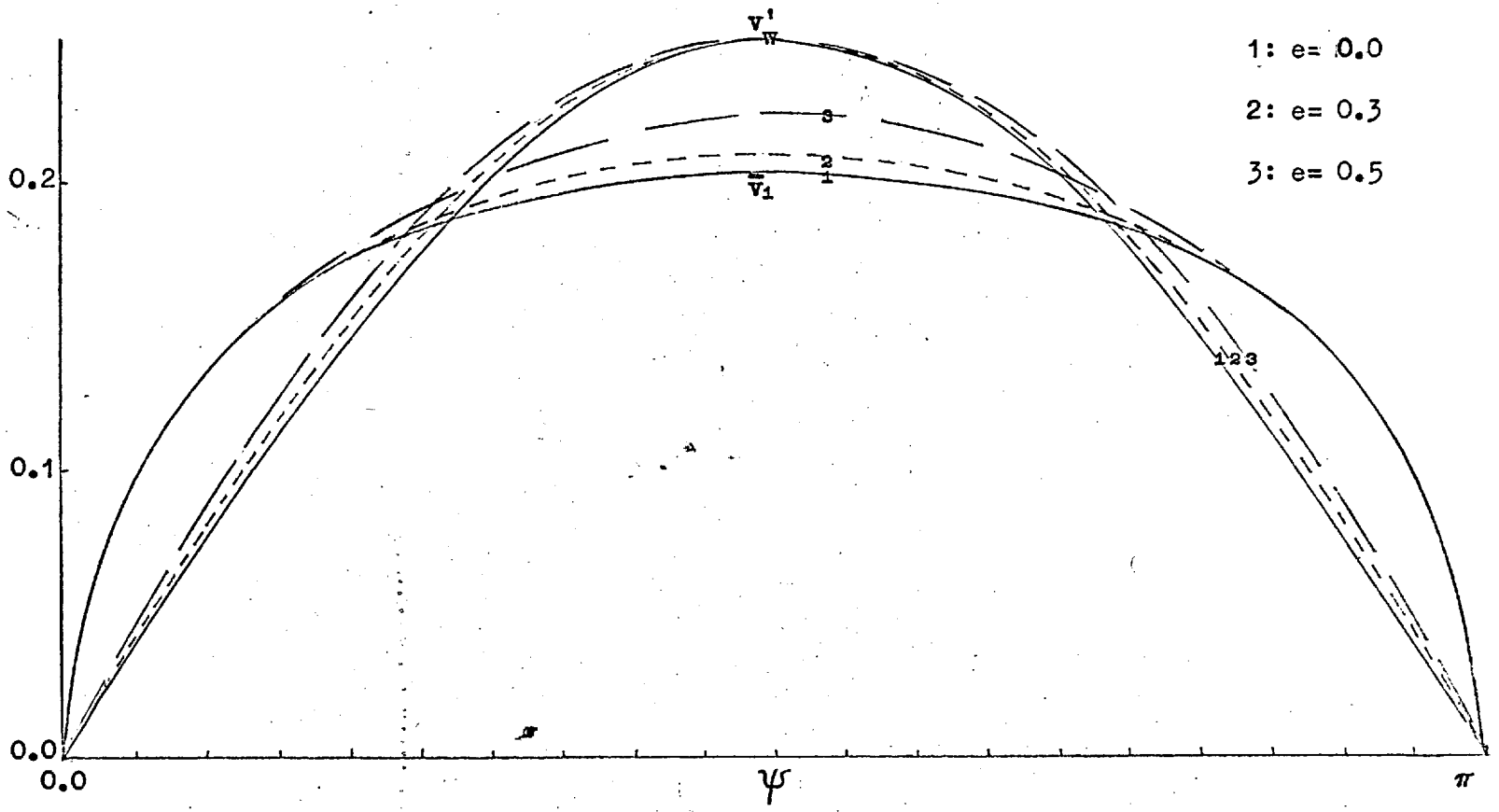

Fig. 8.2b Comparison of $\bar{v}_1$ with v'_w when the major axis of the ellipse lies in the plane in which the pipe is coiled.

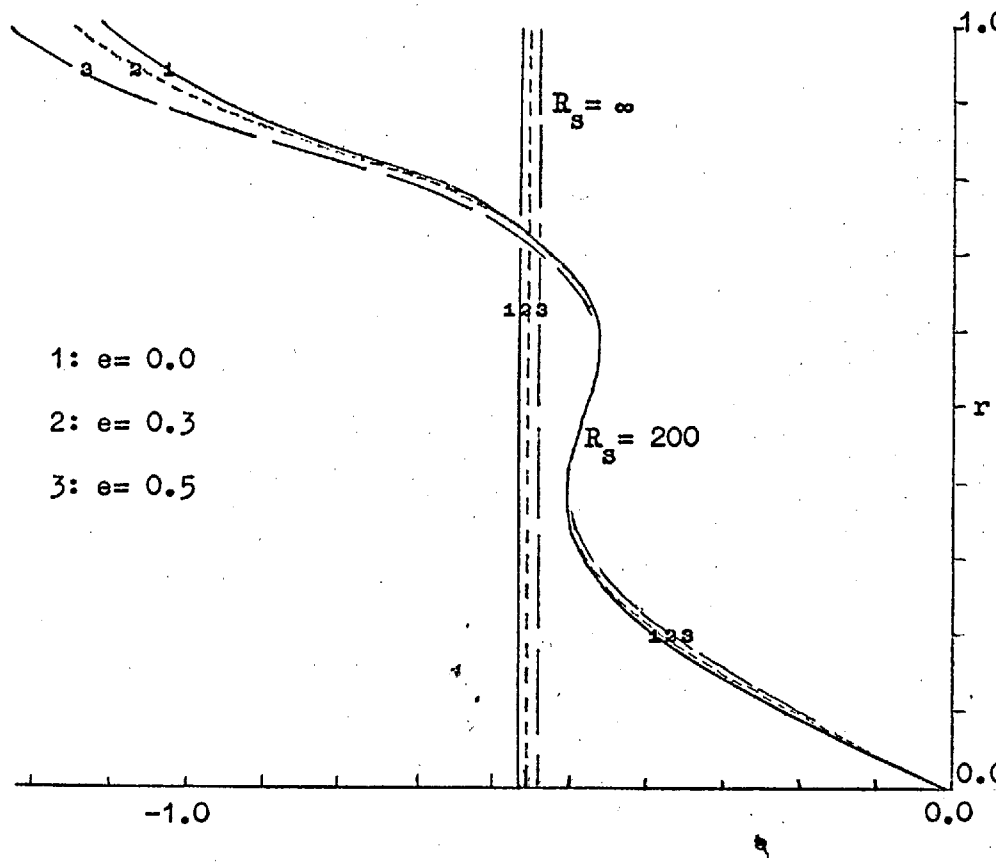

Fig. 8.3a: The secondary flow's vorticity in the outer region along $\psi=\pi/2$ when $\beta=0$ and the minor axis of the ellipse lies in the plane in which the pipe is coiled.

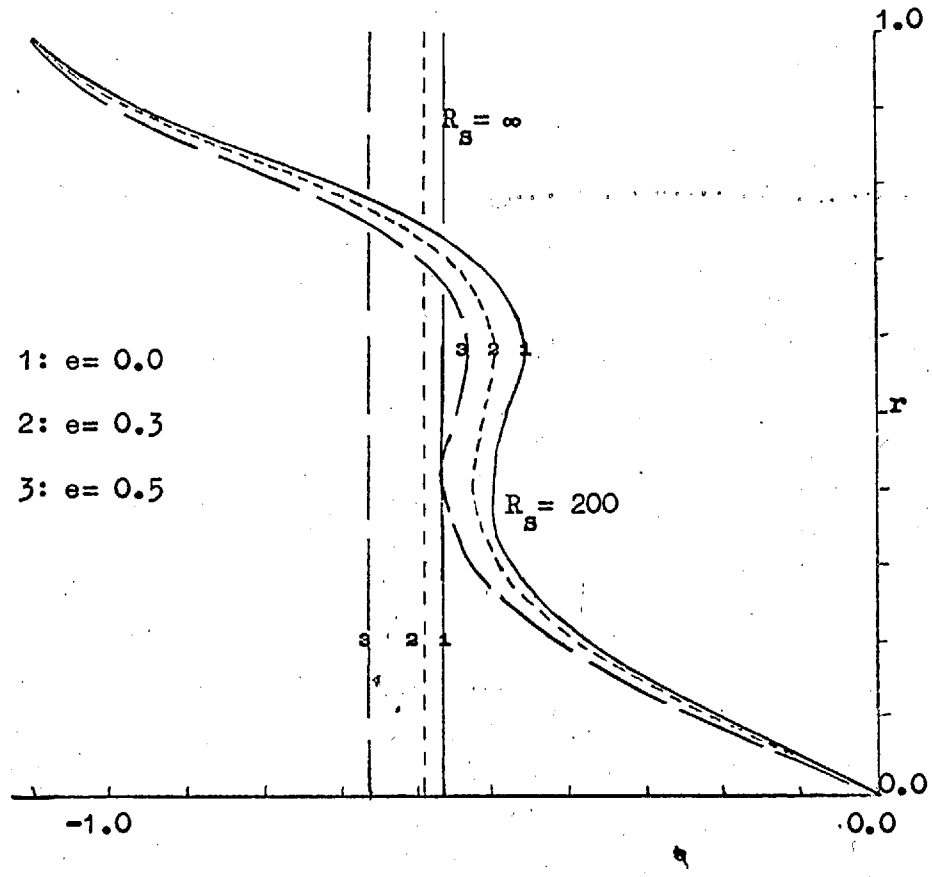

Fig. 8.3b: The secondary flow's vortioity in the outer region along $\psi=\pi/2$ when $\beta=0$ and the major axis of the ellipse lies in the plane in which the pipe is coiled.

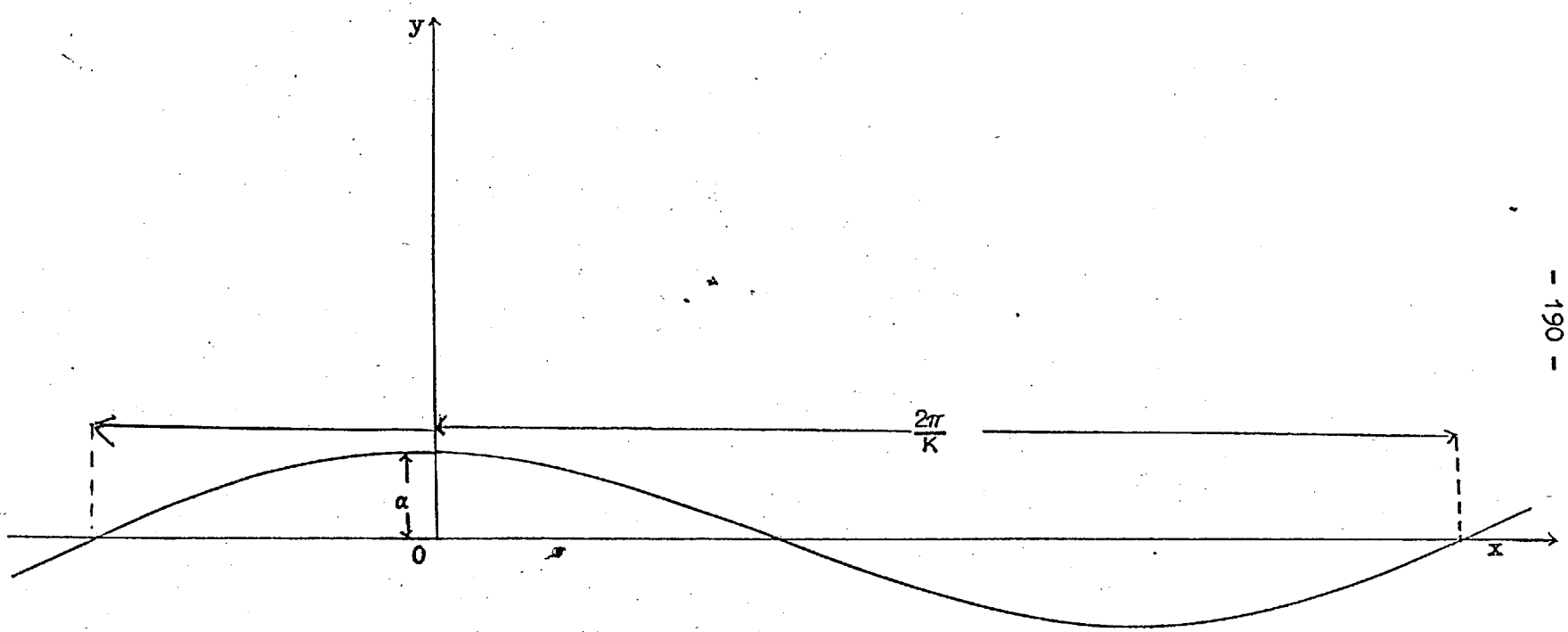

Fig. 10.1: The co-ordinate system for the wavy wall.

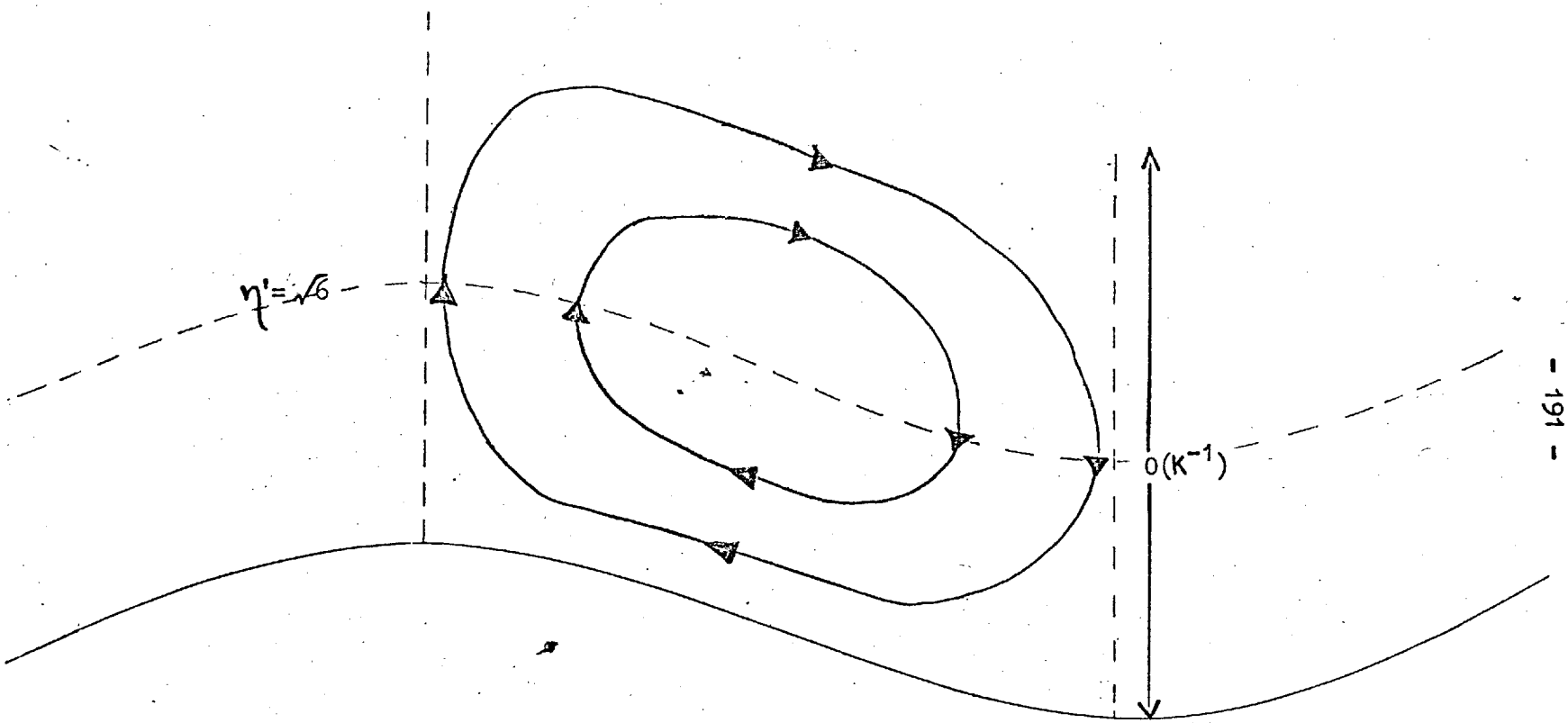

Fig. 11.1: Sketch of steady streaming when $kR \to 0$ and $k \gg 1$.

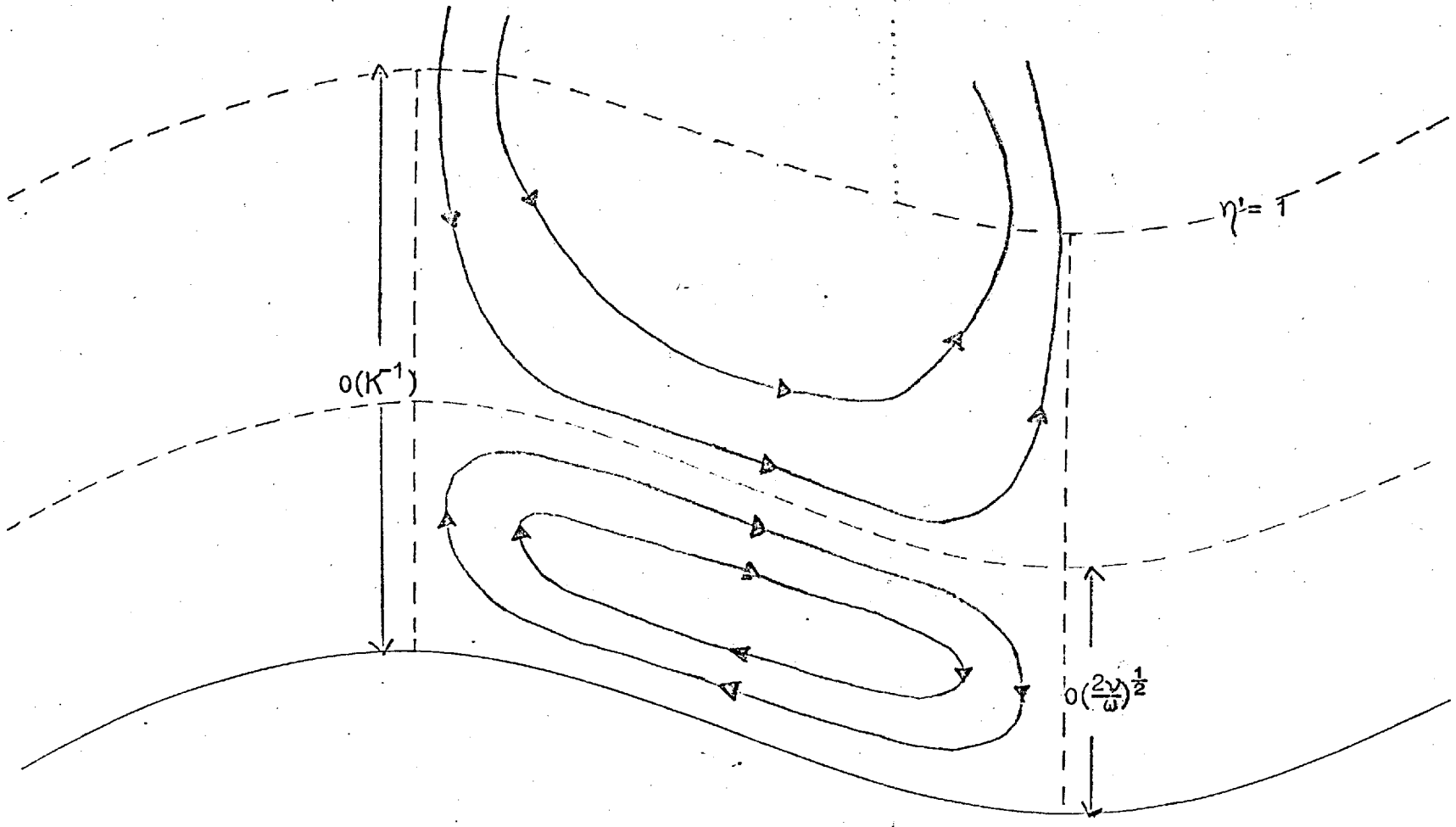

Fig. 11.2: Sketch of steady streaming when kR→ 0 and k<< 1.

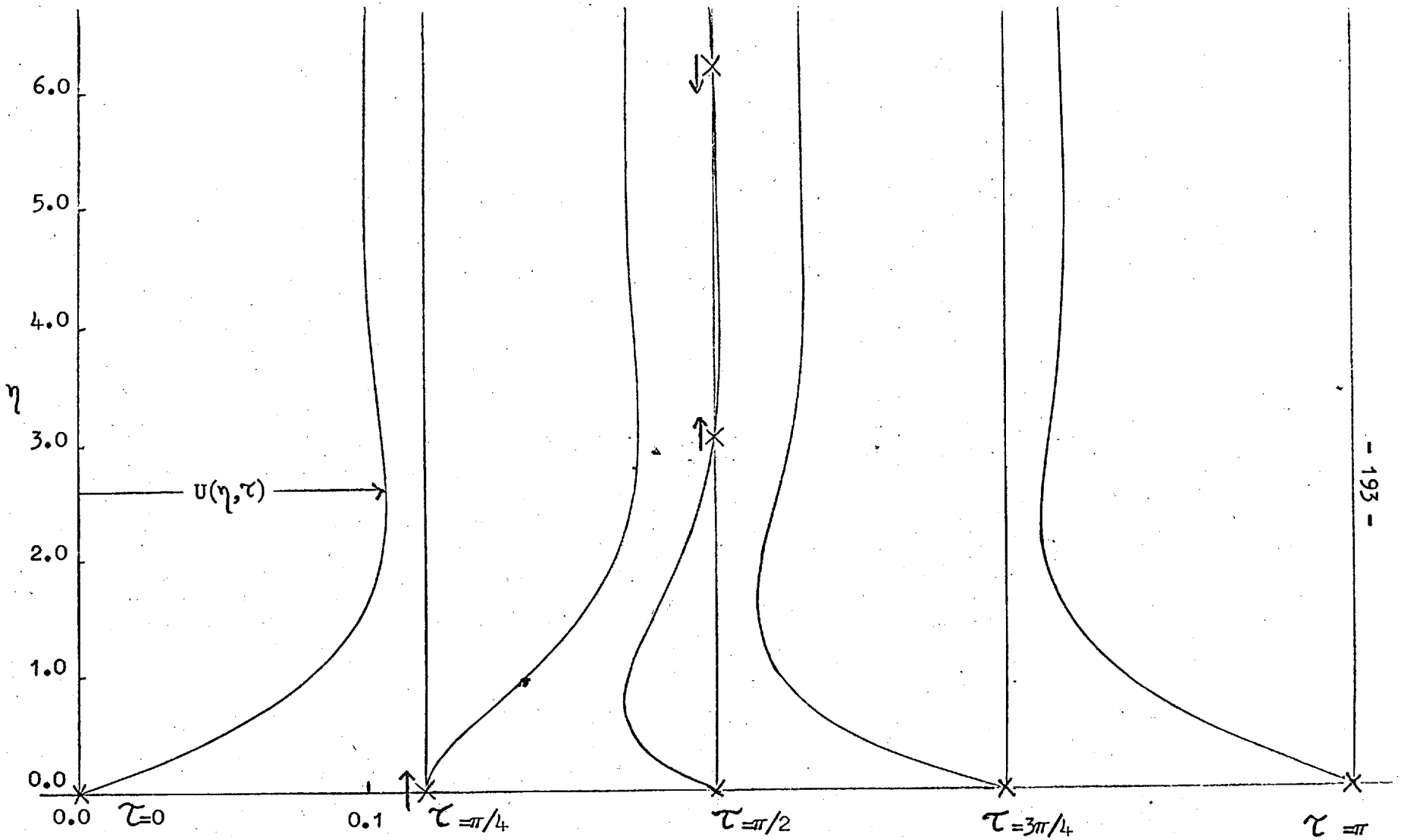

Fig. 12.1: The profiles of $U(\eta,\tau)$ and the associated viscous layers .

↑X = viscous layer and its direction of propagation.

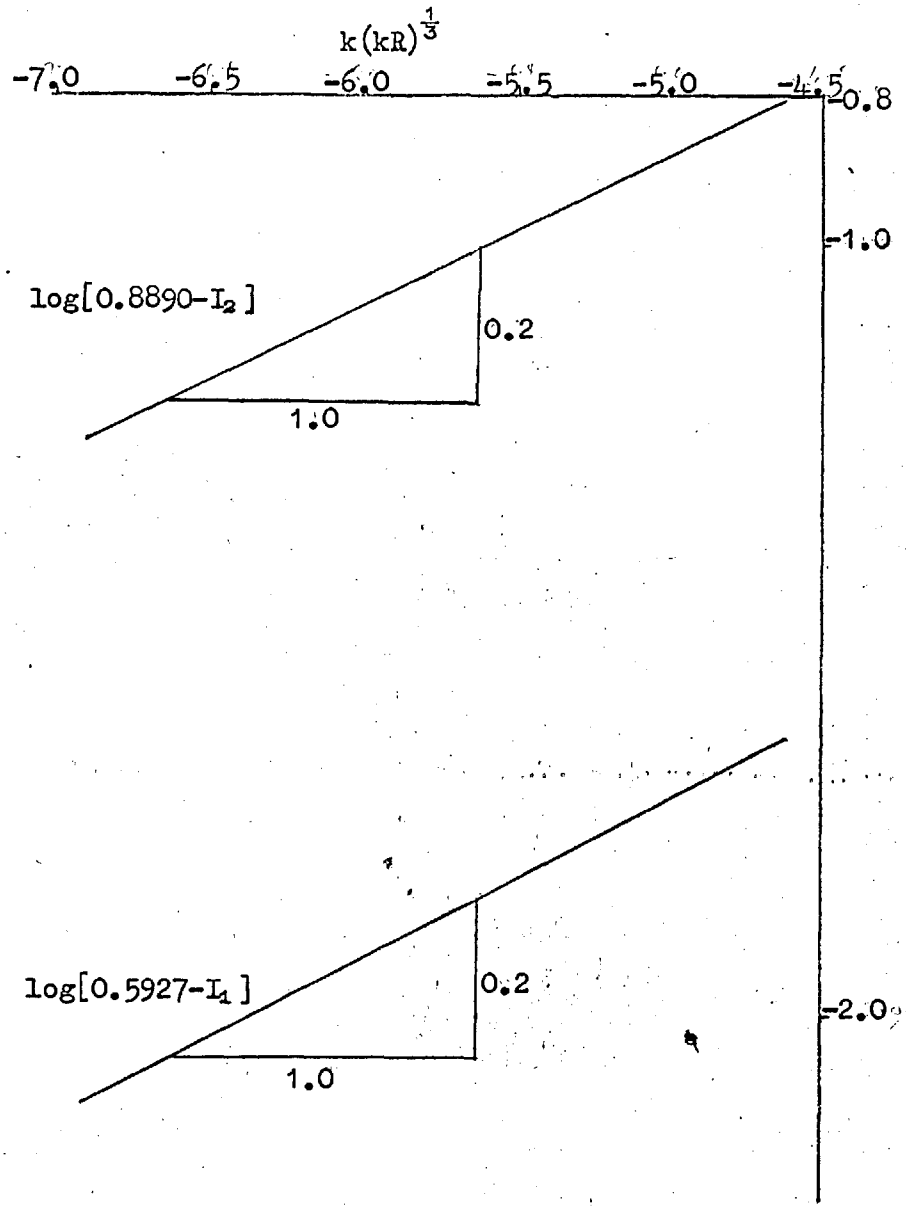

Fig. 12.2: Graph of $\log[0.5927-I_1]$ and $\log[0.8890-I_2]$ plotted against $\log[k(kR)^{\frac{1}{3}}]$ for $0.001 \leq k(kR)^{\frac{1}{3}} \leq 0.010$.

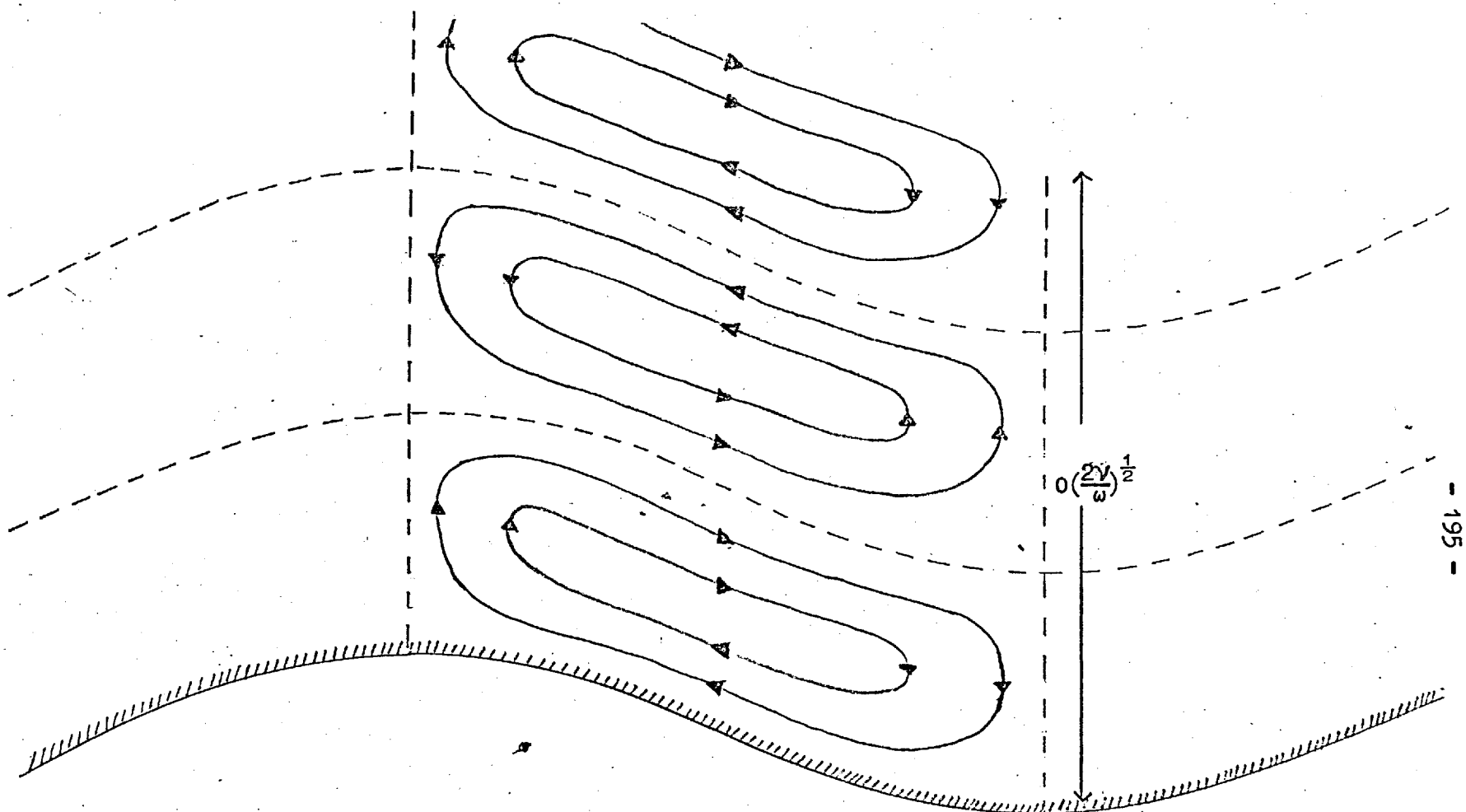

Fig. 12.3: Sketch of steady streaming when $kR \to \infty$ and $k \to 0$ such that $k(kR)^{\frac{1}{3}} \sim O$.

////// =viscous layer of thickness $O[\varepsilon(\frac{2\nu}{\omega})^{\frac{1}{2}}]$.

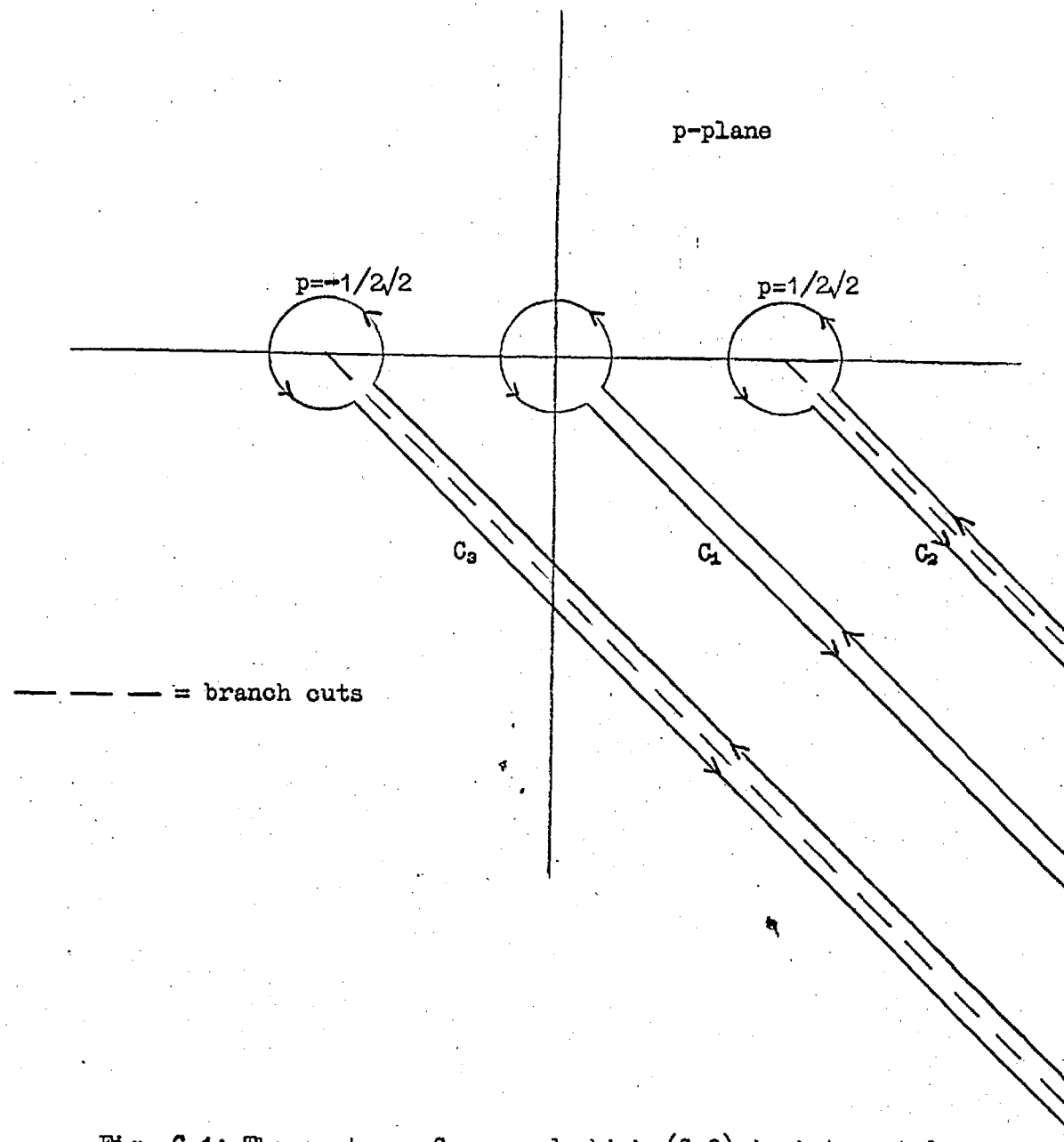

Fig. C.1: The contours C_i around whioh (C.9) is integrated when $U_0'' > 0$.

CORRIGENDA

Page 66

Dr. R. Nerem has pointed out to me that, owing to the mean flow, a fluid particle remains in the aortic arch for a time of only $O(\omega^{-1})$. The time taken for the secondary flow to diffuse into the interior is $O(a^2/\nu)$ (see Chapter 7), and, since the ratio of these is $O(\vartheta^{-2}) >> 1$, then the flow would have no time to develop. However, since the Stokes layer is formed in a time of $O(\omega^{-1})$ (see Chapter 7), this would be in existence at the end of the arch. Because this is the mechanism for driving the secondary flow in the interior, this might still develop further along the artery. In conclusion, it has to be pointed out that the effects due to branching of the aorta may considerably outweigh the centrifugal effects described here.

Dr. Nerem has further pointed out that the ratio a/R is more probably 0.4 and thus the value of the ratio in (6.5) is amended to $0.4/\sqrt{2}$.

pp. 140-141 : (12.68) & (12.69) should include the integral $\int_0^1 \frac{1}{(1-y^6)^{1/2}}\,dy$